PHYSICAL REVIEW D **94,** 113005 (2016)

Nonleptonic decays of $B \to (f_1(1285), f_1(1420))V$ in the perturbative QCD approach

Xin Liu[*]

School of Physics and Electronic Engineering, Jiangsu Normal University, Xuzhou, Jiangsu 221116, People's Republic of China

Zhen-Jun Xiao[†]

Department of Physics and Institute of Theoretical Physics, Nanjing Normal University, Nanjing, Jiangsu 210023, People's Republic of China

Zhi-Tian Zou[‡]

Department of Physics, Yantai University, Yantai, Shandong 264005, People's Republic of China

(Received 6 September 2016; published 15 December 2016)

We investigate the branching ratios, the polarization fractions, the direct CP-violating asymmetries, and the relative phases in 20 nonleptonic decay modes of $B \to f_1 V$ within the framework of the perturbative QCD approach at leading order with f_1 including two $^3P_1$-axial-vector states $f_1(1285)$ and $f_1(1420)$. Here, B denotes B^+, B^0, and B_s^0 mesons and V stands for the lightest vector mesons ρ, K^*, ω, and ϕ, respectively. The $B_s^0 \to f_1 V$ decays are studied theoretically for the first time in the literature. Together with the angle $\phi_{f_1} \approx (24^{+3.2}_{-2.7})^\circ$ extracted from the measurement through $B_{d/s} \to J/\psi f_1(1285)$ modes for the $f_1(1285) - f_1(1420)$ mixing system, it is of great interest to find phenomenologically some modes such as the tree-dominated $B^+ \to f_1\rho^+$ and the penguin-dominated $B^{+,0} \to f_1 K^{*+,0}$, $B_s^0 \to f_1\phi$ with large branching ratios around $\mathcal{O}(10^{-6})$ or even $\mathcal{O}(10^{-5})$, which are expected to be measurable at the LHCb and/or the Belle-II experiments in the near future. The good agreement (sharp contrast) of branching ratios and decay pattern for $B^+ \to f_1\rho^+$, $B^{+,0} \to f_1(1285)K^{*+,0}[B^{+,0} \to f_1(1420)K^{*+,0}]$ decays between QCD factorization and perturbative QCD factorization predictions can help us to distinguish these two rather different factorization approaches via precision measurements, which would also be helpful for us in exploring the annihilation decay mechanism through its important roles for the considered $B \to f_1 V$ decays.

DOI: 10.1103/PhysRevD.94.113005

I. INTRODUCTION

The studies on nonleptonic B meson weak decays are generally expected to provide not only good opportunities for testing the standard model (SM), but also powerful means for probing both weak and strong dynamics, even different new physics (NP) scenarios beyond the SM. It has been discussed that the naive expectations of polarization fractions, i.e., the longitudinal one $f_L \sim 1$ and the transverse two $f_\parallel \approx f_\perp \sim \mathcal{O}(m_V^2/m_B^2)$ [1,2] with m_V (m_B) being the mass of the light vector (B) meson, are violated mainly in the penguin-dominated vector-vector B meson decays [3–7], e.g., $f_L \sim f_T (= f_\parallel + f_\perp)$ in the famous $B \to \phi K^*$ process [8–10], which has resulted in many investigations from various ways based on different mechanisms, such as large penguin-induced annihilation contributions [1], form-factor tuning [11], final-state interactions [2,12], and even possible NP [13], to interpret anomalous polarizations in those considered $B \to VV$ modes. Analogous to $B \to VV$ decays with rich physics involved in three polarization states, it is therefore of particular interest to explore the $B \to VA, AV$ (A is an axial-vector state) modes to shed light on the underlying helicity structure of the decay mechanism [3] through polarization studies. Furthermore, stringent comparisons between theoretical predictions and experimental data for the physical observables may also help us to further understand the hadronic structure of the involved axial-vector bound states [14–18].

Recently, the $B_{d/s} \to J/\psi f_1(1285)$ modes measured by the Large Hadron Collider beauty (LHCb) Collaboration for the first time in the heavy b flavor sector [19] motivated us to study the production of $^3P_1$-axial-vector $f_1(1285)$ and $f_1(1420)$ states in the hadronic B meson decays, such as $B_s^0 \to J/\psi f_1$ [17] and $B \to f_1 P$ [18] within the framework of perturbative QCD (pQCD) approach [20] at leading order [for the sake of simplicity, we use f_1 to denote both $f_1(1285)$ and $f_1(1420)$ unless otherwise stated]. Now, we will extend this pQCD formalism to nonleptonic $B \to f_1 V$ decays, with B^1 (V) being the B^+, B^0, and B_s^0 (the lightest

[*]liuxin@jsnu.edu.cn
[†]xiaozhenjun@njnu.edu.cn
[‡]zouzt@ytu.edu.cn

[1]It is noted that the pure annihilation-type $B_c \to f_1 V$ decays have been studied by two of us (X. L. and Z. J. X.) in the pQCD approach focusing on the predictions of the decay rates and the polarization fractions [21].

vector ρ, K^*, ω, and ϕ) states, in which the $B_s^0 \to f_1 V$ decays are studied theoretically for the first time in the literature, although no data on these $B \to VA, AV$ type modes has been released so far. Though many efforts have been made to develop the next-to-leading order pQCD formalism [22,23], because of a well-known fact that leading order contributions dominate in the perturbation theory, here we will still work at leading order to clarify the physics for convenience. We will calculate the CP-averaged branching ratios, the polarization fractions, the CP-violating asymmetries, and the relative phases of 20 nonleptonic weak decays of $B \to f_1 V$ by employing the low energy effective Hamiltonian [24] and the pQCD approach based on the k_T factorization theorem. Assisted by the techniques of k_T resummation and threshold resummation, we can include all possible contributions by explicitly evaluating the factorizable emission, the nonfactorizable emission, the factorizable annihilation, and the nonfactorizable annihilation Feynman diagrams in the pQCD approach with no end-point singularities. The overall consistency between pQCD predictions and experimental data for the $B \to PP$, PV, and VV decays is very good and indicates the advantage and reliability of the pQCD approach in estimating the hadronic matrix elements of B meson decays.

In the quark model, the two f_1 states, i.e., $f_1(1285)$ and its partner $f_1(1420)$, are classified specifically as the light p-wave axial-vector flavorless mesons carrying quantum number $J^{PC} = 1^{++}$ [8]. In analogy to the pseudoscalar $\eta - \eta'$ mixing [8], these two axial-vector f_1 states are also considered as a mixture induced by nonstrange state $f_{1q} \equiv (u\bar{u} + d\bar{d})/\sqrt{2}$ and strange one $f_{1s} \equiv s\bar{s}$ in the quark-flavor basis and can be described as a 2×2 rotation matrix with mixing angle ϕ_{f_1} as follows [19]:

$$\begin{pmatrix} f_1(1285) \\ f_1(1420) \end{pmatrix} = \begin{pmatrix} \cos\phi_{f_1} & -\sin\phi_{f_1} \\ \sin\phi_{f_1} & \cos\phi_{f_1} \end{pmatrix} \begin{pmatrix} f_{1q} \\ f_{1s} \end{pmatrix}. \quad (1)$$

In fact, there also exists another mixing scheme called the singlet-octet basis with flavor singlet state $f_1 = (u\bar{u} + d\bar{d} + s\bar{s})/\sqrt{3}$ and flavor octet one $f_8 = (u\bar{u} + d\bar{d} - 2s\bar{s})/\sqrt{6}$. The corresponding mixing angle θ_{f_1} is related with ϕ_{f_1} via the equation $\phi_{f_1} = \theta_i - \theta_{f_1}$, with θ_i being the "ideal" mixing angle, specifically, $\theta_i = 35.3°$. It is therefore expected that ϕ_{f_1} can measure the deviation from the ideal mixing. Determination of the magnitude for the mixing angle ϕ_{f_1} is one of the key issues to understand the physical properties of the f_1 states. Furthermore, it is essential to note that ϕ_{f_1} also has an important role in constraining the mixing angle θ_{K_1}, which arises from the mixing between two distinct types of axial-vector $K_{1A}(^3P_1)$ and $K_{1B}(^1P_1)$ states, through the Gell-Mann–Okubo mass formula [8,25]. It is therefore definitely interesting to investigate the mixing angle ϕ_{f_1} in different ways. However, the value of ϕ_{f_1} is still a controversy presently [17,18], though there are several explorations that have been performed at both theoretical and experimental aspects. Of course, it is expected that this status will be greatly improved with the successful upgrade of LHC RUN-II and the scheduled running of Belle-II experiments ever since the $f_1(1285)$ state, as well as the value of ϕ_{f_1}, has been measured preliminarily in the B decay system [19].

Up to now, to our best knowledge, the nonleptonic $B^{+,0} \to f_1 V$ decays have been theoretically investigated by G. Calderón *et al.* [26] in the naive factorization approach and by Cheng and Yang [3] within QCD factorization (QCDF), respectively. However, the conclusion that $\mathrm{Br}(B \to f_1 V)[\mathcal{O}(10^{-8} - 10^{-6})] < \mathrm{Br}(B \to f_1 P)[\mathcal{O}(10^{-5})]$, predicted in Ref. [26], seems to contradict our naive expectation. As pointed out in Ref. [3], the authors believed that, because of the existence of three polarization states for the vector meson, the $B \to f_1 V$ decays may generally have larger decay rates than the $B \to f_1 P$ ones correspondingly. Furthermore, due to the similar QCD behavior between vector and $^3P_1$-axial-vector states [27], the analogy between $B \to f_1 V$ and $B \to (\omega, \phi) V$ decays can be naively anticipated. For example, if $f_1(1285)$ is highly dominated by the f_{1q} flavor state, then $\mathrm{Br}(B^+ \to f_1(1285)\rho^+)$ can be comparable with $\mathrm{Br}(B^+ \to \omega\rho^+)$. Actually, because $f_1(1285)$ mixes with the $s\bar{s}$ component around 20% ($\sim \sin^2\phi_{f_1}$) based on Eq. (1) and the preliminary value $\phi_{f_1} \sim 24°$ given by the LHCb Collaboration [19], it is therefore estimated that the decay rate of $B^+ \to f_1(1285)\rho^+$ may be somewhat smaller than that of $B^+ \to \omega\rho^+$. As a matter of fact, the branching ratios of $B^+ \to f_1(1285)\rho^+$ predicted within the QCDF and pQCD formalisms, as far as the central values are concerned, are $(9\text{–}10) \times 10^{-6}$ [3] and 11.1×10^{-6} in this work, respectively, which are indeed comparative and slightly smaller than that of $B^+ \to \omega\rho^+$, with updated values 16.9×10^{-6} [5] and 12.1×10^{-6} [6] correspondingly. Moreover, the polarization fractions for the $B^{+,0} \to f_1 V$ channels were also given within the framework of QCDF [3]. But, frankly speaking, lack of experimental constraints on the parametrized hard-spectator scattering and weak annihilation contributions in QCDF greatly weakens the reliability of predictions for $B^{+,0} \to f_1 V$ decays, which will limit the hints to relevant experiments, even to understand the physics hidden in relevant modes. It is therefore definitely interesting to investigate these aforementioned $B \to f_1 V$ decays in other frameworks, e.g., the pQCD approach in the present work, to clarify the discrepancies and further distinguish the factorization approaches through experimental examinations with good precision.

The paper is organized as follows. In Sec. II, we present the formalism, hadron wave functions, and analytic pQCD calculations of 20 nonleptonic $B \to f_1 V$ decays. The numerical results and phenomenological analyses are addressed in Sec. III explicitly. Finally, Sec. IV contains the main conclusions and a short summary.

II. FORMALISM AND PERTURBATIVE CALCULATIONS

In this section, we first make a brief introduction to the pQCD formalism at leading order. For more details, the readers can refer to the review article in Ref. [20]. Nowadays, the pQCD approach has been known as one of the important factorization methods based on QCD dynamics to perturbatively evaluate hadronic matrix elements in the decays of heavy b flavor mesons. The unique point of this pQCD approach is that it picks up the transverse momentum k_T of the valence quarks in all the initial and final states, as a result of which the calculations of hadronic matrix elements free of end-point singularities always occur in the collinear factorization theorem employed in the QCDF approach [28] and soft-collinear effective theory (SCET) [29]. Hence, all topologies of Feynman diagrams in the hadronic B meson decays are effectively calculable in the pQCD framework, where three energy scales m_W (mass of W boson); m_b (mass of b quark); and $t \approx \sqrt{m_b\Lambda_{\rm QCD}}$ (factorization hard-collinear scale with $\Lambda_{\rm QCD}$, the hadronic scale) are involved [20,30]. Note that, unlike the QCDF approach [31], the annihilation contributions in the pQCD formalism can be calculated without introducing any parameters. When t is no less than the factorization scale, i.e., $\geq \sqrt{m_b\Lambda_{\rm QCD}}$, the running of Wilson coefficients $C_i(t)$ will be perturbatively controlled through the renormalization group equation. The soft dynamics below $\sqrt{m_b\Lambda_{\rm QCD}}$ will be described by hadron wave functions Φ, which are nonperturbative but universal for all channels and usually determined by employing nonperturbative QCD techniques such as QCD sum rules and/or lattice QCD or extracted experimentally from other well-measured processes. It is worth emphasizing that the physics between m_b and $\sqrt{m_b\Lambda_{\rm QCD}}$ will be absorbed into the so-called "hard kernel" H and perturbatively evaluated in the pQCD approach. The decay amplitude for $B \to f_1 V$ decays in the pQCD approach can therefore be conceptually written as follows:

$$A(B \to f_1 V) \sim \int dx_1 dx_2 dx_3 b_1 db_1 b_2 db_2 b_3 db_3 \cdot \mathrm{Tr}[C(t)\Phi_B(x_1,b_1)\Phi_V(x_2,b_2)\Phi_{f_1}(x_3,b_3) \times H(x_i,b_i,t)S_t(x_i)e^{-S(t)}], \quad (2)$$

where $x_i (i = 1,2,3)$ is the momentum fraction of the valence quark in the involved mesons; b_i is the conjugate space coordinate of k_{iT}; t is the largest running energy scale in hard kernel $H(x_i,b_i,t)$; Tr denotes the trace over Dirac and SU(3) color indices; $C(t)$ stands for the Wilson coefficients, including the large logarithms $\ln(m_W/t)$ [20]; and Φ is the wave function describing the hadronization of quarks and antiquarks to the meson. The jet function $S_t(x_i)$ comes from threshold resummation, which exhibits a strong suppression effect in the small x region [32,33], while the Sudakov factor $e^{-S(t)}$ arises from k_T resummation, which provides a strong suppression in the small k_T (or large b) region [34,35]. These resummation effects therefore guarantee the removal of the end-point singularities. The detailed expressions for $S_t(x_i)$ and $e^{-S(t)}$ can be easily found in the original Refs. [32–35]. Thus, with Eq. (2), we can give the convoluted amplitudes of the $B \to f_1 V$ decays explicitly, which will be presented in the next section, through the evaluations of the hard kernel $H(x_i,b_i,t)$ at leading order in the α_s expansion with the pQCD approach.

A. Hadron wave functions

The heavy B meson is usually treated as a heavy-light system and its light-cone wave function can generally be defined as [20,36]

$$\Phi_B = \frac{i}{\sqrt{2N_c}}\{(P\!\!\!/ + m_B)\gamma_5\phi_B(x,k_T)\}_{\alpha\beta}, \quad (3)$$

where α, β are the color indices; P is the momentum of B meson; N_c is the color factor; and k_T is the intrinsic transverse momentum of the light quark in B meson.

In Eq. (3), $\phi_B(x,k_T)$ is the B meson distribution amplitude and obeys the following normalization condition,

$$\int_0^1 dx\phi_B(x,b=0) = \frac{f_B}{2\sqrt{2N_c}}, \quad (4)$$

where b is the conjugate space coordinate of transverse momentum k_T and f_B is the decay constant of the B meson.

The light-cone wave functions of light vector meson V and axial-vector state f_1 have been given in the QCD sum rule method up to twist-3 as [37,38]

$$\Phi_V^L = \frac{1}{\sqrt{2N_c}}\{m_V\epsilon\!\!\!/_L\phi_V(x) + \epsilon\!\!\!/_L P\!\!\!/\phi_V^t(x) + m_V\phi_V^s(x)\}_{\alpha\beta}, \quad (5)$$

$$\Phi_V^T = \frac{1}{\sqrt{2N_c}}\{m_V\epsilon\!\!\!/_T\phi_V^v(x) + \epsilon\!\!\!/_T P\!\!\!/\phi_V^T(x) + m_V i\epsilon_{\mu\nu\rho\sigma}\gamma_5\gamma^\mu\epsilon_T^\nu n^\rho v^\sigma\phi_V^a(x)\}_{\alpha\beta}, \quad (6)$$

and [27,39]

$$\Phi_{f_1}^L = \frac{1}{\sqrt{2N_c}}\gamma_5\{m_{f_1}\epsilon\!\!\!/_L\phi_{f_1}(x) + \epsilon\!\!\!/_L P\!\!\!/\phi_{f_1}^t(x) + m_{f_1}\phi_{f_1}^s(x)\}_{\alpha\beta}, \quad (7)$$

$$\Phi_{f_1}^T = \frac{1}{\sqrt{2N_c}}\gamma_5\{m_{f_1}\epsilon\!\!\!/_T\phi_{f_1}^v(x) + \epsilon\!\!\!/_T P\!\!\!/\phi_{f_1}^T(x) + m_{f_1} i\epsilon_{\mu\nu\rho\sigma}\gamma_5\gamma^\mu\epsilon_T^\nu n^\rho v^\sigma\phi_{f_1}^a(x)\}_{\alpha\beta}, \quad (8)$$

for longitudinal and transverse polarizations, respectively, with the polarization vectors ϵ_L and ϵ_T of V or f_1, satisfying $P\cdot\epsilon = 0$, where x denotes the momentum fraction carried by quarks in the meson; $n = (1,0,\mathbf{0}_T)$ and $v = (0,1,\mathbf{0}_T)$ are dimensionless lightlike unit vectors; and m_{f_1} stands for the mass of light axial-vector f_1 states. We adopt the

convention $\epsilon^{0123}=1$ for the Levi-Cività tensor $\epsilon^{\mu\nu\alpha\beta}$. Note that the explicit expressions for all the above-mentioned distribution amplitudes $\phi(x)$ with different twists can be found later in the Appendix.

B. Perturbative calculations in the pQCD approach

For the considered 20 $B\to f_1V$ decays induced by the $\bar{b}\to\bar{q}(q=d\,\text{or}\,s)$ transition at the quark level, the related weak effective Hamiltonian H_{eff} can be written as [24]

$$H_{\text{eff}}=\frac{G_F}{\sqrt{2}}\left\{V_{ub}^*V_{uq}[C_1(\mu)O_1^u(\mu)+C_2(\mu)O_2^u(\mu)]-V_{tb}^*V_{tq}\left[\sum_{i=3}^{10}C_i(\mu)O_i(\mu)\right]\right\}+\text{H.c.},\tag{9}$$

with the Fermi constant $G_F=1.16639\times10^{-5}\,\text{GeV}^{-2}$, Cabibbo-Kobayashi-Maskawa (CKM) matrix elements V, and Wilson coefficients $C_i(\mu)$ at the renormalization scale μ. The local four-quark operators $O_i(i=1,\ldots,10)$ are written as

(1) Current-current (tree) operators

$$O_1^u=(\bar{q}_\alpha u_\beta)_{V-A}(\bar{u}_\beta b_\alpha)_{V-A},\qquad O_2^u=(\bar{q}_\alpha u_\alpha)_{V-A}(\bar{u}_\beta b_\beta)_{V-A};\tag{10}$$

(2) QCD penguin operators

$$O_3=(\bar{q}_\alpha b_\alpha)_{V-A}\sum_{q'}(\bar{q}'_\beta q'_\beta)_{V-A},\qquad O_4=(\bar{q}_\alpha b_\beta)_{V-A}\sum_{q'}(\bar{q}'_\beta q'_\alpha)_{V-A},$$
$$O_5=(\bar{q}_\alpha b_\alpha)_{V-A}\sum_{q'}(\bar{q}'_\beta q'_\beta)_{V+A},\qquad O_6=(\bar{q}_\alpha b_\beta)_{V-A}\sum_{q'}(\bar{q}'_\beta q'_\alpha)_{V+A};\tag{11}$$

(3) Electroweak penguin operators

$$O_7=\frac{3}{2}(\bar{q}_\alpha b_\alpha)_{V-A}\sum_{q'}e_{q'}(\bar{q}'_\beta q'_\beta)_{V+A},\qquad O_8=\frac{3}{2}(\bar{q}_\alpha b_\beta)_{V-A}\sum_{q'}e_{q'}(\bar{q}'_\beta q'_\alpha)_{V+A},$$
$$O_9=\frac{3}{2}(\bar{q}_\alpha b_\alpha)_{V-A}\sum_{q'}e_{q'}(\bar{q}'_\beta q'_\beta)_{V-A},\qquad O_{10}=\frac{3}{2}(\bar{q}_\alpha b_\beta)_{V-A}\sum_{q'}e_{q'}(\bar{q}'_\beta q'_\alpha)_{V-A},\tag{12}$$

with the color indices α, β and the notations $(\bar{q}'q')_{V\pm A}=\bar{q}'\gamma_\mu(1\pm\gamma_5)q'$. The index q' in the summation of the above operators runs through u, d, s, c, and b.

From the effective Hamiltonian (9), there are eight types of diagrams contributing to $B\to f_1V$ decays in the pQCD approach at leading order as illustrated in Fig. 1. The possible contributions to the considered decays can be easily obtained by exchanging the positions of f_1 and V. We calculate the contributions arising from various operators as shown in Eqs. (10)–(12). As presented in Ref. [16] [see Eqs. (33)–(57) for details], we have given the analytic $B\to VA$ decay amplitudes only with a $B\to A$ transition. This part will be repeated in this work, in order to present the analytically complete expressions for $B\to VA$ and AV decays. It should be mentioned that, hereafter, for the sake of simplicity, we will use F and M to describe the factorizable and nonfactorizable amplitudes induced by the $(V-A)(V-A)$ operators, F^{P_1} and M^{P_1} to describe the factorizable and nonfactorizable amplitudes arising from the $(V-A)(V+A)$ operators, and F^{P_2} and M^{P_2} to describe the factorizable and nonfactorizable amplitudes coming from the $(S-P)(S+P)$ operators that are obtained by making a Fierz transformation from the $(V-A)(V+A)$ ones, respectively. Furthermore, before starting the

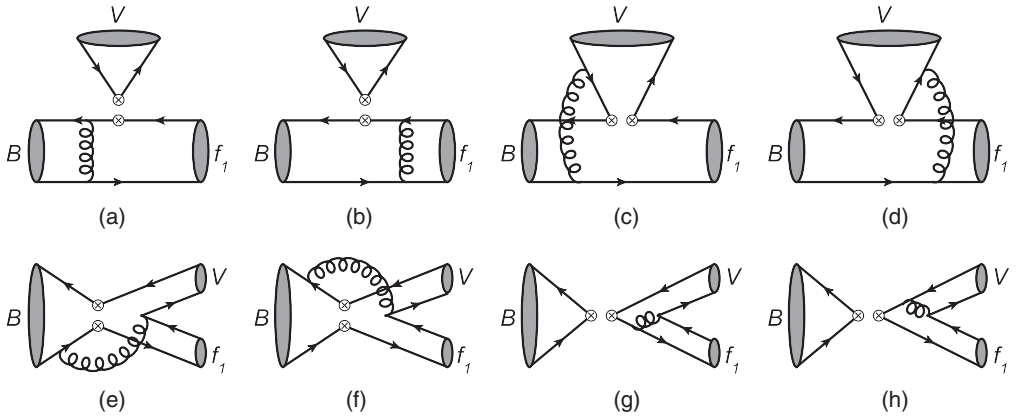

FIG. 1. Typical Feynman diagrams contributing to $B\to f_1V$ decays in the pQCD approach at leading order. The other diagrams contributing to those considered decays can be easily obtained by exchanging the positions of f_1 and V.

perturbative calculations, a comment should be given: in light of the successful clarification of most branching ratios and polarization fractions in the $B \to VV$ decays by keeping the terms proportional to $r_V^2 = m_V^2/m_B^2$ in the denominator of propagators for virtual quarks and gluons with the pQCD approach [6], we will follow this treatment in the present work for 20 nonleptonic $B \to f_1 V$ modes, i.e., retaining the similar terms with r_V^2 and $r_{f_1}^2 = m_{f_1}^2/m_B^2$, which could be examined by future measurements to further clarify its universality.

For the factorizable emission (fe) diagrams in Figs. 1(a) and 1(b), the corresponding Feynman amplitudes with one longitudinal polarization(L) and two transverse polarizations(N and T) can be written as follows:

$$\begin{aligned} F_{fe}^{L} = & -8\pi C_F m_B^2 \int_0^1 dx_1 dx_3 \int_0^\infty b_1 db_1 b_3 db_3 \phi_B(x_1,b_1) \\ & \times \{[(1+x_3)\phi_A(x_3) + r_A(1-2x_3) \\ & \times (\phi_A^t(x_3) + \phi_A^s(x_3))]E_{fe}(t_a)h_{fe}(x_1,x_3,b_1,b_3) \\ & + 2r_A\phi_A^s(x_3)E_{fe}(t_b)h_{fe}(x_3,x_1,b_3,b_1)\}, \end{aligned} \tag{13}$$

$$\begin{aligned} F_{fe}^{N} = & -8\pi C_F m_B^2 \int_0^1 dx_1 dx_3 \int_0^\infty b_1 db_1 b_3 db_3 \phi_B(x_1,b_1) r_V \\ & \times \{[\phi_A^T(x_3) + 2r_A\phi_A^v(x_3) + r_A x_3 \\ & \times (\phi_A^v(x_3) - \phi_A^a(x_3))]E_{fe}(t_a)h_{fe}(x_1,x_3,b_1,b_3) \\ & + r_A[\phi_A^v(x_3) + \phi_A^a(x_3)]E_{fe}(t_b)h_{fe}(x_3,x_1,b_3,b_1)\}, \end{aligned} \tag{14}$$

$$\begin{aligned} F_{fe}^{T} = & -16\pi C_F m_B^2 \int_0^1 dx_1 dx_3 \int_0^\infty b_1 db_1 b_3 db_3 \phi_B(x_1,b_1) \\ & \times r_V\{[\phi_A^T(x_3) + 2r_A\phi_A^a(x_3) - r_A x_3 \\ & \times (\phi_A^v(x_3) - \phi_A^a(x_3))]E_{fe}(t_a)h_{fe}(x_1,x_3,b_1,b_3) \\ & + r_A[\phi_A^v(x_3) + \phi_A^a(x_3)]E_{fe}(t_b)h_{fe}(x_3,x_1,b_3,b_1)\}, \end{aligned} \tag{15}$$

where, in this work, A will specifically denote the axial-vector states $f_1(1285)$ and $f_1(1420)$ and $C_F = 4/3$ is a color factor. For the hard functions h, the running hard scales t, and the convolution functions $E(t)$, refer to the Appendix in Ref. [6].

Since only the vector part of the $(V+A)$ current contributes to the vector meson production, $\langle A|V-A|B\rangle\langle V|V+A|0\rangle = \langle A|V-A|B\rangle\langle V|V-A|0\rangle$, we have

$$F_{fe}^{P_1} = F_{fe}. \tag{16}$$

Because a vector meson cannot be produced via scalar and/or pseudoscalar currents, then the contribution arising from the $(S \pm P)$ operators is

$$F_{fe}^{P_2} = 0. \tag{17}$$

For the nonfactorizable emission (nfe) diagrams in Figs. 1(c) and 1(d), the corresponding Feynman amplitudes are

$$\begin{aligned} M_{nfe}^{L} = & -\frac{16\sqrt{6}}{3}\pi C_F m_B^2 \int_0^1 dx_1 dx_2 dx_3 \int_0^\infty b_1 db_1 b_2 db_2 \phi_B(x_1,b_1)\phi_V(x_2)\{[(1-x_2)\phi_A(x_3) \\ & + r_A x_3(\phi_A^t(x_3) - \phi_A^s(x_3))]E_{nfe}(t_c)h_{nfe}^c(x_1,x_2,x_3,b_1,b_2) - [(x_2+x_3)\phi_A(x_3) \\ & - r_A x_3(\phi_A^t(x_3) + \phi_A^s(x_3))]E_{nfe}(t_d)h_{nfe}^d(x_1,x_2,x_3,b_1,b_2)\}, \end{aligned} \tag{18}$$

$$\begin{aligned} M_{nfe}^{N} = & -\frac{16\sqrt{6}}{3}\pi C_F m_B^2 \int_0^1 dx_1 dx_2 dx_3 \int_0^\infty b_1 db_1 b_2 db_2 \phi_B(x_1,b_1) r_V\{(1-x_2)(\phi_V^v(x_2) + \phi_V^a(x_2)) \\ & \times \phi_A^T(x_3)h_{nfe}^c(x_1,x_2,x_3,b_1,b_2)E_{nfe}(t_c) + [x_2(\phi_V^v(x_2) + \phi_V^a(x_2))\phi_A^T(x_3) \\ & - 2r_A(x_2+x_3)(\phi_V^v(x_2)\phi_A^v(x_3) + \phi_V^a(x_2)\phi_A^a(x_3))]E_{nfe}(t_d)h_{nfe}^d(x_1,x_2,x_3,b_1,b_2)\}, \end{aligned} \tag{19}$$

$$\begin{aligned} M_{nfe}^{T} = & -\frac{32\sqrt{6}}{3}\pi C_F m_B^2 \int_0^1 dx_1 dx_2 dx_3 \int_0^\infty b_1 db_1 b_2 db_2 \phi_B(x_1,b_1) r_V\{(1-x_2)(\phi_V^v(x_2) + \phi_V^a(x_2)) \\ & \times \phi_A^T(x_3)h_{nfe}^c(x_1,x_2,x_3,b_1,b_2)E_{nfe}(t_c) + [x_2(\phi_V^v(x_2) + \phi_V^a(x_2))\phi_A^T(x_3) \\ & - 2r_A(x_2+x_3)(\phi_V^v(x_2)\phi_A^a(x_3) + \phi_V^a(x_2)\phi_A^v(x_3))]E_{nfe}(t_d)h_{nfe}^d(x_1,x_2,x_3,b_1,b_2)\}, \end{aligned} \tag{20}$$

$$M_{nfe}^{L,P_1} = -\frac{16\sqrt{6}}{3}\pi C_F m_B^2 \int_0^1 dx_1 dx_2 dx_3 \int_0^\infty b_1 db_1 b_2 db_2 \phi_B(x_1,b_1) r_V \{[(1-x_2)(\phi_V^t(x_2)+\phi_V^s(x_2)) \times \phi_A(x_3) - r_A(1-x_2)(\phi_V^t(x_2)+\phi_V^s(x_2))(\phi_A^t(x_3)-\phi_A^s(x_3)) - r_A x_3(\phi_V^t(x_2)-\phi_V^s(x_2)) \times(\phi_A^t(x_3)+\phi_A^s(x_3))] E_{nfe}(t_c) h_{nfe}^c(x_1,x_2,x_3,b_1,b_2) + [x_2(\phi_V^t(x_2)-\phi_V^s(x_2))\phi_A(x_3) - r_A x_2(\phi_V^t(x_2)-\phi_V^s(x_2))(\phi_A^t(x_3)-\phi_A^s(x_3)) - r_A x_3(\phi_V^t(x_2)+\phi_V^s(x_2))(\phi_A^t(x_3)+\phi_A^s(x_3))] \times E_{nfe}(t_d) h_{nfe}^d(x_1,x_2,x_3,b_1,b_2)\}, \tag{21}$$

$$M_{nfe}^{N,P_1} = -\frac{16\sqrt{6}}{3}\pi C_F m_B^2 \int_0^1 dx_1 dx_2 dx_3 \int_0^\infty b_1 db_1 b_2 db_2 \phi_B(x_1,b_1) r_A x_3 \phi_V^T(x_2)(\phi_A^v(x_3)-\phi_A^a(x_3)) \times \{E_{nfe}(t_c) h_{nfe}^c(x_1,x_2,x_3,b_1,b_2) + E_{nfe}(t_d) h_{nfe}^d(x_1,x_2,x_3,b_1,b_2)\}, \tag{22}$$

$$M_{nfe}^{T,P_1} = 2M_{nfe}^{N,P_1}, \tag{23}$$

$$M_{nfe}^{L,P_2} = -\frac{16\sqrt{6}}{3}\pi C_F m_B^2 \int_0^1 dx_1 dx_2 dx_3 \int_0^\infty b_1 db_1 b_2 db_2 \phi_B(x_1,b_1)\phi_V(x_2)\{[(1-x_2+x_3)\phi_A(x_3) - r_A x_3(\phi_A^t(x_3)+\phi_A^s(x_3))] E_e(t_c) h_{nfe}^c(x_1,x_2,x_3,b_1,b_2) - h_{nfe}^d(x_1,x_2,x_3,b_1,b_2) E_{nfe}(t_d) \times [x_2\phi_A(x_3) + r_A x_3(\phi_A^t(x_3)-\phi_A^s(x_3))]\}, \tag{24}$$

$$M_{nfe}^{N,P_2} = \frac{16\sqrt{6}}{3}\pi C_F m_B^2 \int_0^1 dx_1 dx_2 dx_3 \int_0^\infty b_1 db_1 b_2 db_2 \phi_B(x_1,b_1) r_V \{[(1-x_2)(\phi_V^v(x_2)-\phi_V^a(x_2)) \times\phi_A^T(x_3) - 2r_A(1-x_2+x_3)(\phi_V^v(x_2)\phi_A^v(x_3)-\phi_V^a(x_2)\phi_A^a(x_3))] h_{nfe}^c(x_1,x_2,x_3,b_1,b_2) \times E_{nfe}(t_c) + x_2(\phi_V^v(x_2)-\phi_V^a(x_2))\phi_A^T(x_3) E_{nfe}(t_d) h_{nfe}^d(x_1,x_2,x_3,b_1,b_2)\}, \tag{25}$$

$$M_{nfe}^{T,P_2} = \frac{32\sqrt{6}}{3}\pi C_F m_B^2 \int_0^1 dx_1 dx_2 dx_3 \int_0^\infty b_1 db_1 b_2 db_2 \phi_B(x_1,b_1) r_V \{[(1-x_2)(\phi_V^v(x_2)-\phi_V^a(x_2)) \times\phi_A^T(x_3) - 2r_A(1-x_2+x_3)(\phi_V^v(x_2)\phi_A^a(x_3)-\phi_V^a(x_2)\phi_A^v(x_3))] h_{nfe}^c(x_1,x_2,x_3,b_1,b_2) \times E_{nfe}(t_c) + x_2(\phi_V^v(x_2)-\phi_V^a(x_2))\phi_A^T(x_3) E_{nfe}(t_d) h_{nfe}^d(x_1,x_2,x_3,b_1,b_2)\}. \tag{26}$$

For the nonfactorizable annihilation(nfa) diagrams in Figs. 1(e) and 1(f), we have

$$M_{nfa}^{L} = -\frac{16\sqrt{6}}{3}\pi C_F m_B^2 \int_0^1 dx_1 dx_2 dx_3 \int_0^\infty b_1 db_1 b_2 db_2 \phi_B(x_1,b_1)\{[(1-x_3)\phi_V(x_2)\phi_A(x_3) + r_V r_A((1+x_2-x_3)(\phi_V^s(x_2)\phi_A^s(x_3)-\phi_V^t(x_2)\phi_A^t(x_3)) - (1-x_2-x_3)(\phi_V^s(x_2)\phi_A^t(x_3) - \phi_V^t(x_2)\phi_A^s(x_3)))] E_{nfa}(t_e) h_{nfa}^e(x_1,x_2,x_3,b_1,b_2) - [x_2\phi_V(x_2)\phi_A(x_3) + 2r_V r_A(\phi_V^t(x_2) \times\phi_A^t(x_3) + \phi_V^s(x_2)\phi_A^s(x_3)) - r_V r_A(1+x_2-x_3)(\phi_V^t(x_2)\phi_A^t(x_3) - \phi_V^s(x_2)\phi_A^s(x_3)) + r_V r_A \times(1-x_2-x_3)(\phi_V^s(x_2)\phi_A^t(x_3) - \phi_V^t(x_2)\phi_A^s(x_3))] E_{nfa}(t_f) h_{nfa}^f(x_1,x_2,x_3,b_1,b_2)\}, \tag{27}$$

$$M_{nfa}^{N} = \frac{32\sqrt{6}}{3}\pi C_F m_B^2 \int_0^1 dx_1 dx_2 dx_3 \int_0^\infty b_1 db_1 b_2 db_2 \phi_B(x_1,b_1) r_V r_A \times [\phi_V^v(x_2)\phi_A^v(x_3) + \phi_V^a(x_2)\phi_A^a(x_3)] E_{nfa}(t_f) h_{nfa}^f(x_1,x_2,x_3,b_1,b_2), \tag{28}$$

$$M_{nfa}^{T} = \frac{64\sqrt{6}}{3}\pi C_F m_B^2 \int_0^1 dx_1 dx_2 dx_3 \int_0^\infty b_1 db_1 b_2 db_2 \phi_B(x_1,b_1) r_V r_A \times [\phi_V^v(x_2)\phi_A^a(x_3) + \phi_V^a(x_2)\phi_A^v(x_3)] E_{nfa}(t_f) h_{nfa}^f(x_1,x_2,x_3,b_1,b_2), \tag{29}$$

$$M_{nfa}^{L,P_1}=-\frac{16\sqrt{6}}{3}\pi C_F m_B^2\int_0^1 dx_1dx_2dx_3\int_0^\infty b_1db_1b_2db_2\phi_B(x_1,b_1)\{[r_A(1-x_3)(\phi_A^s(x_3)-\phi_A^t(x_3))\times\phi_V(x_2)+r_Vx_2(\phi_V^t(x_2)+\phi_V^s(x_2))\phi_A(x_3)]E_{nfa}(t_e)h_{nfa}^e(x_1,x_2,x_3,b_1,b_2)-[r_V(2-x_2)\phi_A(x_3)\times(\phi_V^t(x_2)+\phi_V^s(x_2))-r_A(1+x_3)\phi_V(x_2)(\phi_A^s(x_3)-\phi_A^t(x_3))]E_{nfa}(t_f)h_{nfa}^f(x_1,x_2,x_3,b_1,b_2)\},\tag{30}$$

$$M_{nfa}^{N,P_1}=-\frac{16\sqrt{6}}{3}\pi C_F m_B^2\int_0^1 dx_1dx_2dx_3\int_0^\infty b_1db_1b_2db_2\phi_B(x_1,b_1)\{[r_Vx_2(\phi_V^v(x_2)+\phi_V^a(x_2))\phi_A^T(x_3)-r_A(1-x_3)\phi_V^T(x_2)(\phi_A^a(x_3)-\phi_A^v(x_3))]E_{nfa}(t_e)h_{nfa}^e(x_1,x_2,x_3,b_1,b_2)+[r_V(2-x_2)\phi_A^T(x_3)\times(\phi_V^v(x_2)+\phi_V^a(x_2))-r_A(1+x_3)\phi_V^T(x_2)(\phi_A^a(x_3)-\phi_A^v(x_3))]E_{nfa}(t_f)h_{nfa}^f(x_1,x_2,x_3,b_1,b_2)\},\tag{31}$$

$$M_{nfa}^{T,P_1}=2M_{nfa}^{N,P_1},\tag{32}$$

$$M_{nfa}^{L,P_2}=\frac{16\sqrt{6}}{3}\pi C_F m_B^2\int_0^1 dx_1dx_2dx_3\int_0^\infty b_1db_1b_2db_2\phi_B(x_1,b_1)\{[x_2\phi_V(x_2)\phi_A(x_3)+r_Vr_A((1+x_2-x_3)(\phi_V^s(x_2)\phi_A^s(x_3)-\phi_V^t(x_2)\phi_A^t(x_3))+(1-x_2-x_3)(\phi_V^s(x_2)\phi_A^t(x_3)-\phi_V^t(x_2)\phi_A^s(x_3)))]E_{nfa}(t_e)h_{nfa}^e(x_1,x_2,x_3,b_1,b_2)-[(1-x_3)\phi_V(x_2)\phi_A(x_3)+2r_Vr_A(\phi_V^t(x_2)\times\phi_A^t(x_3)+\phi_V^s(x_2)\phi_A^s(x_3))-r_Vr_A(1+x_2-x_3)(\phi_V^t(x_2)\phi_A^t(x_3)-\phi_V^s(x_2)\phi_A^s(x_3))-r_Vr_A\times(1-x_2-x_3)(\phi_V^s(x_2)\phi_A^t(x_3)-\phi_V^t(x_2)\phi_A^s(x_3))]E_{nfa}(t_f)h_{nfa}^f(x_1,x_2,x_3,b_1,b_2)\},\tag{33}$$

$$M_{nfa}^{N,P_2}=-M_{nfa}^{N},\tag{34}$$

$$M_{nfa}^{T,P_2}=M_{nfa}^{T}.\tag{35}$$

For the factorizable annihilation(fa) diagrams in Figs. 1(g) and 1(h), the contributions are

$$F_{fa}^{L}=-8\pi C_F m_B^2\int_0^1 dx_2dx_3\int_0^\infty b_2db_2b_3db_3\{[x_2\phi_V(x_2)\phi_A(x_3)+2r_Vr_A\phi_A^s(x_3)((1+x_2)\phi_V^s(x_2)-(1-x_2)\phi_V^t(x_2))]E_{fa}(t_g)h_{fa}(x_2,1-x_3,b_2,b_3)-[(1-x_3)\phi_V(x_2)\phi_A(x_3)+2r_Vr_A\phi_V^s(x_2)\times(x_3\phi_A^t(x_3)+(2-x_3)\phi_A^s(x_3))]E_{fa}(t_h)h_{fa}(1-x_3,x_2,b_3,b_2)\},\tag{36}$$

$$F_{fa}^{N}=-8\pi C_F m_B^2\int_0^1 dx_2dx_3\int_0^\infty b_2db_2b_3db_3r_Vr_A\{E_{fa}(t_g)[(1+x_2)(\phi_V^v(x_2)\phi_A^v(x_3)+\phi_V^a(x_2)\phi_A^a(x_3))-(1-x_2)(\phi_V^v(x_2)\phi_A^a(x_3)+\phi_V^a(x_2)\phi_A^v(x_3))]h_{fa}(x_2,1-x_3,b_2,b_3)-[(2-x_3)(\phi_V^v(x_2)\phi_A^v(x_3)+\phi_V^a(x_2)\phi_A^a(x_3))+x_3(\phi_V^v(x_2)\phi_A^a(x_3)+\phi_V^a(x_2)\phi_A^v(x_3))]E_{fa}(t_h)h_{fa}(1-x_3,x_2,b_3,b_2)\},\tag{37}$$

$$F_{fa}^{T}=-16\pi C_F m_B^2\int_0^1 dx_2dx_3\int_0^\infty b_2db_2b_3db_3r_Vr_A\{E_{fa}(t_g)[(1+x_2)(\phi_V^v(x_2)\phi_A^a(x_3)+\phi_V^a(x_2)\phi_A^v(x_3))-(1-x_2)(\phi_V^v(x_2)\phi_A^v(x_3)+\phi_V^a(x_2)\phi_A^a(x_3))]h_{fa}(x_2,1-x_3,b_2,b_3)+[x_3(\phi_V^v(x_2)\phi_A^v(x_3)+\phi_V^a(x_2)\phi_A^a(x_3))+(2-x_3)(\phi_V^v(x_2)\phi_A^a(x_3)+\phi_V^a(x_2)\phi_A^v(x_3))]E_{fa}(t_h)h_{fa}(1-x_3,x_2,b_3,b_2)\};\tag{38}$$

$$F_{fa}^{L,P_1}=-F_{fa}^{L};\tag{39}$$

$$F_{fa}^{N,P_1}=-F_{fa}^{N};\tag{40}$$

$$F_{fa}^{T,P_1}=F_{fa}^{T};\tag{41}$$

$$F_{fa}^{L,P_2} = -16\pi C_F m_B^2 \int_0^1 dx_2 dx_3 \int_0^\infty b_2 db_2 b_3 db_3 \{[2r_A\phi_V(x_2)\phi_A^s(x_3) - r_V x_2(\phi_V^t(x_2) - \phi_V^s(x_2)) \times\phi_A(x_3)]h_{fa}(x_2, 1-x_3, b_2, b_3)E_{fa}(t_g) + [2r_V\phi_V^s(x_2)\phi_A(x_3) + r_A(1-x_3)\phi_V(x_2) \times(\phi_A^t(x_3) + \phi_A^s(x_3))]E_{fa}(t_h)h_{fa}(1-x_3, x_2, b_3, b_2)\}, \tag{42}$$

$$F_{fa}^{N,P_2} = -16\pi C_F m_B^2 \int_0^1 dx_2 dx_3 \int_0^\infty b_2 db_2 b_3 db_3 \{r_A\phi_V^T(x_2)(\phi_A^a(x_3) - \phi_A^v(x_3))h_{fa}(x_2, 1-x_3, b_2, b_3) \times E_{fa}(t_g) + r_V(\phi_V^v(x_2) + \phi_V^a(x_2))\phi_A^T(x_3)E_{fa}(t_h)h_{fa}(1-x_3, x_2, b_3, b_2)\}, \tag{43}$$

$$F_{fa}^{T,P_2} = 2F_{fa}^{N,P_2}. \tag{44}$$

When we exchange the positions of vector and axial-vector states in Fig. 1, the amplitudes F', M', F'^{P_1}, M'^{P_1}, F'^{P_2}, and M'^{P_2} arising from new Feynman diagrams can be easily and correspondingly obtained as follows:

$$F'^{L}_{fe} = -8\pi C_F m_B^2 \int_0^1 dx_1 dx_3 \int_0^\infty b_1 db_1 b_3 db_3 \phi_B(x_1, b_1)\{[(1+x_3)\phi_V(x_3) + r_V(1-2x_3) \times(\phi_V^t(x_3) + \phi_V^s(x_3))]E_{fe}(t'_a)h_{fe}(x_1, x_3, b_1, b_3) + 2r_V\phi_V^s(x_3)E_{fe}(t'_b)h_{fe}(x_3, x_1, b_3, b_1)\}, \tag{45}$$

$$F'^{N}_{fe} = -8\pi C_F m_B^2 \int_0^1 dx_1 dx_3 \int_0^\infty b_1 db_1 b_3 db_3 \phi_B(x_1, b_1) r_A\{[\phi_V^T(x_3) + 2r_V\phi_V^v(x_3) + r_V x_3 \times(\phi_V^v(x_3) - \phi_V^a(x_3))]E_{fe}(t'_a)h_{fe}(x_1, x_3, b_1, b_3) + r_V[\phi_V^v(x_3) + \phi_V^a(x_3)]E_{fe}(t'_b)h_{fe}(x_3, x_1, b_3, b_1)\}, \tag{46}$$

$$F'^{T}_{fe} = -16\pi C_F m_B^2 \int_0^1 dx_1 dx_3 \int_0^\infty b_1 db_1 b_3 db_3 \phi_B(x_1, b_1) r_A\{[\phi_V^T(x_3) + 2r_V\phi_V^a(x_3) - r_V x_3 \times(\phi_V^v(x_3) - \phi_V^a(x_3))]E_{fe}(t'_a)h_{fe}(x_1, x_3, b_1, b_3) + r_V[\phi_V^v(x_3) + \phi_V^a(x_3)]E_{fe}(t'_b)h_{fe}(x_3, x_1, b_3, b_1)\}. \tag{47}$$

For the hard functions h_i, the running hard scales t'_i, and the convolution functions $E_i(t')$, refer to Ref. [6].

Since only the axial-vector part of the $(V+A)$ current contributes to the production of axial-vector states, then $\langle V|V-A|B\rangle\langle A|V+A|0\rangle = -\langle V|V-A|B\rangle\langle A|V-A|0\rangle$, which means

$$F'^{P_1}_{fe} = -F'_{fe}. \tag{48}$$

Analogously, because an axial-vector state also cannot be produced via scalar and/or pseudoscalar currents, then the contribution from the $(S \pm P)$ operators is

$$F'^{P_2}_{fe} = 0. \tag{49}$$

The rest Feynman amplitudes can be presented explicitly as follows:

$$M'^{L}_{nfe} = -\frac{16\sqrt{6}}{3}\pi C_F m_B^2 \int_0^1 dx_1 dx_2 dx_3 \int_0^\infty b_1 db_1 b_2 db_2 \phi_B(x_1, b_1)\phi_A(x_2)\{[(1-x_2)\phi_V(x_3) + r_V x_3(\phi_V^t(x_3) - \phi_V^s(x_3))]E_{nfe}(t'_c)h^c_{nfe}(x_1, x_2, x_3, b_1, b_2) - [(x_2+x_3)\phi_V(x_3) - r_V x_3(\phi_V^t(x_3) + \phi_V^s(x_3))]E_{nfe}(t'_d)h^d_{nfe}(x_1, x_2, x_3, b_1, b_2)\}, \tag{50}$$

$$M'^{N}_{nfe} = -\frac{16\sqrt{6}}{3}\pi C_F m_B^2 \int_0^1 dx_1 dx_2 dx_3 \int_0^\infty b_1 db_1 b_2 db_2 \phi_B(x_1, b_1) r_A\{(1-x_2)(\phi_A^v(x_2) + \phi_A^a(x_2)) \times\phi_V^T(x_3)h^c_{nfe}(x_1, x_2, x_3, b_1, b_2)E_{nfe}(t'_c) + [x_2(\phi_A^v(x_2) + \phi_A^a(x_2))\phi_V^T(x_3) - 2r_V(x_2+x_3)(\phi_A^v(x_2)\phi_V^v(x_3) + \phi_A^a(x_2)\phi_V^a(x_3))]E_{nfe}(t'_d)h^d_{nfe}(x_1, x_2, x_3, b_1, b_2)\}, \tag{51}$$

$$M'^{T}_{nfe} = -\frac{32\sqrt{6}}{3}\pi C_F m_B^2 \int_0^1 dx_1 dx_2 dx_3 \int_0^\infty b_1 db_1 b_2 db_2 \phi_B(x_1,b_1) r_A \{(1-x_2)(\phi_A^v(x_2)+\phi_A^a(x_2)) \times \phi_V^T(x_3) h^c_{nfe}(x_1,x_2,x_3,b_1,b_2) E_{nfe}(t'_c) + [x_2(\phi_A^v(x_2)+\phi_A^a(x_2))\phi_V^T(x_3) - 2r_V(x_2+x_3)(\phi_A^v(x_2)\phi_V^a(x_3)+\phi_A^a(x_2)\phi_V^v(x_3))] E_{nfe}(t'_d) h^d_{nfe}(x_1,x_2,x_3,b_1,b_2)\}, \tag{52}$$

$$M'^{L,P_1}_{nfe} = \frac{16\sqrt{6}}{3}\pi C_F m_B^2 \int_0^1 dx_1 dx_2 dx_3 \int_0^\infty b_1 db_1 b_2 db_2 \phi_B(x_1,b_1) r_A \{[(1-x_2)(\phi_A^t(x_2)+\phi_A^s(x_2)) \times \phi_V(x_3) - r_V(1-x_2)(\phi_A^t(x_2)+\phi_A^s(x_2))(\phi_V^t(x_3)-\phi_V^s(x_3)) - r_V x_3(\phi_A^t(x_2)-\phi_A^s(x_2)) \times (\phi_V^t(x_3)+\phi_V^s(x_3))] E_{nfe}(t'_c) h^c_{nfe}(x_1,x_2,x_3,b_1,b_2) + [x_2(\phi_A^t(x_2)-\phi_A^s(x_2))\phi_V(x_3) - r_V x_2(\phi_A^t(x_2)-\phi_A^s(x_2))(\phi_V^t(x_3)-\phi_V^s(x_3)) - r_V x_3(\phi_A^t(x_2)+\phi_A^s(x_2))(\phi_V^t(x_3)+\phi_V^s(x_3))] \times E_{nfe}(t'_d) h^d_{nfe}(x_1,x_2,x_3,b_1,b_2)\}, \tag{53}$$

$$M'^{N,P_1}_{nfe} = \frac{16\sqrt{6}}{3}\pi C_F m_B^2 \int_0^1 dx_1 dx_2 dx_3 \int_0^\infty b_1 db_1 b_2 db_2 \phi_B(x_1,b_1) r_V x_3 \phi_A^T(x_2)(\phi_V^v(x_3)-\phi_V^a(x_3)) \times \{E_{nfe}(t'_c) h^c_{nfe}(x_1,x_2,x_3,b_1,b_2) + E_{nfe}(t'_d) h^d_{nfe}(x_1,x_2,x_3,b_1,b_2)\}, \tag{54}$$

$$M'^{T,P_1}_{nfe} = 2M'^{N,P_1}_{nfe}, \tag{55}$$

$$M'^{L,P_2}_{nfe} = \frac{16\sqrt{6}}{3}\pi C_F m_B^2 \int_0^1 dx_1 dx_2 dx_3 \int_0^\infty b_1 db_1 b_2 db_2 \phi_B(x_1,b_1)\phi_A(x_2)\{[(1-x_2+x_3)\phi_V(x_3) - r_V x_3(\phi_V^t(x_3)+\phi_V^s(x_3))] E_e(t'_c) h^c_{nfe}(x_1,x_2,x_3,b_1,b_2) - h^d_{nfe}(x_1,x_2,x_3,b_1,b_2) E_{nfe}(t'_d) \times [x_2\phi_V(x_3) + r_V x_3(\phi_V^t(x_3)-\phi_V^s(x_3))]\}, \tag{56}$$

$$M'^{N,P_2}_{nfe} = -\frac{16\sqrt{6}}{3}\pi C_F m_B^2 \int_0^1 dx_1 dx_2 dx_3 \int_0^\infty b_1 db_1 b_2 db_2 \phi_B(x_1,b_1) r_A \{[(1-x_2)(\phi_A^v(x_2)-\phi_A^a(x_2)) \times \phi_V^T(x_3) - 2r_V(1-x_2+x_3)(\phi_A^v(x_2)\phi_V^v(x_3)-\phi_A^a(x_2)\phi_V^a(x_3))] h^c_{nfe}(x_1,x_2,x_3,b_1,b_2) \times E_{nfe}(t'_c) + x_2(\phi_A^v(x_2)-\phi_A^a(x_2))\phi_V^T(x_3) E_{nfe}(t'_d) h^d_{nfe}(x_1,x_2,x_3,b_1,b_2)\}, \tag{57}$$

$$M'^{T,P_2}_{nfe} = -\frac{32\sqrt{6}}{3}\pi C_F m_B^2 \int_0^1 dx_1 dx_2 dx_3 \int_0^\infty b_1 db_1 b_2 db_2 \phi_B(x_1,b_1) r_A \{[(1-x_2)(\phi_A^v(x_2)-\phi_A^a(x_2)) \times \phi_V^T(x_3) - 2r_V(1-x_2+x_3)(\phi_A^v(x_2)\phi_V^a(x_3)-\phi_A^a(x_2)\phi_V^v(x_3))] h^c_{nfe}(x_1,x_2,x_3,b_1,b_2) \times E_{nfe}(t'_c) + x_2(\phi_A^v(x_2)-\phi_A^a(x_2))\phi_V^T(x_3) E_{nfe}(t'_d) h^d_{nfe}(x_1,x_2,x_3,b_1,b_2)\}, \tag{58}$$

$$M'^{L}_{nfa} = -\frac{16\sqrt{6}}{3}\pi C_F m_B^2 \int_0^1 dx_1 dx_2 dx_3 \int_0^\infty b_1 db_1 b_2 db_2 \phi_B(x_1,b_1)\{[(1-x_3)\phi_A(x_2)\phi_V(x_3) - r_A r_V((1+x_2-x_3)(\phi_A^s(x_2)\phi_V^s(x_3)-\phi_A^t(x_2)\phi_V^t(x_3)) - (1-x_2-x_3)(\phi_A^s(x_2)\phi_V^t(x_3) - \phi_A^t(x_2)\phi_V^s(x_3)))] E_{nfa}(t'_e) h^e_{nfa}(x_1,x_2,x_3,b_1,b_2) - [x_2\phi_A(x_2)\phi_V(x_3) - 2r_A r_V(\phi_A^t(x_2) \times \phi_V^t(x_3) + \phi_A^s(x_2)\phi_V^s(x_3)) + r_A r_V(1+x_2-x_3)(\phi_A^t(x_2)\phi_V^t(x_3) - \phi_A^s(x_2)\phi_V^s(x_3)) - r_A r_V \times (1-x_2-x_3)(\phi_A^s(x_2)\phi_V^t(x_3) - \phi_A^t(x_2)\phi_V^s(x_3))] E_{nfa}(t'_f) h^f_{nfa}(x_1,x_2,x_3,b_1,b_2)\}, \tag{59}$$

$$M'^{N}_{nfa} = \frac{32\sqrt{6}}{3}\pi C_F m_B^2 \int_0^1 dx_1 dx_2 dx_3 \int_0^\infty b_1 db_1 b_2 db_2 \phi_B(x_1,b_1) r_A r_V \times [\phi_A^v(x_2)\phi_V^v(x_3) + \phi_A^a(x_2)\phi_V^a(x_3)] E_{nfa}(t'_f) h^f_{nfa}(x_1,x_2,x_3,b_1,b_2), \tag{60}$$

$$M'^{T}_{nfa} = \frac{64\sqrt{6}}{3}\pi C_F m_B^2 \int_0^1 dx_1 dx_2 dx_3 \int_0^\infty b_1 db_1 b_2 db_2 \phi_B(x_1,b_1) r_A r_V \times [\phi_A^v(x_2)\phi_V^a(x_3) + \phi_A^a(x_2)\phi_V^v(x_3)] E_{nfa}(t'_f) h^f_{nfa}(x_1,x_2,x_3,b_1,b_2), \tag{61}$$

$$M'^{L,P_1}_{nfa} = \frac{16\sqrt{6}}{3}\pi C_F m_B^2 \int_0^1 dx_1 dx_2 dx_3 \int_0^\infty b_1 db_1 b_2 db_2 \phi_B(x_1,b_1)\{[r_V(1-x_3)(\phi_V^s(x_3)-\phi_V^t(x_3)) \times \phi_A(x_2) + r_A x_2(\phi_A^t(x_2)+\phi_A^s(x_2))\phi_V(x_3)] E_{nfa}(t'_e) h^e_{nfa}(x_1,x_2,x_3,b_1,b_2) + [r_A(2-x_2)\phi_V(x_3) \times(\phi_A^t(x_2)+\phi_A^s(x_2)) + r_V(1+x_3)\phi_A(x_2)(\phi_V^s(x_3)-\phi_V^t(x_3))] E_{nfa}(t'_f) h^f_{nfa}(x_1,x_2,x_3,b_1,b_2)\}, \tag{62}$$

$$M'^{N,P_1}_{nfa} = -\frac{16\sqrt{6}}{3}\pi C_F m_B^2 \int_0^1 dx_1 dx_2 dx_3 \int_0^\infty b_1 db_1 b_2 db_2 \phi_B(x_1,b_1)\{[r_A x_2(\phi_A^v(x_2)+\phi_A^a(x_2))\phi_V^T(x_3) + r_A(1-x_3)\phi_A^T(x_2)(\phi_V^a(x_3)-\phi_V^v(x_3))] E_{nfa}(t'_e) h^e_{nfa}(x_1,x_2,x_3,b_1,b_2) + [r_A(2-x_2)\phi_V^T(x_3) \times(\phi_A^v(x_2)+\phi_A^a(x_2)) + r_V(1+x_3)\phi_A^T(x_2)(\phi_V^a(x_3)-\phi_V^v(x_3))] E_{nfa}(t'_f) h^f_{nfa}(x_1,x_2,x_3,b_1,b_2)\}, \tag{63}$$

$$M'^{T,P_1}_{nfa} = 2M'^{N,P_1}_{nfa}, \tag{64}$$

$$M'^{L,P_2}_{nfa} = \frac{16\sqrt{6}}{3}\pi C_F m_B^2 \int_0^1 dx_1 dx_2 dx_3 \int_0^\infty b_1 db_1 b_2 db_2 \phi_B(x_1,b_1)\{[x_2\phi_A(x_2)\phi_V(x_3) - r_A r_V((1+x_2-x_3)(\phi_A^s(x_2)\phi_V^s(x_3)-\phi_A^t(x_2)\phi_V^t(x_3)) + (1-x_2-x_3)(\phi_A^s(x_2)\phi_V^t(x_3) - \phi_A^t(x_2)\phi_V^s(x_3)))] E_{nfa}(t'_e) h^e_{nfa}(x_1,x_2,x_3,b_1,b_2) - [(1-x_3)\phi_A(x_2)\phi_V(x_3) - 2r_A r_V(\phi_A^t(x_2) \times\phi_V^t(x_3) + \phi_A^s(x_2)\phi_V^s(x_3)) + r_A r_V(1+x_2-x_3)(\phi_A^t(x_2)\phi_V^t(x_3) - \phi_A^s(x_2)\phi_V^s(x_3)) + r_A r_V \times(1-x_2-x_3)(\phi_A^s(x_2)\phi_V^t(x_3) - \phi_A^t(x_2)\phi_V^s(x_3))] E_{nfa}(t'_f) h^f_{nfa}(x_1,x_2,x_3,b_1,b_2)\}, \tag{65}$$

$$M'^{N,P_2}_{nfa} = -M'^{N}_{nfa}, \tag{66}$$

$$M'^{T,P_2}_{nfa} = M'^{T}_{nfa}, \tag{67}$$

$$F'^{L}_{fa} = -8\pi C_F m_B^2 \int_0^1 dx_2 dx_3 \int_0^\infty b_2 db_2 b_3 db_3 \{[x_2\phi_A(x_2)\phi_V(x_3) - 2r_A r_V \phi_V^s(x_3)((1+x_2)\phi_A^s(x_2) - (1-x_2)\phi_A^t(x_2))] E_{fa}(t'_g) h_{fa}(x_2,1-x_3,b_2,b_3) - [(1-x_3)\phi_A(x_2)\phi_V(x_3) - 2r_A r_V \phi_A^s(x_2) \times(x_3\phi_V^t(x_3) + (2-x_3)\phi_V^s(x_3))] E_{fa}(t'_h) h_{fa}(1-x_3,x_2,b_3,b_2)\}, \tag{68}$$

$$F'^{N}_{fa} = -8\pi C_F m_B^2 \int_0^1 dx_2 dx_3 \int_0^\infty b_2 db_2 b_3 db_3 r_A r_V \{E_{fa}(t'_g)[(1+x_2)(\phi_A^v(x_2)\phi_V^v(x_3) + \phi_A^a(x_2)\phi_V^a(x_3)) - (1-x_2)(\phi_A^v(x_2)\phi_V^a(x_3) + \phi_A^a(x_2)\phi_V^v(x_3))] h_{fa}(x_2,1-x_3,b_2,b_3) - [(2-x_3)(\phi_A^v(x_2)\phi_V^v(x_3) + \phi_A^a(x_2)\phi_V^a(x_3)) + x_3(\phi_A^v(x_2)\phi_V^a(x_3) + \phi_A^a(x_2)\phi_V^v(x_3))] E_{fa}(t'_h) h_{fa}(1-x_3,x_2,b_3,b_2)\}, \tag{69}$$

$$F'^{T}_{fa} = -16\pi C_F m_B^2 \int_0^1 dx_2 dx_3 \int_0^\infty b_2 db_2 b_3 db_3 r_A r_V \{E_{fa}(t'_g)[(1+x_2)(\phi_A^v(x_2)\phi_V^a(x_3) + \phi_A^a(x_2)\phi_V^v(x_3)) - (1-x_2)(\phi_A^v(x_2)\phi_V^v(x_3) + \phi_A^a(x_2)\phi_V^a(x_3))] h_{fa}(x_2,1-x_3,b_2,b_3) - [x_3(\phi_A^v(x_2)\phi_V^v(x_3) + \phi_A^a(x_2)\phi_V^a(x_3)) + (2-x_3)(\phi_A^v(x_2)\phi_V^a(x_3) + \phi_A^a(x_2)\phi_V^v(x_3))] E_{fa}(t'_h) h_{fa}(1-x_3,x_2,b_3,b_2)\}; \tag{70}$$

$$F'^{L,P_1}_{fa} = -F'^{L}_{fa}; \tag{71}$$

$$F'^{N,P_1}_{fa} = -F'^{N}_{fa}; \tag{72}$$

$$F'^{T,P_1}_{fa} = F'^{T}_{fa}; \tag{73}$$

$$F'^{L,P_2}_{fa} = -16\pi C_F m_B^2 \int_0^1 dx_2 dx_3 \int_0^\infty b_2 db_2 b_3 db_3 \{[2r_V\phi_A(x_2)\phi_V^s(x_3) + r_A x_2(\phi_A^t(x_2) - \phi_A^s(x_2)) \times\phi_V(x_3)]h_{fa}(x_2, 1-x_3, b_2, b_3)E_{fa}(t'_g) - [2r_A\phi_A^s(x_2)\phi_V(x_3) - r_V(1-x_3)\phi_A(x_2) \times(\phi_V^t(x_3) + \phi_V^s(x_3))]E_{fa}(t'_h)h_{fa}(1-x_3, x_2, b_3, b_2)\}, \tag{74}$$

$$F'^{N,P_2}_{fa} = 16\pi C_F m_B^2 \int_0^1 dx_2 dx_3 \int_0^\infty b_2 db_2 b_3 db_3 \{r_V\phi_A^T(x_2)(\phi_V^a(x_3) - \phi_V^v(x_3))h_{fa}(x_2, 1-x_3, b_2, b_3) \times E_{fa}(t'_g) - r_A(\phi_A^v(x_2) + \phi_A^a(x_2))\phi_V^T(x_3)E_{fa}(t'_h)h_{fa}(1-x_3, x_2, b_3, b_2)\}, \tag{75}$$

$$F'^{T,P_2}_{fa} = 2F'^{N,P_2}_{fa}. \tag{76}$$

Thus, by combining various contributions from different diagrams as presented in Eqs. (13)–(76) and the mixing pattern in Eq. (1), the total decay amplitudes for 10 nonleptonic decays of $B \to f_1(1285)V$ can be written as follows (the superscript h in the following formulas describes the helicity amplitudes with longitudinal, normal, and transverse polarizations, respectively):

(1) $B^+ \to f_1(1285)(\rho^+, K^{*+})$ decays

$$\begin{aligned}
A^h(B^+ \to f_1(1285)\rho^+) = {} & \{[a_1](f_\rho F^h_{fe} + f_B F^h_{fa} + f_B F'^h_{fa}) + [a_2]f_{f_{1q}}F'^h_{fe} + [C_1](M^h_{nfe} + M^h_{nfa} + M'^h_{nfa}) \\
& + [C_2]M'^h_{nfe}\}\lambda_u^d\zeta_{f_{1q}} - \lambda_t^d\zeta_{f_{1q}}\Big\{[a_4 + a_{10}](f_\rho F^h_{fe} + f_B F^h_{fa} + f_B F'^h_{fa}) + [a_6 + a_8] \\
& \times (f_B F^{h,P_2}_{fa} + f_B F'^{h,P_2}_{fa}) + [C_3 + C_9](M^h_{nfe} + M^h_{nfa} + M'^h_{nfa}) + [C_5 + C_7] \\
& \times (M^{h,P_1}_{nfe} + M^{h,P_1}_{nfa} + M'^{h,P_1}_{nfa}) + \left[2a_3 + a_4 - 2a_5 - \frac{1}{2}(a_7 - a_9 + a_{10})\right]f_{f_{1q}}F'^h_{fe} \\
& + \left[C_3 + 2C_4 - \frac{1}{2}(C_9 - C_{10})\right]M'^h_{nfe} + \left[C_5 - \frac{1}{2}C_7\right]M'^{h,P_1}_{nfe} + \left[2C_6 + \frac{1}{2}C_8\right]M'^{h,P_2}_{nfe}\Big\} \\
& - \lambda_t^d\zeta_{f_{1s}}\Big\{\left[a_3 - a_5 + \frac{1}{2}(a_7 - a_9)\right]f_{f_{1s}}F'^h_{fe} + \left[C_4 - \frac{1}{2}C_{10}\right]M'^h_{nfe} \\
& + \left[C_6 - \frac{1}{2}C_8\right]M'^{h,P_2}_{nfe}\Big\};
\end{aligned} \tag{77}$$

$$\begin{aligned}
A^h(B^+ \to f_1(1285)K^{*+}) = {} & \lambda_u^s\{[a_1]((f_{K^*}F^h_{fe} + f_B F^h_{fa})\zeta_{f_{1q}} + f_B F'^h_{fa}\zeta_{f_{1s}}) + [a_2]f_{f_{1q}}F'^h_{fe}\zeta_{f_{1q}} + [C_1] \\
& \times (M'^h_{nfa}\zeta_{f_{1s}} + (M^h_{nfe} + M^h_{nfa})\zeta_{f_{1q}}) + [C_2]M'^h_{nfe}\zeta_{f_{1q}}\} - \lambda_t^s\Big\{[a_4 + a_{10}] \\
& \times ((f_{K^*}F^h_{fe} + f_B F^h_{fa})\zeta_{f_{1q}} + f_B F'^h_{fa}\zeta_{f_{1s}}) + (f_B F^{h,P_2}_{fa}\zeta_{f_{1q}} + f_B F'^{h,P_2}_{fa}\zeta_{f_{1s}}) \\
& \times [a_6 + a_8] + [C_3 + C_9](M'^h_{nfa}\zeta_{f_{1s}} + (M^h_{nfe} + M^h_{nfa})\zeta_{f_{1q}}) + [C_5 + C_7] \\
& \times ((M^{h,P_1}_{nfe} + M^{h,P_1}_{nfa})\zeta_{f_{1q}} + M'^{h,P_1}_{nfa}\zeta_{f_{1s}}) + \Bigg(\left[2a_3 - 2a_5 - \frac{1}{2}(a_7 - a_9)\right]f_{f_{1q}}F'^h_{fe} \\
& + \left[2C_4 + \frac{1}{2}C_{10}\right]M'^h_{nfe} + \left[2C_6 + \frac{1}{2}C_8\right]M'^{h,P_2}_{nfe}\Bigg)\zeta_{f_{1q}} + \Bigg(\left[C_3 + C_4 - \frac{1}{2}(C_9 + C_{10})\right] \\
& \times M'^h_{nfe} + \left[a_3 + a_4 - a_5 + \frac{1}{2}(a_7 - a_9 - a_{10})\right]f_{f_{1s}}F'^h_{fe} + \left[C_5 - \frac{1}{2}C_7\right]M'^{h,P_1}_{nfe} \\
& + \left[C_6 - \frac{1}{2}C_8\right]M'^{h,P_2}_{nfe}\Bigg)\zeta_{f_{1s}}\Big\};
\end{aligned} \tag{78}$$

(2) $B^0 \to f_1(1285)(\rho^0, K^{*0}, \omega, \phi)$ decays

$$\begin{aligned}\sqrt{2}A^h(B^0 \to f_1(1285)\rho^0) = {} & \{a_2(f_\rho F^h_{fe} + f_B F^h_{fa} + f_B F'^h_{fa} - f_{f_{1q}} F'^h_{fe}) + C_2(M^h_{nfe} + M^h_{nfa} + M'^h_{nfa} - M'^h_{nfe})\} \\ & \times \lambda_u^d \zeta_{f_{1q}} - \lambda_t^d \zeta_{f_{1q}} \Big\{ \Big[-a_4 - \frac{1}{2}(3a_7 - 3a_9 - a_{10})\Big] f_\rho F^h_{fe} + \Big[-a_4 + \frac{1}{2}(3a_7 + 3a_9 + a_{10})\Big] \\ & \times (f_B F^h_{fa} + f_B F'^h_{fa}) - \Big[2a_3 + a_4 - 2a_5 - \frac{1}{2}(a_7 - a_9 + a_{10})\Big] f_{f_{1q}} F'^h_{fe} - \Big[a_6 - \frac{1}{2}a_8\Big] \\ & \times (f_B F^{h,P_2}_{fa} + f_B F'^{h,P_2}_{fa}) + \Big[-C_3 + \frac{1}{2}(C_9 + 3C_{10})\Big](M^h_{nfe} + M^h_{nfa} + M'^h_{nfa}) + \Big[\frac{3}{2}C_8\Big] \\ & \times (M^{h,P_2}_{nfe} + M^{h,P_2}_{nfa} + M'^{h,P_2}_{nfa}) - \Big[C_5 - \frac{1}{2}C_7\Big](M^{h,P_1}_{nfe} + M^{h,P_1}_{nfa} + M'^{h,P_1}_{nfa} + M'^{h,P_1}_{nfe}) \\ & - \Big[C_3 + 2C_4 - \frac{1}{2}(C_9 - C_{10})\Big] M'^h_{nfe} - \Big[2C_6 + \frac{1}{2}C_8\Big] M'^{h,P_2}_{nfe}\Big\} - \lambda_t^d \Big\{ - \Big[a_3 - a_5 + \frac{1}{2} \\ & \times (a_7 - a_9)\Big] f_{f_{1s}} F'^h_{fe} - \Big[C_4 - \frac{1}{2}C_{10}\Big] M'^h_{nfe} - \Big[C_6 - \frac{1}{2}C_8\Big] M'^{h,P_2}_{nfe}\Big\} \zeta_{f_{1s}}; \end{aligned} \tag{79}$$

$$\begin{aligned}A^h(B^0 \to f_1(1285)K^{*0}) = {} & \lambda_u^s \{[a_2] f_{f_{1q}} F'^h_{fe} + [C_2] M'^h_{nfe}\} \zeta_{f_{1q}} - \lambda_t^s \Big\{ \Big[a_4 - \frac{1}{2}a_{10}\Big]((f_{K^*} F^h_{fe} + f_B F^h_{fa}) \zeta_{f_{1q}} + \zeta_{f_{1s}} f_B F'^h_{fa}) \\ & + \Big[a_6 - \frac{1}{2}a_8\Big](f_B F^{h,P_2}_{fa} \zeta_{f_{1q}} + f_B F'^{h,P_2}_{fa} \zeta_{f_{1s}}) + \Big[C_3 - \frac{1}{2}C_9\Big]((M^h_{nfe} + M^h_{nfa}) \zeta_{f_{1q}} + M'^h_{nfa} \zeta_{f_{1s}}) \\ & + \Big[C_5 - \frac{1}{2}C_7\Big]((M^{h,P_1}_{nfe} + M^{h,P_1}_{nfa}) \zeta_{f_{1q}} + M'^{h,P_1}_{nfa} \zeta_{f_{1s}}) + \Big(\Big[2a_3 - 2a_5 - \frac{1}{2}(a_7 - a_9)\Big] f_{f_{1q}} F'^h_{fe} \\ & + \Big[2C_4 + \frac{1}{2}C_{10}\Big] M'^h_{nfe} + \Big[2C_6 + \frac{1}{2}C_8\Big] M'^{h,P_2}_{nfe}\Big) \zeta_{f_{1q}} \\ & + \Big(\Big[a_3 + a_4 - a_5 + \frac{1}{2}(a_7 - a_9 - a_{10})\Big] f_{f_{1s}} F'^h_{fe} + \Big[C_3 + C_4 - \frac{1}{2}(C_9 + C_{10})\Big] M'^h_{nfe} \\ & + \Big[C_5 - \frac{1}{2}C_7\Big] M'^{h,P_1}_{nfe} + \Big[C_6 - \frac{1}{2}C_8\Big] M'^{h,P_2}_{nfe}\Big) \zeta_{f_{1s}}\Big\}; \end{aligned} \tag{80}$$

$$\begin{aligned}\sqrt{2}A^h(B^0 \to f_1(1285)\omega) = {} & \lambda_u^d \{a_2(f_\omega F^h_{fe} + f_B F^h_{fa} + f_B F'^h_{fa} + f_{f_{1q}} F'^h_{fe}) + C_2(M^h_{nfe} + M^h_{nfa} + M'^h_{nfa} + M'^h_{nfe})\} \cdot \zeta_{f_{1q}} \\ & - \lambda_t^d \Big\{ \Big[2a_3 + a_4 - 2a_5 - \frac{1}{2}(a_7 - a_9 + a_{10})\Big](f_\omega F^h_{fe} + f_{f_{1q}} F'^h_{fe}) \\ & + \Big[2a_3 + a_4 + 2a_5 + \frac{1}{2}(a_7 + a_9 - a_{10})\Big](f_B F^h_{fa} + f_B F'^h_{fa}) + (f_B F^{h,P_2}_{fa} + f_B F'^{h,P_2}_{fa}) \\ & \times \Big[a_6 - \frac{1}{2}a_8\Big] + \Big[C_3 + 2C_4 - \frac{1}{2}(C_9 - C_{10})\Big](M^h_{nfe} + M'^h_{nfe} + M^h_{nfa} + M'^h_{nfa}) \\ & + \Big[C_5 - \frac{1}{2}C_7\Big](M^{h,P_1}_{nfe} + M^{h,P_1}_{nfa} + M'^{h,P_1}_{nfa} + M'^{h,P_1}_{nfe}) \\ & + \Big[2C_6 + \frac{1}{2}C_8\Big](M^{h,P_2}_{nfe} + M'^{h,P_2}_{nfe} + M^{h,P_2}_{nfa} + M'^{h,P_2}_{nfa})\Big\} \cdot \zeta_{f_{1q}} \\ & - \lambda_t^d \Big\{ \Big[a_3 - a_5 + \frac{1}{2}(a_7 - a_9)\Big] f_{f_{1s}} F'^h_{fe} + \Big[C_4 - \frac{1}{2}C_{10}\Big] M'^h_{nfe} \\ & + \Big[C_6 - \frac{1}{2}C_8\Big] M'^{h,P_2}_{nfe}\Big\} \cdot \zeta_{f_{1s}}; \end{aligned} \tag{81}$$

$$A^h(B^0 \to f_1(1285)\phi) = -\lambda_t^d\Big\{\Big[a_3 - a_5 + \frac{1}{2}(a_7 - a_9)\Big]f_\phi F^h_{fe}\zeta_{f_{1q}} + \Big[a_3 + a_5 - \frac{1}{2}(a_7 + a_9)\Big](f_B F^h_{fa} + f_B F'^h_{fa})\zeta_{f_{1s}} + \Big[C_4 - \frac{1}{2}C_{10}\Big](M^h_{nfe}\zeta_{f_{1q}} + (M^h_{nfa} + M'^h_{nfa})\zeta_{f_{1s}}) + \Big[C_6 - \frac{1}{2}C_8\Big]((M^{h,P_2}_{nfa} + M'^{h,P_2}_{nfa})\zeta_{f_{1s}} + M^{h,P_2}_{nfe}\zeta_{f_{1q}})\Big\}; \quad (82)$$

(3) $B_s^0 \to f_1(1285)(\rho^0, \overline{K}^{*0}, \omega, \phi)$ decays

$$\sqrt{2}A^h(B_s^0 \to f_1(1285)\rho^0) = \lambda_u^s\{a_2(f_\rho F^h_{fe}\zeta_{f_{1s}} + (f_B F^h_{fa} + f_B F'^h_{fa})\zeta_{f_{1q}}) + C_2(M^h_{nfe}\zeta_{f_{1s}} + (M^h_{nfa} + M'^h_{nfa})\cdot\zeta_{f_{1q}})\} - \lambda_t^s\cdot\frac{3}{2}\cdot\{[a_9 - a_7]f_\rho F^h_{fe}\zeta_{f_{1s}} + [a_7 + a_9](f_B F^h_{fa} + f_B F'^h_{fa})\zeta_{f_{1q}} + C_{10} \times (M^h_{nfe}\zeta_{f_{1s}} + (M^h_{nfa} + M'^h_{nfa})\zeta_{f_{1q}}) + C_8(M^{h,P_2}_{nfe}\zeta_{f_{1s}} + (M^{h,P_2}_{nfa} + M'^{h,P_2}_{nfa})\zeta_{f_{1q}})\}; \quad (83)$$

$$A^h(B_s^0 \to f_1(1285)\overline{K}^{*0}) = \lambda_u^d\{a_2 f_{f_{1q}}F'^h_{fe} + C_2 M'^h_{nfe}\}\cdot\zeta_{f_{1q}} - \lambda_t^d\Big\{\Big[a_4 - \frac{1}{2}a_{10}\Big]((f_{K^*}F^h_{fe} + f_B F^h_{fa})\cdot\zeta_{f_{1s}} + f_B F'^h_{fa}\cdot\zeta_{f_{1q}}) + \Big[a_6 - \frac{1}{2}a_8\Big](f_B F^{h,P_2}_{fa}\zeta_{f_{1s}} + f_B F'^{h,P_2}_{fa}\zeta_{f_{1q}}) + \Big[C_3 - \frac{1}{2}C_9\Big](M'^h_{nfa}\zeta_{f_{1q}} + (M^h_{nfe} + M^h_{nfa})\zeta_{f_{1s}}) + \Big[C_5 - \frac{1}{2}C_7\Big]((M^{h,P_1}_{nfe} + M^{h,P_1}_{nfa})\zeta_{f_{1s}} + \zeta_{f_{1q}}M'^{h,P_1}_{nfa}) + \Big(\Big[2a_3 + a_4 - 2a_5 - \frac{1}{2}(a_7 - a_9 + a_{10})\Big]f_{f_{1q}}F'^h_{fe} + \Big[C_3 + 2C_4 - \frac{1}{2}(C_9 - C_{10})\Big]M'^h_{nfe} + \Big[C_5 - \frac{1}{2}C_7\Big]M'^{h,P_1}_{nfe} + \Big[2C_6 + \frac{1}{2}C_8\Big]M'^{h,P_2}_{nfe}\Big)\zeta_{f_{1q}} + \Big(\Big[a_3 - a_5 + \frac{1}{2}(a_7 - a_9)\Big]f_{f_{1s}}F'^h_{fe} + \Big[C_4 - \frac{1}{2}C_{10}\Big]M'^h_{nfe} + \Big[C_6 - \frac{1}{2}C_8\Big]M'^{h,P_2}_{nfe}\Big)\zeta_{f_{1s}}\Big\}; \quad (84)$$

$$\sqrt{2}A^h(B_s^0 \to f_1(1285)\omega) = \{\zeta_{f_{1s}}\cdot(a_2 f_\omega F^h_{fe} + C_2 M^h_{nfe}) + \zeta_{f_{1q}}\cdot(a_2(f_B F^h_{fa} + f_B F'^h_{fa}) + C_2(M^h_{nfa} + M'^h_{nfa}))\} \times \lambda_u^s - \lambda_t^s\Big\{\zeta_{f_{1q}}\cdot\Big(\Big(2C_4 + \frac{1}{2}C_{10}\Big)(M^h_{nfa} + M'^h_{nfa}) + \Big(2C_6 + \frac{1}{2}C_8\Big)(M^{h,P_2}_{nfa} + M'^{h,P_2}_{nfa}) + \Big(2a_3 + 2a_5 + \frac{1}{2}(a_7 + a_9)\Big)(f_B F^h_{fa} + f_B F'^h_{fa})\Big) + \zeta_{f_{1s}}\cdot\Big(\Big(2a_3 - 2a_5 - \frac{1}{2}(a_7 - a_9)\Big)f_\omega F^h_{fe} + \Big(2C_4 + \frac{1}{2}C_{10}\Big)M^h_{nfe} + \Big(2C_6 + \frac{1}{2}C_8\Big)M^{h,P_2}_{nfe}\Big)\Big\}; \quad (85)$$

$$A^h(B_s^0 \to f_1(1285)\phi) = \lambda_u^s\{\zeta_{f_{1q}} \cdot (a_2 f_{f_{1q}} F'^h_{fe} + C_2 M'^h_{nfe})\} - \lambda_t^s\Big\{\zeta_{f_{1s}} \cdot \Big(\Big(a_3 + a_4 - a_5 + \frac{1}{2}(a_7 - a_9 - a_{10})\Big) \times (f_\phi F^h_{fe} + f_{f_{1s}} F'^h_{fe}) + \Big(a_6 - \frac{1}{2}a_8\Big)(f_B F^{h,P_2}_{fa} + f_B F'^{h,P_2}_{fa}) + \Big(C_3 + C_4 - \frac{1}{2}(C_9 + C_{10})\Big) \times (M^h_{nfe} + M'^h_{nfe} + M^h_{nfa} + M'^h_{nfa}) + \Big(C_5 - \frac{1}{2}C_7\Big)(M^{h,P_1}_{nfe} + M'^{h,P_1}_{nfe} + M^{h,P_1}_{nfa} + M'^{h,P_1}_{nfa}) + \Big(C_6 - \frac{1}{2}C_8\Big)(M^{h,P_2}_{nfe} + M'^{h,P_2}_{nfe} + M^{h,P_2}_{nfa} + M'^{h,P_2}_{nfa}) + \Big(a_3 + a_4 + a_5 - \frac{1}{2}(a_7 + a_9 + a_{10})\Big) \times (f_B F^h_{fa} + f_B F'^h_{fa})\Big) + \zeta_{f_{1q}} \cdot \Big(\Big(2a_3 - 2a_5 - \frac{1}{2}(a_7 - a_9)\Big) f_{1s} F'^h_{fe} + \Big(2C_4 + \frac{1}{2}C_{10}\Big) M'^h_{nfe} + \Big(2C_6 + \frac{1}{2}C_8\Big) M'^{h,P_2}_{nfe}\Big)\Big\}; \quad (86)$$

where $\lambda_u^{d(s)} = V_{ub}^* V_{ud(s)}$ and $\lambda_t^{d(s)} = V_{tb}^* V_{td(s)}$, and $\zeta_{f_{1q}} = \cos\phi_{f_1}/\sqrt{2}$ and $\zeta_{f_{1s}} = -\sin\phi_{f_1}$. Also, a_i is the standard combination of the Wilson coefficients C_i defined as follows:

$$a_1 = C_2 + \frac{C_1}{3}; \qquad a_2 = C_1 + \frac{C_2}{3};$$
$$a_i = C_i + C_{i\pm1}/3, \qquad i = 3\text{–}10, \quad (87)$$

where $C_2 \sim 1$ is the largest one among all the Wilson coefficients and the upper (lower) sign applies, when i is odd (even). When we make the replacements with $\zeta_{f_{1q}} \to \zeta'_{f_{1q}} = \sin\phi_{f_1}/\sqrt{2}$ and $\zeta_{f_{1s}} \to \zeta'_{f_{1s}} = \cos\phi_{f_1}$ in the above equations, i.e., Eqs. (77)–(86), the decay amplitudes of other 10 $B \to f_1(1420)V$ modes will be straightforwardly obtained.

III. NUMERICAL RESULTS AND DISCUSSIONS

In this section, we will present numerically the pQCD predictions of the CP-averaged branching ratios, the polarization fractions, the CP-violating asymmetries, and the relative phases for those considered 20 nonleptonic $B \to f_1 V$ decays. Some comments are essentially given on the input quantities for axial-vector f_1 states:

(a) $f_{1q(s)}$ state distribution amplitude

In light of the similar behavior between vector and $^3P_1$-axial-vector mesons [27] and the same form for ρ and ω distribution amplitudes in the vector meson sector but with different decay constants f_ρ and f_ω, we argue that the f_{1q} distribution amplitude can be taken with the same one as that of the $a_1(1260)$ state with decay constant $f_{f_{1q}} = 0.193$ GeV [40]. While, for simplicity, we adopt the same distribution amplitude as the flavor singlet f_1 state [not to be confused with the abbreviation f_1 of $f_1(1285)$ and $f_1(1420)$ mesons] [17] for the f_{1s} state with decay constant $f_{f_{1s}} = 0.230$ GeV [40].

(b) $f_{1q(s)}$ state mass and mixing angle

As mentioned in the Introduction, the value of the mixing angle $\phi_{f_1} = (24.0^{+3.2}_{-2.7})^\circ$ has been measured preliminarily by the LHCb Collaboration in 2013 in the heavy b flavor sector [19]. Because of the good agreement between this measurement and the latest update $(27 \pm 2)^\circ$ in lattice QCD calculations [41], we will adopt experimental data $\phi_{f_1} = 24.0^\circ$ to predict the quantities numerically in this work. On the other hand, as exhibited in Ref. [18], the predictions of $\mathrm{Br}(B^{+,0} \to AP)_{\mathrm{pQCD}}$ with the measured angle are generally consistent with those $\mathrm{Br}(B^{+,0} \to AP)_{\mathrm{QCDF}}$ based on the same mixing matrix for the $f_1(1285) - f_1(1420)$ system with $\alpha_{^3P_1} \sim 18^\circ$, i.e., the second entry $\theta_{^3P_1} \sim 53^\circ$ in the flavor singlet-octet basis [14]. Moreover, for the masses of two f_{1q} and f_{1s} states, we adopt $m_{f_{1q}} \sim m_{f_1(1285)}$ and $m_{f_{1s}} \sim m_{f_1(1420)}$ for convenience.

In numerical calculations, central values of the input parameters will be used implicitly unless otherwise stated. The relevant QCD scale (GeV), masses (GeV), and B meson lifetime (ps) are the following [19,20,27,40,42]:

$$\Lambda^{(f=4)}_{\overline{\mathrm{MS}}} = 0.250, \qquad m_W = 80.41, \qquad m_B = 5.28,$$
$$m_{B_s} = 5.37, \qquad m_b = 4.8;$$
$$f_{f_{1q}} = 0.193^{+0.043}_{-0.038}, \qquad f_{f_{1s}} = 0.230 \pm 0.009,$$
$$m_{f_{1q}} = 1.28, m_{f_{1s}} = 1.42;$$
$$\tau_{B^+} = 1.641, \qquad \tau_{B^0} = 1.519, \qquad \tau_{B_s^0} = 1.497,$$
$$\phi_{f_1} = (24.0^{+3.2}_{-2.7})^\circ. \quad (88)$$

For the CKM matrix elements, we adopt the Wolfenstein parametrization at leading order [43] and the updated parameters $A = 0.814$, $\lambda = 0.22537$, $\bar{\rho} = 0.117 \pm 0.021$, and $\bar{\eta} = 0.353 \pm 0.013$ [8].

TABLE I. Theoretical predictions of physical quantities of $B^+ \to f_1\rho^+$ decays obtained in the pQCD approach with mixing angle $\phi_{f_1} = 24°$ in the quark-flavor ($f_{1q} - f_{1s}$) basis. For comparison, we also quote the estimations in the framework of the QCDF approach with mixing angle $\theta_{^3P_1} \sim 53°$ in the flavor singlet-octet (f_1–f_8) basis.

Decay modes		$B^+ \to f_1(1285)\rho^+$		$B^+ \to f_1(1420)\rho^+$	
Parameter	Definition	This work	QCDF [3]	This work	QCDF [3]
BR (10^{-6})	$\Gamma/\Gamma_{\rm total}$	$11.1^{+3.2+5.4+6.0+0.4+0.2+0.8}_{-2.5-4.0-4.8-0.6-0.3-0.9}$	$8.9^{+5.1+0.4}_{-3.2-0.3}$	$2.3^{+0.7+1.1+1.2+0.6+0.0+0.2}_{-0.5-0.8-0.9-0.4-0.0-0.2}$	$1.3^{+0.6+0.2}_{-0.3-0.0}$
$f_L(\%)$	$\lvert\mathcal{A}_L\rvert^2$	$96.3^{+0.2+0.2+0.4+0.0+0.1+0.0}_{-0.1-0.2-0.3-0.0-0.1-0.0}$	90^{+4}_{-3}	$90.5^{+0.0+1.7+1.8+1.2+1.2+0.7}_{-0.1-2.5-3.7-1.4-1.8-0.8}$	93^{+4}_{-3}
$f_\parallel(\%)$	$\lvert\mathcal{A}_\parallel\rvert^2$	$2.3^{+0.0+0.1+0.2+0.0+0.1+0.0}_{-0.1-0.1-0.2-0.0-0.1-0.0}$	…	$5.5^{+0.0+1.3+2.0+0.7+1.0+0.4}_{-0.1-0.9-1.1-0.7-0.7-0.4}$	…
$f_\perp(\%)$	$\lvert\mathcal{A}_\perp\rvert^2$	$1.4^{+0.1+0.1+0.1+0.0+0.1+0.0}_{-0.1-0.1-0.1-0.0-0.0-0.0}$	…	$4.1^{+0.0+1.1+1.6+0.6+0.8+0.3}_{-0.1-0.9-0.9-0.6-0.6-0.4}$	…
$\phi_\parallel$ (rad)	$\arg\frac{\mathcal{A}_\parallel}{\mathcal{A}_L}$	$3.1^{+0.0+0.0+0.0+0.0+0.0+0.0}_{-0.0-0.1-0.1-0.0-0.0-0.0}$	…	$3.1^{+0.1+0.1+0.2+0.1+0.1+0.0}_{-0.0-0.0-0.0-0.0-0.0-0.0}$	…
$\phi_\perp$ (rad)	$\arg\frac{\mathcal{A}_\perp}{\mathcal{A}_L}$	$3.1^{+0.0+0.0+0.1+0.0+0.0+0.0}_{-0.0-0.0-0.0-0.0-0.0-0.0}$	…	$3.2^{+0.0+0.0+0.0+0.0+0.0+0.0}_{-0.0-0.0-0.1-0.0-0.0-0.0}$	…
$\mathcal{A}_{CP}^{\rm dir}(\%)$	$\frac{\bar\Gamma-\Gamma}{\bar\Gamma+\Gamma}$	$-6.7^{+0.1+0.3+2.1+0.1+0.5+0.4}_{-0.0-0.2-2.9-0.0-0.5-0.3}$	–	$-3.7^{+0.4+0.7+1.8+0.3+0.6+0.1}_{-0.4-0.7-2.1-0.4-0.8-0.1}$	–
$\mathcal{A}_{CP}^{\rm dir}(L)(\%)$	$\frac{\bar f_L-f_L}{\bar f_L+f_L}$	$-7.0^{+0.1+0.1+2.1+0.1+0.5+0.4}_{-0.0-0.1-2.8-0.0-0.6-0.3}$	…	$-5.4^{+0.7+0.4+1.8+0.2+1.0+0.2}_{-0.6-0.4-2.1-0.2-1.4-0.3}$	…
$\mathcal{A}_{CP}^{\rm dir}(\parallel)(\%)$	$\frac{\bar f_\parallel-f_\parallel}{\bar f_\parallel+f_\parallel}$	$0.7^{+0.6+2.8+2.8+0.7+2.1+0.0}_{-0.4-3.5-3.8-0.8-1.2-0.0}$	–	$13.8^{+1.6+3.7+10.9+0.4+0.8+0.7}_{-1.8-3.7-11.0-0.6-0.6-0.8}$	–
$\mathcal{A}_{CP}^{\rm dir}(\perp)(\%)$	$\frac{\bar f_\perp-f_\perp}{\bar f_\perp+f_\perp}$	$1.3^{+0.7+3.0+3.0+0.7+2.4+0.1}_{-0.5-3.9-4.1-0.8-1.3-0.0}$	…	$10.5^{+2.5+4.0+11.9+0.5+0.5+0.5}_{-3.2-3.9-12.2-0.6-0.3-0.6}$	…

A. *CP*-averaged branching ratios

For the considered $B \to f_1 V$ decays, the decay rate can be written as

$$\Gamma = \frac{G_F^2|P_c|}{16\pi m_B^2}\sum_{\sigma=L,N,T} A^{(\sigma)\dagger}A^{(\sigma)}, \tag{89}$$

where $|\mathbf{P_c}| \equiv |\mathbf{P_{2z}}| = |\mathbf{P_{3z}}|$ is the momentum of either the outgoing axial-vector meson or vector meson and $A^{(\sigma)}$ can be found, for example, in Eqs. (77)–(86). Using the decay amplitudes obtained in last section, it is straightforward to calculate the *CP*-averaged branching ratios with uncertainties for the considered decays in the pQCD approach.

The numerical results of the physical quantities are presented in Tables I–X, in which the six major errors are induced by the uncertainties of the shape parameter $\omega_b = 0.40 \pm 0.04 (\omega_b = 0.50 \pm 0.05)$ GeV in the $B^{+,0}(B_s^0)$ meson wave function; of the combined decay constants f_M from the $^3P_1$-axial-vector state decay constants $f_{f_{1q}} = 0.193^{+0.043}_{-0.038}$ and $f_{f_{1s}} = 0.230 \pm 0.009$ GeV and vector meson decay constants f_V and f_V^T; of the combined Gegenbauer moments a_i^M from $a_2^\parallel$ and $a_1^\perp$ for the axial-vector f_{1q} and f_{1s} states and from $a_{(1)2V}^{\parallel,\perp}$ for the light vector meson in both longitudinal and transverse polarizations; of the mixing angle $\phi_{f_1} = (24.0^{+3.2}_{-2.7})°$ for the

TABLE II. Same as Table I but for $B^+ \to f_1 K^{*+}$ decays.

Decay modes		$B^+ \to f_1(1285)K^{*+}$		$B^+ \to f_1(1420)K^{*+}$	
Parameter	Definition	This work	QCDF [3]	This work	QCDF [3]
BR (10^{-6})	$\Gamma/\Gamma_{\rm total}$	$6.4^{+0.5+2.4+1.6+0.3+2.1+0.1}_{-0.3-1.7-1.3-0.2-1.2-0.0}$	$5.7^{+3.8+21.4}_{-2.2-4.8}$	$4.5^{+0.7+0.4+1.3+0.2+0.8+0.0}_{-0.6-0.4-1.2-0.3-0.5-0.1}$	$15.6^{+10.9+10.4}_{-5.2-4.7}$
$f_L(\%)$	$\lvert\mathcal{A}_L\rvert^2$	$23.5^{+0.8+2.3+4.8+1.3+1.8+0.5}_{-0.5-1.6-3.2-1.0-1.3-0.5}$	47^{+49}_{-45}	$69.3^{+1.0+0.9+10.2+0.5+4.8+0.4}_{-1.2-1.3-10.4-0.6-6.6-0.3}$	64^{+37}_{-61}
$f_\parallel(\%)$	$\lvert\mathcal{A}_\parallel\rvert^2$	$42.1^{+0.2+0.9+1.8+0.6+0.8+0.3}_{-0.4-1.2-2.4-0.7-1.0-0.2}$	…	$16.5^{+0.8+0.8+5.9+0.4+3.5+0.2}_{-0.6-0.7-5.7-0.4-2.6-0.2}$	…
$f_\perp(\%)$	$\lvert\mathcal{A}_\perp\rvert^2$	$34.4^{+0.2+0.7+1.5+0.4+0.6+0.2}_{-0.4-1.1-2.4-0.6-0.8-0.2}$	…	$14.2^{+0.5+0.5+3.8+0.2+3.0+0.2}_{-0.4-0.3-4.4-0.1-2.2-0.2}$	…
$\phi_\parallel$ (rad)	$\arg\frac{\mathcal{A}_\parallel}{\mathcal{A}_L}$	$4.4^{+0.0+0.1+0.1+0.0+0.1+0.1}_{-1.3-0.2-1.8-0.0-0.2-0.1}$	…	$3.6^{+0.1+0.2+0.3+0.1+0.1+0.1}_{-0.0-0.1-0.1-0.0-0.1-0.0}$	…
$\phi_\perp$ (rad)	$\arg\frac{\mathcal{A}_\perp}{\mathcal{A}_L}$	$4.4^{+0.0+0.1+0.1+0.0+0.1+0.1}_{-1.3-0.2-1.8-0.0-0.2-0.1}$	…	$3.6^{+0.0+0.1+0.2+0.0+0.1+0.0}_{-0.1-0.1-0.3-0.1-0.1-0.0}$	…
$\mathcal{A}_{CP}^{\rm dir}(\%)$	$\frac{\bar\Gamma-\Gamma}{\bar\Gamma+\Gamma}$	$-16.0^{+0.9+1.0+4.4+0.3+2.3+0.5}_{-0.9-0.9-4.2-0.3-2.2-0.5}$	…	$13.9^{+0.9+3.0+3.7+2.0+0.5+0.5}_{-0.8-2.8-4.0-1.7-0.8-0.4}$	…
$\mathcal{A}_{CP}^{\rm dir}(L)(\%)$	$\frac{\bar f_L-f_L}{\bar f_L+f_L}$	$-94.5^{+3.3+7.3+20.7+4.1+8.0+1.4}_{-1.1-4.4-3.7-2.8-4.0-1.2}$	…	$25.4^{+1.1+4.9+2.3+3.4+1.5+1.0}_{-0.9-4.7-3.7-2.8-1.1-0.9}$	…
$\mathcal{A}_{CP}^{\rm dir}(\parallel)(\%)$	$\frac{\bar f_\parallel-f_\parallel}{\bar f_\parallel+f_\parallel}$	$8.2^{+0.3+0.5+2.1+0.1+1.0+0.3}_{-0.3-0.5-2.1-0.1-1.0-0.3}$	…	$-14.1^{+1.1+3.0+4.9+1.8+2.2+0.5}_{-1.1-2.9-5.6-2.1-2.1-0.6}$	…
$\mathcal{A}_{CP}^{\rm dir}(\perp)(\%)$	$\frac{\bar f_\perp-f_\perp}{\bar f_\perp+f_\perp}$	$7.9^{+0.4+0.6+2.1+0.1+0.8+0.3}_{-0.3-0.4-2.0-0.1-0.9-0.2}$	…	$-9.7^{+1.0+2.2+4.1+1.3+1.5+0.4}_{-0.9-2.0-4.0-1.4-1.4-0.3}$	…

TABLE III. Same as Table I but for $B^0 \to f_1\rho^0$ decays.

Decay modes		$B^0 \to f_1(1285)\rho^0$		$B^0 \to f_1(1420)\rho^0$	
Parameter	Definition	This work	QCDF [3]	This work	QCDF [3]
BR (10^{-7})	$\Gamma/\Gamma_{\rm total}$	$1.1^{+0.3+0.5+0.8+0.1+0.1+0.1}_{-0.2-0.3-0.2-0.0-0.0-0.0}$	$2.0^{+1.0+3.0}_{-1.0-0.0}$	$0.7^{+0.2+0.1+0.1+0.0+0.2+0.0}_{-0.2-0.1-0.1-0.0-0.2-0.0}$	$0.4^{+1.2+0.8}_{-0.3-0.0}$
$f_L(\%)$	$\lvert\mathcal{A}_L\rvert^2$	$90.5^{+0.1+1.6+5.4+0.0+1.1+0.7}_{-0.0-2.0-12.8-0.3-1.1-0.8}$	71^{+9}_{-36}	$7.2^{+1.8+3.7+5.6+2.0+4.1+0.1}_{-1.1-2.4-1.7-1.7-2.6-0.0}$	87^{+8}_{-40}
$f_\parallel(\%)$	$\lvert\mathcal{A}_\parallel\rvert^2$	$4.5^{+0.0+1.1+6.8+0.2+0.5+0.4}_{-0.1-0.8-2.1-0.1-0.5-0.4}$	...	$49.3^{+0.4+1.0+0.9+0.7+1.3+0.0}_{-0.9-1.8-2.8-1.0-2.1-0.1}$	...
$f_\perp(\%)$	$\lvert\mathcal{A}_\perp\rvert^2$	$5.0^{+0.1+1.0+6.1+0.1+0.6+0.4}_{-0.1-0.8-3.3-0.0-0.6-0.4}$	...	$43.5^{+0.7+1.5+0.7+1.0+1.3+0.1}_{-0.9-1.9-2.8-1.0-2.0-0.0}$	...
$\phi_\parallel$ (rad)	$\arg\frac{\mathcal{A}_\parallel}{\mathcal{A}_L}$	$3.3^{+0.1+0.3+0.4+0.1+0.1+0.0}_{-0.0-0.1-0.1-0.0-0.0-0.0}$	...	$3.5^{+0.0+0.4+0.2+0.2+0.1+0.0}_{-0.0-0.1-0.4-0.1-0.0-0.0}$	...
$\phi_\perp$ (rad)	$\arg\frac{\mathcal{A}_\perp}{\mathcal{A}_L}$	$3.3^{+0.1+0.2+0.4+0.1+0.1+0.1}_{-0.0-0.0-0.1-0.0-0.0-0.0}$	...	$3.5^{+0.0+0.4+0.2+0.2+0.1+0.0}_{-0.0-0.1-0.3-0.1-0.0-0.0}$	...
$\mathcal{A}_{CP}^{\rm dir}(\%)$	$\frac{\bar{\Gamma}-\Gamma}{\bar{\Gamma}+\Gamma}$	$18.0^{+12.9+3.9+40.6+2.3+1.6+0.6}_{-12.0-4.5-27.5-2.6-1.4-0.6}$	...	$24.1^{+0.5+7.5+17.2+4.5+5.1+1.1}_{-0.4-6.7-22.4-3.7-5.4-1.3}$	...
$\mathcal{A}_{CP}^{\rm dir}(L)(\%)$	$\frac{\bar{f}_L-f_L}{\bar{f}_L+f_L}$	$24.7^{+13.7+1.3+39.2+0.5+3.0+1.1}_{-12.7-1.5-32.5-0.5-2.9-1.0}$	...	$-72.5^{+24.1+27.2+29.5+16.1+19.2+2.8}_{-20.8-26.1-14.7-18.2-18.6-2.7}$	...
$\mathcal{A}_{CP}^{\rm dir}(\parallel)(\%)$	$\frac{\bar{f}_\parallel-f_\parallel}{\bar{f}_\parallel+f_\parallel}$	$-56.6^{+4.9+31.4+40.2+19.5+5.5+2.6}_{-5.2-26.4-11.4-17.8-2.3-2.7}$	...	$29.8^{+0.6+6.6+20.4+3.7+3.1+1.4}_{-0.6-6.2-23.3-3.2-3.4-1.5}$	...
$\mathcal{A}_{CP}^{\rm dir}(\perp)(\%)$	$\frac{\bar{f}_\perp-f_\perp}{\bar{f}_\perp+f_\perp}$	$-36.9^{+6.2+30.0+27.3+19.4+7.0+1.9}_{-6.6-30.8-11.8-20.3-3.5-1.9}$	...	$33.6^{+0.7+7.0+19.5+4.1+3.8+1.7}_{-0.9-6.6-22.8-7.0-4.0-1.6}$	...

TABLE IV. Same as Table I but for $B^0 \to f_1K^{*0}$ decays.

Decay modes		$B^0 \to f_1(1285)K^{*0}$		$B^0 \to f_1(1420)K^{*0}$	
Parameter	Definition	This work	QCDF [3]	This work	QCDF [3]
BR (10^{-6})	$\Gamma/\Gamma_{\rm total}$	$5.0^{+0.1+1.6+1.3+0.2+1.7+0.0}_{-0.2-1.3-1.2-0.2-1.1-0.1}$	$5.1^{+3.6+20.0}_{-2.1-4.7}$	$4.4^{+0.6+0.4+1.4+0.2+0.7+0.0}_{-0.6-0.4-1.2-0.3-0.5-0.0}$	$14.9^{+10.2+10.1}_{-5.0-4.6}$
$f_L(\%)$	$\lvert\mathcal{A}_L\rvert^2$	$15.8^{+0.9+2.8+5.8+1.6+0.7+0.1}_{-1.0-1.8-2.4-1.2-0.2-0.1}$	45^{+55}_{-50}	$71.0^{+1.3+1.7+10.9+1.2+4.4+0.1}_{-1.7-2.2-11.1-1.0-6.3-0.1}$	64^{+38}_{-61}
$f_\parallel(\%)$	$\lvert\mathcal{A}_\parallel\rvert^2$	$46.1^{+0.5+0.9+1.3+0.5+0.1+0.0}_{-0.5-1.4-3.3-0.8-0.4-0.1}$	...	$16.0^{+1.0+1.4+6.4+0.8+3.4+0.0}_{-0.9-1.2-6.3-0.8-2.4-0.1}$	...
$f_\perp(\%)$	$\lvert\mathcal{A}_\perp\rvert^2$	$38.1^{+0.5+1.1+1.1+0.7+0.1+0.1}_{-0.4-1.4-2.6-0.8-0.3-0.0}$	...	$13.0^{+0.6+0.9+4.7+0.5+2.9+0.1}_{-0.4-0.6-4.5-0.4-2.0-0.0}$	...
$\phi_\parallel$ (rad)	$\arg\frac{\mathcal{A}_\parallel}{\mathcal{A}_L}$	$3.9^{+0.1+0.1+0.5+0.0+0.1+0.0}_{-0.1-0.2-0.4-0.1-0.1-0.0}$	...	$3.7^{+0.1+0.2+0.3+0.1+0.1+0.0}_{-0.0-0.1-0.1-0.0-0.1-0.0}$	...
$\phi_\perp$ (rad)	$\arg\frac{\mathcal{A}_\perp}{\mathcal{A}_L}$	$3.9^{+0.1+0.1+0.5+0.0+0.1+0.0}_{-0.1-0.1-0.4-0.1-0.1-0.0}$	...	$3.7^{+0.0+0.0+0.1+0.0+0.0+0.0}_{-0.1-0.3-0.4-0.1-0.2-0.0}$	...
$\mathcal{A}_{CP}^{\rm dir}(\%)$	$\frac{\bar{\Gamma}-\Gamma}{\bar{\Gamma}+\Gamma}$	$-7.8^{+0.8+0.2+2.0+0.1+1.2+0.3}_{-0.9-0.0-1.8-0.0-1.0-0.3}$	...	$4.7^{+0.0+0.9+0.2+0.6+0.8+0.2}_{-0.0-0.9-0.4-0.5-1.0-0.2}$	...
$\mathcal{A}_{CP}^{\rm dir}(L)(\%)$	$\frac{\bar{f}_L-f_L}{\bar{f}_L+f_L}$	$1.7^{+0.0+3.3+6.0+2.0+2.7+0.1}_{-0.2-2.6-10.6-1.7-2.4-0.0}$	...	$3.4^{+0.0+0.9+0.3+0.5+1.0+0.1}_{-0.1-0.8-0.5-0.5-1.6-0.2}$	...
$\mathcal{A}_{CP}^{\rm dir}(\parallel)(\%)$	$\frac{\bar{f}_\parallel-f_\parallel}{\bar{f}_\parallel+f_\parallel}$	$-9.3^{+0.9+0.5+0.9+0.3+0.9+0.4}_{-0.9-0.4-0.9-0.2-0.8-0.3}$	...	$7.9^{+0.3+1.6+2.0+1.1+0.7+0.3}_{-0.4-1.6-1.8-0.9-0.8-0.3}$	...
$\mathcal{A}_{CP}^{\rm dir}(\perp)(\%)$	$\frac{\bar{f}_\perp-f_\perp}{\bar{f}_\perp+f_\perp}$	$-9.9^{+0.8+0.4+0.7+0.2+1.0+0.3}_{-1.0-0.5-0.9-0.2-1.0-0.4}$	...	$8.0^{+0.1+1.2+1.2+0.8+0.8+0.3}_{-0.2-1.4-1.5-0.8-0.8-0.3}$	...

$f_1(1285) - f_1(1420)$ mixing system; of the maximal running hard scale $t_{\rm max}$; and of the combined CKM matrix elements from parameters $\bar{\rho}$ and $\bar{\eta}$, respectively. It is worth mentioning that, though parts of next-to-leading order corrections to two-body hadronic B meson decays have been proposed in the pQCD approach [22,23], the higher order QCD contributions to $B \to VV$ modes beyond leading order are not yet available presently. Therefore, as displayed in the above-mentioned tables, the higher order contributions in this work are simply investigated by exploring the variation of hard scale $t_{\rm max}$, i.e., from $0.8t$ to $1.2t$ (not changing $1/b_i$, $i = 1, 2, 3$), in the hard kernel, which have been counted into one of the sources of theoretical uncertainties. It looks like the penguin-dominated decays such as $B^{+,0} \to f_1K^{*+,0}$, $B^0 \to f_1\phi$, and $B_s^0 \to f_1(\overline{K}^{*0}, \omega, \phi)$ are more sensitive to the potential higher order corrections, as can be clearly seen in Tables II,IV,VI,VIII,IX, and X, correspondingly.

(1) According to the effective Hamiltonian shown in Eq. (9), the considered 20 nonleptonic $B \to f_1V$ decays contain two kinds of transitions, i.e., the $\overline{b} \to \overline{d}$ one with $\Delta S = 0$ and the $\overline{b} \to \overline{s}$ one with $\Delta S = 1$ (here, the capital S describes strange flavor number), in which $B^{+,0} \to f_1(\rho, \omega, \phi)$ and $B_s^0 \to f_1\overline{K}^{*0}$ belong to the former class, while $B^{+,0} \to f_1K^{*+,0}$ and $B_s^0 \to f_1(\rho, \omega, \phi)$ are classified into the latter one. Also, in principle, if the decays with these two kinds of transitions are dominated by the penguin amplitudes, it can be roughly anticipated that because $|\lambda_t^d| : |\lambda_t^s| \sim 0.22:1$ in magnitude, $\mathrm{Br}(B \to f_1V)_{\overline{b}\to\overline{d}}$ is basically less than $\mathrm{Br}(B \to f_1V)_{\overline{b}\to\overline{s}}$. Undoubtedly, the

TABLE V. Same as Table I but for $B^0 \to f_1\omega$ decays.

Decay modes		$B^0 \to f_1(1285)\omega$		$B^0 \to f_1(1420)\omega$	
Parameter	Definition	This work	QCDF [3]	This work	QCDF [3]
BR (10^{-6})	$\Gamma/\Gamma_{\rm total}$	$1.0^{+0.2+0.5+0.3+0.0+0.1+0.1}_{-0.2-0.3-0.1-0.0-0.0-0.0}$	$0.9^{+1.0+2.2}_{-0.4-0.1}$	$0.2^{+0.0+0.1+0.0+0.0+0.0+0.0}_{-0.0-0.1-0.0-0.0-0.0-0.0}$	$0.1^{+0.2+0.3}_{-0.1-0.0}$
$f_L(\%)$	$\lvert\mathcal{A}_L\rvert^2$	$60.1^{+2.3+1.2+8.1+0.0+2.4+0.5}_{-2.4-1.3-7.6-0.1-1.6-0.6}$	86^{+7}_{-62}	$45.3^{+3.2+3.9+9.7+2.3+4.4+1.4}_{-3.4-4.7-9.3-2.4-3.0-1.4}$	86^{+4}_{-76}
$f_\parallel(\%)$	$\lvert\mathcal{A}_\parallel\rvert^2$	$20.1^{+1.3+0.7+4.0+0.1+1.0+0.3}_{-1.2-0.6-4.2-0.0-1.3-0.2}$	···	$28.3^{+1.8+2.5+4.8+1.3+1.7+0.7}_{-1.8-2.3-5.1-1.3-2.5-0.9}$	···
$f_\perp(\%)$	$\lvert\mathcal{A}_\perp\rvert^2$	$19.8^{+1.1+0.6+3.5+0.1+0.6+0.3}_{-1.1-0.6-3.9-0.1-1.1-0.3}$	···	$26.5^{+1.5+2.0+4.4+1.0+1.2+0.6}_{-1.5-1.8-4.7-1.0-2.0-0.7}$	···
$\phi_\parallel$ (rad)	$\arg\frac{\mathcal{A}_\parallel}{\mathcal{A}_L}$	$1.7^{+0.1+0.1+1.5+0.0+1.3+0.1}_{-0.0-0.0-0.1-0.0-0.0-0.0}$	···	$3.2^{+0.0+0.0+0.1+0.0+0.2+0.0}_{-0.1-0.0-0.2-0.0-0.2-0.0}$	···
$\phi_\perp$ (rad)	$\arg\frac{\mathcal{A}_\perp}{\mathcal{A}_L}$	$1.7^{+0.1+0.1+0.3+0.0+2.9+0.1}_{-0.0-0.0-0.1-0.0-0.0-0.0}$	···	$3.2^{+0.0+0.0+0.1+0.0+0.2+0.0}_{-0.1-0.0-0.2-0.0-0.2-0.0}$	···
$\mathcal{A}_{CP}^{\rm dir}(\%)$	$\frac{\bar\Gamma-\Gamma}{\bar\Gamma+\Gamma}$	$-59.3^{+0.2+1.6+4.2+0.6+4.5+1.8}_{-0.0-1.7-1.8-0.6-1.0-1.5}$	···	$-6.0^{+2.8+12.2+18.7+6.5+9.2+0.2}_{-2.7-11.2-17.3-6.7-6.5-0.3}$	···
$\mathcal{A}_{CP}^{\rm dir}(L)(\%)$	$\frac{\bar f_L-f_L}{\bar f_L+f_L}$	$-88.7^{+2.8+1.2+11.7+0.8+6.0+1.6}_{-2.7-1.6-6.3-0.9-0.0-1.6}$	···	$-7.3^{+5.6+25.1+17.9+13.5+24.2+0.3}_{-4.5-19.5-20.3-12.6-13.8-0.4}$	···
$\mathcal{A}_{CP}^{\rm dir}(\parallel)(\%)$	$\frac{\bar f_\parallel-f_\parallel}{\bar f_\parallel+f_\parallel}$	$-15.8^{+0.0+1.5+5.2+0.1+0.4+0.6}_{-0.1-1.7-3.8-0.1-0.3-0.7}$	···	$-4.3^{+0.7+3.7+21.3+1.2+0.9+0.2}_{-0.9-4.1-17.6-1.3-1.9-0.3}$	···
$\mathcal{A}_{CP}^{\rm dir}(\perp)(\%)$	$\frac{\bar f_\perp-f_\perp}{\bar f_\perp+f_\perp}$	$-14.3^{+0.1+1.4+5.3+0.1+0.5+0.6}_{-0.0-1.4-5.8-0.0-0.4-0.5}$	···	$-5.6^{+0.7+3.5+19.7+1.0+0.8+0.3}_{-0.9-3.9-16.2-1.1-1.9-0.4}$	···

TABLE VI. Same as Table I but for $B^0 \to f_1\phi$ decays.

Decay modes		$B^0 \to f_1(1285)\phi$		$B^0 \to f_1(1420)\phi$	
Parameter	Definition	This work	QCDF [3]	This work	QCDF [3]
BR (10^{-9})	$\Gamma/\Gamma_{\rm total}$	$8.9^{+1.8+3.3+3.4+0.3+2.2+0.4}_{-1.4-2.3-2.2-0.2-1.4-0.3}$	$2.0^{+2.0+9.0}_{-1.0-0.0}$	$3.7^{+0..2+0.3+2.6+0.2+0.9+0.1}_{-0.4-0.5-2.1-0.3-0.9-0.2}$	$0.8^{+0.9+0.9}_{-0.1-0.1}$
$f_L(\%)$	$\lvert\mathcal{A}_L\rvert^2$	$68.9^{+0.9+3.9+19.5+2.5+1.7+0.0}_{-0.9-3.3-17.7-2.1-2.4-0.0}$	90^{+3}_{-71}	$85.9^{+1.6+5.7+11.4+3.6+0.0+0.0}_{-2.0-7.7-16.7-5.1-1.1-0.0}$	98^{+2}_{-44}
$f_\parallel(\%)$	$\lvert\mathcal{A}_\parallel\rvert^2$	$17.3^{+0.5+1.9+9.9+1.2+1.3+0.0}_{-0.4-2.0-10.5-1.3-0.9-0.0}$	···	$7.4^{+1.1+4.3+9.0+2.8+0.6+0.0}_{-0.8-3.0-6.2-1.9-0.0-0.0}$	···
$f_\perp(\%)$	$\lvert\mathcal{A}_\perp\rvert^2$	$13.7^{+0.5+1.5+7.9+1.0+1.2+0.0}_{-0.4-1.7-8.5-1.1-0.8-0.0}$	···	$6.7^{+0.9+3.5+7.7+2.3+0.5+0.0}_{-0.7-2.6-5.3-1.7-0.0-0.0}$	···
$\phi_\parallel$ (rad)	$\arg\frac{\mathcal{A}_\parallel}{\mathcal{A}_L}$	$3.7^{+0.0+0.0+0.0+0.0+0.0+0.0}_{-0.1-0.1-0.1-0.0-0.0-0.0}$	···	$4.3^{+0.1+0.0+0.1+0.0+0.0+0.0}_{-0.1-0.1-0.2-0.0-0.0-0.0}$	···
$\phi_\perp$ (rad)	$\arg\frac{\mathcal{A}_\perp}{\mathcal{A}_L}$	$3.7^{+0.0+0.0+0.1+0.0+0.0+0.0}_{-0.0-0.0-0.1-0.0-0.0-0.0}$	···	$4.4^{+0.1+0.0+0.1+0.0+0.0+0.0}_{-0.1-0.1-0.2-0.0-0.0-0.0}$	···
$\mathcal{A}_{CP}^{\rm dir}(\%)$	$\frac{\bar\Gamma-\Gamma}{\bar\Gamma+\Gamma}$	~ 0.0	···	~ 0.0	···
$\mathcal{A}_{CP}^{\rm dir}(L)(\%)$	$\frac{\bar f_L-f_L}{\bar f_L+f_L}$	~ 0.0	···	~ 0.0	···
$\mathcal{A}_{CP}^{\rm dir}(\parallel)(\%)$	$\frac{\bar f_\parallel-f_\parallel}{\bar f_\parallel+f_\parallel}$	~ 0.0	···	~ 0.0	···
$\mathcal{A}_{CP}^{\rm dir}(\perp)(\%)$	$\frac{\bar f_\perp-f_\perp}{\bar f_\perp+f_\perp}$	~ 0.0	···	~ 0.0	···

tree-dominated $B^+ \to f_1\rho^+$ modes are exceptional. A convincing example is directly observed from the ratios between $B^0 \to f_1 K^{*0}$ and $B_s^0 \to f_1\overline{K}^{*0}$ decay rates. From the numerical branching ratios predicted in the pQCD approach as given in Tables IV and VIII, the ratios $R^{d/s}_{f_{(1285)}K^*}$ and $R^{d/s}_{f_{(1420)}K^*}$ can be written as

$$R^{d/s}_{f_1(1285)K^*} \equiv \frac{\mathrm{Br}(B^0 \to f_1(1285)K^{*0})_{\rm pQCD}}{\mathrm{Br}(B_s^0 \to f_1(1285)\overline{K}^{*0})_{\rm pQCD}} \sim 9,$$
$$R^{d/s}_{f_1(1420)K^*} \equiv \frac{\mathrm{Br}(B^0 \to f_1(1420)K^{*0})_{\rm pQCD}}{\mathrm{Br}(B_s^0 \to f_1(1420)\overline{K}^{*0})_{\rm pQCD}} \sim 13, \quad (90)$$

where, for the sake of simplicity, only central values are quoted for clarification. The difference between these two ratios $R^{d/s}_{f_1(1285)K^*}$ and $R^{d/s}_{f_1(1420)K^*}$ is mainly induced by the fact that $f_1(1285)[f_1(1420)]$ has a dominant $u\bar{u}+d\bar{d}(s\bar{s})$ component with $\cos\phi \sim 0.9$, which confirms somewhat large tree contaminations in $B_{d/s} \to f_1(1285)K^{*0}$ decays. Numerically, in terms of central values, $\mathrm{Br}(B^0 \to f_1(1285)[f_1(1420)]K^{*0})$ varies from $4.96(4.37)\times 10^{-6}$ to $5.08(4.34)\times 10^{-6}$, while $\mathrm{Br}(B_s^0 \to f_1(1285)[f_1(1420)]\overline{K}^{*0})$ changes from $5.47(3.40)\times 10^{-7}$ to $1.99(2.84)\times 10^{-7}$ by neglecting the tree contributions.

(2) Based on the theoretical predictions given at leading order in the pQCD approach, as collected in Tables I–X, large CP-averaged branching ratios

TABLE VII. Same as Table I but for $B_s^0 \to f_1\rho^0$ decays.

Decay modes		$B_s^0 \to f_1(1285)\rho^0$		$B_s^0 \to f_1(1420)\rho^0$	
Parameter	Definition	This work	QCDF	This work	QCDF
BR (10^{-7})	$\Gamma/\Gamma_{\rm total}$	$0.5^{+0.2+0.1+0.3+0.1+0.1+0.0}_{-0.1-0.0-0.2-0.1-0.0-0.0}$	...	$2.5^{+0.8+0.2+1.4+0.1+0.2+0.0}_{-0.6-0.2-1.1-0.1-0.2-0.1}$	...
$f_L(\%)$	$\lvert\mathcal{A}_L\rvert^2$	$79.8^{+0.3+0.3+1.9+0.2+0.2+0.8}_{-0.3-0.0-3.6-0.1-0.1-0.8}$	...	$80.8^{+0.0+0.1+1.6+0.1+0.1+0.8}_{-0.0-0.1-2.7-0.0-0.1-0.8}$	...
$f_\parallel(\%)$	$\lvert\mathcal{A}_\parallel\rvert^2$	$10.9^{+0.1+0.0+1.9+0.0+0.0+0.3}_{-0.2-0.2-1.0-0.1-0.1-0.4}$	...	$10.4^{+0.1+0.1+1.5+0.1+0.1+0.4}_{-0.0-0.0-0.8-0.0-0.0-0.4}$	...
$f_\perp(\%)$	$\lvert\mathcal{A}_\perp\rvert^2$	$9.3^{+0.1+0.0+1.7+0.1+0.1+0.3}_{-0.1-0.1-0.8-0.1-0.1-0.3}$	...	$8.7^{+0.1+0.2+1.4+0.1+0.1+0.4}_{-0.0-0.0-0.7-0.0-0.0-0.3}$	...
$\phi_\parallel$ (rad)	$\arg\frac{\mathcal{A}_\parallel}{\mathcal{A}_L}$	$3.1^{+0.0+0.1+0.1+0.0+0.0+0.0}_{-0.0-0.0-0.1-0.0-0.0-0.0}$	...	$2.9^{+0.1+0.0+0.2+0.0+0.0+0.1}_{-0.0-0.0-0.0-0.0-0.0-0.0}$	...
$\phi_\perp$ (rad)	$\arg\frac{\mathcal{A}_\perp}{\mathcal{A}_L}$	$3.1^{+0.0+0.1+0.1+0.0+0.0+0.0}_{-0.0-0.0-0.1-0.0-0.0-0.0}$	...	$3.0^{+0.0+0.0+0.1+0.0+0.0+0.0}_{-0.1-0.0-0.1-0.0-0.0-0.0}$	...
$\mathcal{A}_{CP}^{\rm dir}(\%)$	$\frac{\bar{\Gamma}-\Gamma}{\bar{\Gamma}+\Gamma}$	$-26.4^{+3.3+2.2+3.8+5.2+1.5+1.0}_{-3.3-8.1-3.3-5.1-1.4-0.9}$	...	$23.7^{+2.0+1.9+15.6+1.3+1.8+0.8}_{-2.0-1.6-9.4-1.0-1.9-0.8}$	...
$\mathcal{A}_{CP}^{\rm dir}(L)(\%)$	$\frac{\bar{f}_L-f_L}{\bar{f}_L+f_L}$	$-30.6^{+3.6+2.5+5.8+6.4+1.8+1.1}_{-3.7-10.1-8.1-6.5-1.8-1.2}$	...	$31.8^{+3.0+2.2+17.2+1.5+2.2+1.1}_{-3.0-2.0-10.4-1.3-1.5-1.1}$	...
$\mathcal{A}_{CP}^{\rm dir}(\parallel)(\%)$	$\frac{\bar{f}_\parallel-f_\parallel}{\bar{f}_\parallel+f_\parallel}$	$-13.8^{+2.5+0.1+12.7+0.4+0.5+0.7}_{-2.9-0.8-7.2-0.5-0.6-0.8}$	...	$-9.6^{+2.2+0.1+14.8+0.1+0.3+0.5}_{-2.5-0.2-8.4-0.1-0.4-0.6}$	...
$\mathcal{A}_{CP}^{\rm dir}(\perp)(\%)$	$\frac{\bar{f}_\perp-f_\perp}{\bar{f}_\perp+f_\perp}$	$-4.2^{+1.6+1.2+15.4+0.8+0.2+0.2}_{-1.6-0.3-8.9-0.7-0.4-0.2}$	...	$-10.8^{+2.4+0.3+13.8+0.2+0.1+0.6}_{-2.4-0.2-7.6-0.1-0.2-0.6}$	...

of the order of 10^{-6}–10^{-5} can be found in the channels such as $B^+ \to f_1(\rho^+, K^{*+})$, $B^0 \to f_1 K^{*0}$, $B^0 \to f_1(1285)\omega$, and $B_s^0 \to f_1\phi$, which can be detected at the LHCb and Belle-II experiments in the near future. Of course, relative to the $B_s^0 \to \phi\phi$ decay, it is of particular interest to study the $B_s - \overline{B}_s$ mixing phase and even possible NP through the detectable $B_s^0 \to f_1\phi$ decays with large decay rates complementarily, which is mainly because these two modes contain the tiny and safely negligible tree pollution. More relevant discussions will be given below.

(3) From Table I, one can easily find that the CP-averaged branching ratios of color-allowed tree-dominated $B^+ \to f_1\rho^+$ decays are

$$\begin{aligned}
&\mathrm{Br}(B^+ \to f_1(1285)\rho^+)_{\rm pQCD} = 11.1^{+8.7}_{-6.8} \times 10^{-6},\\
&\mathrm{Br}(B^+ \to f_1(1420)\rho^+)_{\rm pQCD} = 2.3^{+1.9}_{-1.4} \times 10^{-6},
\end{aligned} \tag{91}$$

where various errors arising from the input parameters have been added in quadrature. It is known that the $B^+ \to f_1\rho^+$ decays are induced by the interferences between $B^+ \to f_{1q}\rho^+$ and $f_{1s}\rho^+$ modes. The values of the branching ratios indicate a constructive (destructive) interference in the $B^+ \to f_1(1285)[f_1(1420)]\rho^+$ decay. In fact, due to the dominance of $f_{1q}(f_{1s})$ in the $f_1(1285)[f_1(1420)]$ state, it is therefore naturally expected that

TABLE VIII. Same as Table I but for $B_s^0 \to f_1\bar{K}^{*0}$ decays.

Decay modes		$B_s^0 \to f_1(1285)\bar{K}^{*0}$		$B_s^0 \to f_1(1420)\bar{K}^{*0}$	
Parameter	Definition	This work	QCDF	This work	QCDF
BR (10^{-7})	$\Gamma/\Gamma_{\rm total}$	$5.5^{+1.0+2.2+1.0+0.0+1.1+0.3}_{-0.8-1.7-0.9-0.0-0.6-0.3}$	...	$3.4^{+0.6+0.4+1.8+0.0+0.6+0.0}_{-0.5-0.3-1.3-0.0-0.4-0.0}$	...
$f_L(\%)$	$\lvert\mathcal{A}_L\rvert^2$	$39.2^{+0.0+1.6+8.4+0.4+3.2+0.9}_{-0.3-1.6-8.2-0.4-1.5-0.8}$	...	$51.1^{+2.7+4.3+12.0+0.6+5.2+0.5}_{-2.8-4.5-15.5-0.7-6.5-0.6}$	...
$f_\parallel(\%)$	$\lvert\mathcal{A}_\parallel\rvert^2$	$31.8^{+0.2+0.9+4.3+0.3+1.1+0.5}_{-0.0-0.9-4.4-0.3-1.9-0.4}$	...	$25.8^{+1.5+2.6+8.2+0.5+3.6+0.3}_{-1.4-2.5-6.4-0.4-2.8-0.2}$	...
$f_\perp(\%)$	$\lvert\mathcal{A}_\perp\rvert^2$	$29.0^{+0.2+0.6+3.8+0.1+0.4+0.5}_{-0.1-0.8-4.0-0.2-1.3-0.5}$	...	$23.1^{+1.3+2.0+7.4+0.2+2.9+0.3}_{-1.2-2.0-5.7-0.2-2.4-0.3}$	...
$\phi_\parallel$ (rad)	$\arg\frac{\mathcal{A}_\parallel}{\mathcal{A}_L}$	$3.0^{+1.0+1.1+2.1+1.3+1.3+1.3}_{-0.0-0.1-0.1-0.0-0.0-0.0}$	...	$2.9^{+0.0+0.1+0.2+0.1+0.1+0.1}_{-0.0-0.0-0.1-0.0-0.0-0.0}$	...
$\phi_\perp$ (rad)	$\arg\frac{\mathcal{A}_\perp}{\mathcal{A}_L}$	$3.2^{+1.1+1.2+0.2+0.1+0.0+0.1}_{-0.0-0.2-0.4-0.2-0.1-0.2}$	...	$3.0^{+0.0+0.0+0.2+0.0+0.0+0.0}_{-0.0-0.2-0.3-0.1-0.1-0.1}$	...
$\mathcal{A}_{CP}^{\rm dir}(\%)$	$\frac{\bar{\Gamma}-\Gamma}{\bar{\Gamma}+\Gamma}$	$-52.9^{+4.2+3.0+12.7+1.9+7.5+1.0}_{-2.7-2.2-13.2-1.5-4.4-0.9}$	...	$-5.9^{+2.3+5.0+11.5+2.2+4.2+0.1}_{-2.6-5.9-10.8-4.0-3.8-0.2}$	...
$\mathcal{A}_{CP}^{\rm dir}(L)(\%)$	$\frac{\bar{f}_L-f_L}{\bar{f}_L+f_L}$	$17.7^{+7.0+11.3+18.7+6.9+26.0+0.7}_{-6.0-9.9-23.0-6.1-20.9-0.8}$	...	$-71.1^{+1.3+11.2+23.8+6.6+2.4+2.3}_{-0.5-10.0-26.2-7.0-3.2-2.1}$	...
$\mathcal{A}_{CP}^{\rm dir}(\parallel)(\%)$	$\frac{\bar{f}_\parallel-f_\parallel}{\bar{f}_\parallel+f_\parallel}$	$-99.0^{+2.4+1.1+3.4+0.6+1.0+0.6}_{-0.0-0.5-1.3-0.2-0.4-0.5}$	...	$61.7^{+3.1+5.1+6.9+3.3+4.2+1.8}_{-3.9-7.7-7.6-4.1-5.4-1.8}$	...
$\mathcal{A}_{CP}^{\rm dir}(\perp)(\%)$	$\frac{\bar{f}_\perp-f_\perp}{\bar{f}_\perp+f_\perp}$	$-97.8^{+3.6+1.9+3.7+1.1+1.8+1.0}_{-1.2-1.3-3.1-0.9-1.4-0.7}$	...	$62.5^{+2.5+4.2+6.0+2.8+4.2+1.7}_{-3.4-7.3-7.4-3.9-5.5-1.8}$	...

TABLE IX. Same as Table I but for $B_s^0 \to f_1\omega$ decays.

Decay modes		$B_s^0 \to f_1(1285)\omega$		$B_s^0 \to f_1(1420)\omega$	
Parameter	Definition	This work	QCDF	This work	QCDF
BR (10^{-7})	$\Gamma/\Gamma_{\rm total}$	$1.9^{+0.5+0.6+0.7+0.2+0.7+0.1}_{-0.3-0.4-0.3-0.1-0.4-0.0}$	⋯	$3.5^{+1.5+0.2+3.2+0.1+1.1+0.0}_{-1.1-0.3-2.2-0.2-0.8-0.1}$	⋯
$f_L(\%)$	$\lvert\mathcal{A}_L\rvert^2$	$81.8^{+1.1+4.0+10.0+2.6+0.1+0.2}_{-1.4-4.8-9.9-3.0-0.5-0.3}$	⋯	$50.9^{+4.0+0.6+3.4+0.4+0.3+0.6}_{-3.9-0.4-2.8-0.3-1.4-0.7}$	⋯
$f_\parallel(\%)$	$\lvert\mathcal{A}_\parallel\rvert^2$	$9.9^{+0.7+2.5+5.3+1.6+0.3+0.2}_{-0.6-2.1-5.5-1.4-0.1-0.2}$	⋯	$26.5^{+2.0+0.3+1.7+0.2+0.8+0.4}_{-2.1-0.3-2.2-0.2-0.1-0.3}$	⋯
$f_\perp(\%)$	$\lvert\mathcal{A}_\perp\rvert^2$	$8.3^{+0.6+2.2+4.5+1.4+0.3+0.2}_{-0.5-1.8-4.6-1.2-0.0-0.1}$	⋯	$22.6^{+1.8+0.1+1.1+0.1+0.6+0.3}_{-1.9-0.3-1.3-0.2-0.1-0.3}$	⋯
$\phi_\parallel$ (rad)	$\arg\frac{\mathcal{A}_\parallel}{\mathcal{A}_L}$	$3.9^{+0.0+0.0+0.4+0.0+0.0+0.0}_{-0.1-0.1-0.3-0.1-0.1-0.0}$	⋯	$2.7^{+0.0+0.1+0.3+0.0+0.0+0.0}_{-0.1-0.1-0.2-0.1-0.0-0.0}$	⋯
$\phi_\perp$ (rad)	$\arg\frac{\mathcal{A}_\perp}{\mathcal{A}_L}$	$3.9^{+0.0+0.0+0.4+0.0+0.0+0.0}_{-0.1-0.1-0.3-0.1-0.1-0.0}$	⋯	$2.7^{+0.1+0.1+0.3+0.1+0.0+0.0}_{-0.1-0.1-0.2-0.0-0.0-0.0}$	⋯
$\mathcal{A}_{CP}^{\rm dir}(\%)$	$\frac{\bar\Gamma-\Gamma}{\bar\Gamma+\Gamma}$	$10.9^{+1.1+0.9+2.0+0.5+0.3+0.4}_{-1.1-0.5-4.6-0.3-0.9-0.4}$	⋯	$29.5^{+2.0+0.8+13.9+0.6+3.9+1.1}_{-2.2-0.7-7.6-0.4-4.6-1.0}$	⋯
$\mathcal{A}_{CP}^{\rm dir}(L)(\%)$	$\frac{\bar f_L-f_L}{\bar f_L+f_L}$	$7.7^{+1.1+0.2+2.2+0.1+1.5+0.2}_{-1.1-0.1-3.8-0.0-2.2-0.3}$	⋯	$34.3^{+5.3+1.4+20.4+1.0+2.8+1.2}_{-4.7-1.5-11.1-0.9-3.4-1.2}$	⋯
$\mathcal{A}_{CP}^{\rm dir}(\parallel)(\%)$	$\frac{\bar f_\parallel-f_\parallel}{\bar f_\parallel+f_\parallel}$	$23.5^{+0.1+0.1+5.3+0.1+4.7+1.1}_{-0.1-0.0-3.7-0.0-5.2-0.9}$	⋯	$23.9^{+0.1+0.0+6.5+0.0+4.7+1.0}_{-0.2-0.0-4.1-0.0-5.4-1.1}$	⋯
$\mathcal{A}_{CP}^{\rm dir}(\perp)(\%)$	$\frac{\bar f_\perp-f_\perp}{\bar f_\perp+f_\perp}$	$27.6^{+0.0+0.3+7.6+0.2+5.3+1.1}_{-0.3-0.4-5.0-0.3-6.2-1.2}$	⋯	$25.4^{+0.0+0.1+5.2+0.1+5.2+1.1}_{-0.1-0.1-4.2-0.0-5.9-1.1}$	⋯

TABLE X. Same as Table I but for $B_s^0 \to f_1\phi$ decays.

Decay modes		$B_s^0 \to f_1(1285)\phi$		$B_s^0 \to f_1(1420)\phi$	
Parameter	Definition	This work	QCDF	This work	QCDF
BR (10^{-6})	$\Gamma/\Gamma_{\rm total}$	$14.7^{+6.1+3.3+3.0+1.7+3.9+0.1}_{-4.1-2.7-2.6-1.4-2.8-0.0}$	⋯	$16.2^{+5.9+2.0+7.4+1.3+1.8+0.0}_{-4.1-1.9-5.7-1.6-1.6-0.0}$	⋯
$f_L(\%)$	$\lvert\mathcal{A}_L\rvert^2$	$56.7^{+0.6+2.4+3.2+1.5+0.6+0.1}_{-0.4-2.3-3.7-1.5-1.0-0.1}$	⋯	$82.1^{+1.8+2.0+3.2+1.1+2.4+0.1}_{-1.9-1.8-3.1-0.9-3.6-0.0}$	⋯
$f_\parallel(\%)$	$\lvert\mathcal{A}_\parallel\rvert^2$	$23.7^{+0.2+1.2+1.9+0.7+0.5+0.0}_{-0.3-1.3-1.9-0.8-0.4-0.1}$	⋯	$10.5^{+1.1+1.0+1.8+0.5+2.1+0.0}_{-1.0-1.1-1.7-0.6-1.4-0.0}$	⋯
$f_\perp(\%)$	$\lvert\mathcal{A}_\perp\rvert^2$	$19.6^{+0.2+1.2+1.7+0.7+0.5+0.1}_{-0.3-1.1-1.4-0.7-0.2-0.0}$	⋯	$7.4^{+0.8+0.7+1.4+0.4+1.5+0.0}_{-0.8-0.9-1.5-0.5-1.0-0.0}$	⋯
$\phi_\parallel$ (rad)	$\arg\frac{\mathcal{A}_\parallel}{\mathcal{A}_L}$	$2.9^{+0.1+0.0+0.1+0.0+0.0+0.0}_{-0.0-0.0-0.0-0.0-0.0-0.0}$	⋯	$2.6^{+0.0+0.0+0.2+0.0+0.0+0.0}_{-0.0-0.0-0.0-0.0-0.0-0.0}$	⋯
$\phi_\perp$ (rad)	$\arg\frac{\mathcal{A}_\perp}{\mathcal{A}_L}$	$2.9^{+0.1+0.1+0.1+0.0+0.0+0.0}_{-0.0-0.0-0.0-0.0-0.0-0.0}$	⋯	$2.6^{+0.0+0.0+0.2+0.0+0.0+0.0}_{-0.0-0.0-0.0-0.0-0.0-0.0}$	⋯
$\mathcal{A}_{CP}^{\rm dir}(\%)$	$\frac{\bar\Gamma-\Gamma}{\bar\Gamma+\Gamma}$	$-5.3^{+0.3+0.7+0.7+0.4+0.8+0.2}_{-0.2-0.4-0.5-0.3-0.7-0.1}$	⋯	$2.5^{+0.1+0.7+0.4+0.5+0.2+0.1}_{-0.1-0.6-0.4-0.4-0.3-0.1}$	⋯
$\mathcal{A}_{CP}^{\rm dir}(L)(\%)$	$\frac{\bar f_L-f_L}{\bar f_L+f_L}$	$-7.2^{+0.5+1.1+1.2+0.7+0.9+0.3}_{-0.4-1.0-1.1-0.6-1.0-0.2}$	⋯	$2.4^{+0.1+0.6+0.4+0.4+0.5+0.1}_{-0.1-0.5-0.4-0.3-0.2-0.1}$	⋯
$\mathcal{A}_{CP}^{\rm dir}(\parallel)(\%)$	$\frac{\bar f_\parallel-f_\parallel}{\bar f_\parallel+f_\parallel}$	$-2.7^{+0.1+0.3+0.4+0.1+0.4+0.1}_{-0.0-0.1-0.3-0.0-0.3-0.1}$	⋯	$2.6^{+0.1+1.1+0.2+0.7+0.3+0.1}_{-0.1-0.7-0.4-0.4-0.2-0.1}$	⋯
$\mathcal{A}_{CP}^{\rm dir}(\perp)(\%)$	$\frac{\bar f_\perp-f_\perp}{\bar f_\perp+f_\perp}$	$-2.8^{+0.0+0.2+0.4+0.1+0.4+0.1}_{-0.0-0.1-0.4-0.1-0.4-0.1}$	⋯	$3.1^{+0.2+1.1+0.2+0.9+0.4+0.1}_{-0.1-0.9-0.4-0.6-0.3-0.1}$	⋯

TABLE XI. The decay amplitudes (in units of 10^{-3} GeV^3) of the $B^+ \to f_{1q}\rho^+$ and $B^+ \to f_{1s}\rho^+$ channels in the $B^+ \to f_1\rho^+$ decays with three polarizations in the pQCD approach, where only the central values are quoted for clarification. Note that the numerical results in the parentheses are the corresponding amplitudes without annihilation contributions.

Decay modes	$B^+ \to f_1(1285)\rho^+$		$B^+ \to f_1(1420)\rho^+$	
Channels	$B^+ \to \rho^+ f_{1q}$	$B^+ \to \rho^+ f_{1s}$	$B^+ \to \rho^+ f_{1q}$	$B^+ \to \rho^+ f_{1s}$
A_L	$-2.217 - i3.790$	$-0.127 + i0.058$	$-0.987 - i1.688$	$0.285 - i0.131$
	$(-2.359 - i3.718)$	$(-0.127 + i0.058)$	$(-1.050 - i1.655)$	$(0.285 - i0.131)$
A_N	$-0.166 - i0.424$	$-0.089 + i0.041$	$-0.073 - i0.187$	$0.201 - i0.091$
	$(-0.179 - i0.447)$	$(-0.089 + i0.041)$	$(-0.079 - i0.197)$	$(0.201 - i0.091)$
A_T	$-0.224 - i0.757$	$-0.184 + i0.080$	$-0.107 - i0.331$	$0.413 - i0.180$
	$(-0.325 - i0.810)$	$(-0.184 + i0.080)$	$(-0.152 - i0.355)$	$(0.413 - i0.180)$

TABLE XII. Same as Table XI but for $B^+ \to f_1 K^{*+}$ decays.

Decay modes	$B^+ \to f_1(1285)K^{*+}$		$B^+ \to f_1(1420)K^{*+}$	
Channels	$B^+ \to K^{*+} f_{1q}$	$B^+ \to K^{*+} f_{1s}$	$B^+ \to K^{*+} f_{1q}$	$B^+ \to K^{*+} f_{1s}$
A_L	$0.284 - i1.423$	$-0.679 - i0.791$	$0.127 - i0.634$	$1.524 + i1.776$
	$(0.292 - i0.832)$	$(-0.672 - i0.224)$	$(0.130 - i0.370)$	$(1.510 + i0.502)$
A_N	$-1.078 + i0.436$	$-0.089 + i0.446$	$-0.465 + i0.188$	$0.200 - i1.003$
	$(-0.747 - i0.123)$	$(0.127 - i0.027)$	$(-0.318 - i0.060)$	$(-0.285 + i0.062)$
A_T	$-2.166 + i0.866$	$-0.152 + i0.896$	$-0.965 + i0.386$	$0.340 - i2.013$
	$(-1.509 - i0.281)$	$(0.287 - i0.043)$	$(-0.672 - i0.125)$	$(-0.643 + i0.097)$

$\mathrm{Br}(B^+ \to f_1(1285)[f_1(1420)]\rho^+)_{\mathrm{pQCD}}$ is more like $\mathrm{Br}(B^+ \to \omega[\phi]\rho^+)$. However, relative to $B^+ \to \phi\rho^+$ decay, the $B^+ \to f_1(1420)\rho^+$ mode receives an extra and significant interference from the dominant factorizable $B^+ \to f_{1q}$ transition with a factor $(\sin\phi_{f_1}) \sim 0.4$, which finally results in a larger $\mathrm{Br}(B^+ \to f_1(1420)\rho^+)$ than $\mathrm{Br}(B^+ \to \phi\rho^+)$ as it should be. Careful analysis of the decay amplitudes with three polarizations presented in Table XI confirms the above-mentioned arguments.

The $B^+ \to f_1\rho^+$ decays have been investigated within the framework of the QCDF approach [3].[2] The branching ratios were predicted as follows:

$$\mathrm{Br}(B^+ \to f_1(1285)\rho^+)_{\mathrm{QCDF}} = 8.9^{+5.1}_{-3.2} \times 10^{-6},$$
$$\mathrm{Br}(B^+ \to f_1(1420)\rho^+)_{\mathrm{QCDF}} = 1.3^{+0.6}_{-0.3} \times 10^{-6}, \quad (92)$$

where the errors are also added in quadrature. Note that, as discussed in Ref. [18], the QCDF predictions only with the mixing angle $\theta_{^3P_1} \sim 53.2°$ are basically consistent with the pQCD ones for $B^{+,0} \to f_1 P$ decay rates. Therefore, as listed in Eq. (92), we still quote the theoretical predictions for $B \to f_1 V$ decays with $\theta_{^3P_1} \sim 53.2°$ to make concrete comparisons with those in the pQCD approach. One can easily observe the good agreement of the $B^+ \to f_1\rho^+$ decay rates predicted in both the QCDF and pQCD approaches within uncertainties.

(4) According to Table II, the CP-averaged branching ratios of $B^+ \to f_1 K^{*+}$ decays can be written as

$$\mathrm{Br}(B^+ \to f_1(1285)K^{*+})_{\mathrm{pQCD}} = 6.4^{+3.6}_{-2.5} \times 10^{-6},$$
$$\mathrm{Br}(B^+ \to f_1(1420)K^{*+})_{\mathrm{pQCD}} = 4.5^{+1.7}_{-1.5} \times 10^{-6}. \quad (93)$$

Here, we have added all the errors in quadrature. For the former $B^+ \to f_1(1285)K^{*+}$ decay, our predicted branching ratio is in good consistency with the value $5.7^{+21.7}_{-5.3} \times 10^{-6}$ derived in the QCDF approach within theoretical errors. Generally speaking, in light of the constructive or destructive interference between $f_{1q}V$ and $f_{1s}V$ states, the latter $\mathrm{Br}(B^+ \to f_1(1420)K^{*+})$ is naturally expected to be larger or smaller than $\mathrm{Br}(B^+ \to f_1(1285)K^{*+})$ in principle. Although $\mathrm{Br}(B^+ \to f_1(1285)K^{*+})_{\mathrm{pQCD}}$ is, in terms of the central values, somewhat larger than $\mathrm{Br}(B^+ \to f_1(1420)K^{*+})_{\mathrm{pQCD}}$, the pQCD predictions of the $B^+ \to f_1 K^{*+}$ decay rates within errors are approximately equivalent to each other in this work, which make a sharp contrast to the pattern obtained in the framework of QCDF. The authors predicted the $B^+ \to f_1(1420)K^{*+}$ branching fraction as $\mathrm{Br}(B^+ \to f_1(1420)K^{*+})_{\mathrm{QCDF}} = 15.6^{+15.1}_{-7.0} \times 10^{-6}$ [3]. It seems that the predicted branching ratio for $B^+ \to f_1(1420)K^{*+}$ indicates a strongly constructive (moderately destructive) interference in QCDF (pQCD) between $B^+ \to f_{1q}K^{*+}$ and $B^+ \to f_{1s}K^{*+}$ channels. In order to understand the branching ratios of $B^+ \to f_1 K^{*+}$ decays, different from those QCDF predictions, the numerical values of decay amplitudes are presented in Table XII explicitly involving three polarizations within the pQCD framework. One can easily see the dominated $B^+ \to f_{1q}K^{*+}(B^+ \to f_{1s}K^{*+})$ contributions induced by the dominance of $f_{1q}(f_{1s})$ in the $f_1(1285)[f_1(1420)]$ state [see Eq. (1) with $\phi_{f_1} \sim 24°$] and the moderately constructive (destructive) interferences between $B^+ \to f_{1q}K^{*+}$ and $B^+ \to f_{1s}K^{*+}$ in the $B^+ \to f_1(1285)[f_1(1420)]K^{*+}$ decays in the pQCD approach.

However, it should be pointed out that when the very large errors are taken into account, $\mathrm{Br}(B^+ \to f_1(1285)K^{*+})_{\mathrm{QCDF}} \sim \mathrm{Br}(B^+ \to f_1(1420)K^{*+})_{\mathrm{QCDF}}$ can be observed. Moreover, objectively speaking, as discussed in Ref. [5], different predictions of $B \to VV$ decays have been theoretically obtained by fitting the parameters through different well-measured channels such as $B \to \phi K^*$ [7] and $B \to \rho K^*$ [3,5],

[2] In light of the crude predictions given in Ref. [26] and the consistent results presented in Refs. [14] and [18] for the branching ratios of $B \to f_1 P$ decays, we will mainly focus on the theoretical predictions of $B^{+,0} \to f_1 V$ modes obtained with QCDF and make comprehensive analyses and comparisons in this work.

respectively, because of inevitable end-point singularities in the framework of QCDF. This indefiniteness may render misunderstandings of the dynamics involved in these kinds of decays with polarizations. It will be very interesting and probably a challenge for the theorists to further understand the QCD dynamics of axial-vector f_1 mesons and the decay mechanism of $B \to f_1 K^*$ with helicity in depth once the experiments at LHCb and/or Belle-II confirm the aforementioned decay rates and decay pattern in the near future.

Similar phenomena also occur in the $B^0 \to f_1 K^{*0}$ modes (see Table IV), in which few contributions arising from the color-suppressed tree amplitudes are involved. Specifically, the branching ratios will numerically decrease (increase) from $6.43(4.46) \times 10^{-6}$ to $5.65(4.61) \times 10^{-6}$ for $B^+ \to f_1(1285)[f_1(1420)]K^{*+}$ decay, and increase (decrease) from $4.96(4.37) \times 10^{-6}$ to $5.08(4.34) \times 10^{-6}$ for the $B^0 \to f_1(1285)[f_1(1420)]K^{*0}$ mode, when the contributions induced by tree operators are turned off. The stringent tests on the CP-averaged branching ratios for $B \to f_1 K^*$ decays predicted in the QCDF and pQCD approaches may provide an experimental check on these two competing frameworks.

(5) As discussed in Refs. [3,27], the behavior of axial-vector $^3P_1$ states is similar to that of vector mesons, which will consequently result in the branching ratio of $B \to f_1(1285)[f_1(1420)]K^*$ analogous to that of $B \to \omega[\phi]K^*$ decays in the pQCD approach as expected, if the $f_1(1285)[f_1(1420)]$ state is almost governed by the $f_{1q}(f_{1s})$ component. However, from Tables II, IV, and XII, it can be clearly observed that the predicted branching ratios of $B \to f_1(1285)[f_1(1420)]K^*$ decays in this work are larger (smaller) than those of $B \to \omega[\phi]K^*$ decays [5–8]. The underlying reason is that, for the $B^0 \to f_1(1285)[f_1(1420)]K^{*0}$ mode for example, a constructive (destructive) interference arising from $B^0 \to f_{1s}[f_{1q}]K^{*0}$ (as can be seen in Table XII) with a factor $\sin\phi_{f_1} \sim 0.4$ will enhance (reduce) the amplitude of $B^0 \to f_{1q}[f_{1s}]K^{*0}$, which finally leads to somewhat larger (smaller) branching ratio $5.0^{+2.7}_{-2.1}[4.4^{+1.7}_{-1.5}] \times 10^{-6}$ than that of $B^0 \to \omega[\phi]K^{*0}$, with $2.0^{+3.1}_{-1.4}[9.3^{+11.4}_{-6.5}] \times 10^{-6}$ in [7], $2.5^{+2.5}_{-1.6}[9.5^{+12.0}_{-6.0}] \times 10^{-6}$ in [5], $4.7^{+2.6}_{-2.0}[9.8^{+4.9}_{-3.8}] \times 10^{-6}$ in [6], and $2.0 \pm 0.5[10.0 \pm 0.5] \times 10^{-6}$ in [8], respectively.

(6) The CP-averaged branching ratios for penguin-dominated $B^0 \to f_1\rho^0$, color-suppressed tree-dominated $B^0 \to f_1\omega$, and pure penguin $B^0 \to f_1\phi$ decays with the CKM suppressed $\bar{b} \to \bar{d}$ transition in the pQCD approach have been given in Tables III, V, and VI, in which only $B^0 \to f_1(1285)\omega$ has a large and measurable decay rate, $1.0^{+0.6}_{-0.4} \times 10^{-6}$, and the other five decays have such small branching ratios in the range of $10^{-9} - 10^{-7}$ that it is hard to detect them precisely in a short period. Note that the ideal mixing has been assumed for ω and ϕ mesons, i.e., $\omega \equiv (u\bar{u} + d\bar{d})/\sqrt{2}$ and $\phi \equiv s\bar{s}$. By employing the same distribution amplitudes but with slightly different decay constants for ρ and ω, the corresponding $(u\bar{u} - d\bar{d})/\sqrt{2}$ and $(u\bar{u} + d\bar{d})/\sqrt{2}$ components have dramatically different effects, i.e., being destructive (constructive) to $B^0 \to f_1\rho^0(\omega)$ decays. Together with interferences at different levels between $f_{1q}(\rho^0, \omega)$ and $f_{1s}(\rho^0, \omega)$, we finally obtain $\mathrm{Br}(B^0 \to f_1(1285)\rho^0)_{\mathrm{pQCD}} \gtrsim \mathrm{Br}(B^0 \to f_1(1420)\rho^0)_{\mathrm{pQCD}}$ and $\mathrm{Br}(B^0 \to f_1(1285)\omega)_{\mathrm{pQCD}} > \mathrm{Br}(B^0 \to f_1(1420)\omega)_{\mathrm{pQCD}}$ within uncertainties, but with a very consistent decay rate and decay pattern as given in the QCDF approach. Careful analysis shows that $B^0 \to f_1\rho^0$ decays only include negligible color-suppressed tree contributions. For the $B^0 \to f_1\phi$ mode, the CP-averaged branching ratios predicted in the pQCD approach are $8.9^{+5.5}_{-3.8} \times 10^{-9}$ and $3.7^{+2.8}_{-2.4} \times 10^{-9}$, respectively, which are basically consistent with but slightly larger than those obtained in the QCDF approach.

(7) As shown in Tables VII–X, the $B_s^0 \to f_1 V$ decays are studied for the first time in the literature. The CP-averaged branching ratios of $B_s^0 \to f_1(\rho^0, \omega, \overline{K}^{*0})$ predicted in the pQCD approach are of the order of 10^{-7} within large theoretical errors, apart from $B_s^0 \to f_1\phi$ modes with large decay rates around $\mathcal{O}(10^{-5})$. In light of the measurements of $B_d^0 \to K^+K^-$ with decay rate $1.3 \pm 0.5 \times 10^{-7}$ and $B_s^0 \to \pi^+\pi^-$ with branching ratio $7.6 \pm 1.9 \times 10^{-7}$ [8,44,45], it is therefore expected that the above-mentioned $B_s^0 \to f_1 V$ decay modes can be generally accessed at the running of LHCb and the forthcoming Belle-II experiments with a large number of $B_s^0\overline{B}_s^0$ events in the near future. The interferences between $B_s^0 \to f_{1q}V$ and $B_s^0 \to f_{1s}V$ channels lead to the following relations in $B_s^0 \to f_1 V$ decays with errors:

$$\begin{aligned}
&\mathrm{Br}(B_s^0 \to f_1(1285)(\rho^0, \omega))_{\mathrm{pQCD}} \\
&\quad < \mathrm{Br}(B_s^0 \to f_1(1420)(\rho^0, \omega))_{\mathrm{pQCD}}, \\
&\mathrm{Br}(B_s^0 \to f_1(1285)(\overline{K}^{*0}, \phi))_{\mathrm{pQCD}} \\
&\quad \sim \mathrm{Br}(B_s^0 \to f_1(1420)(\overline{K}^{*0}, \phi))_{\mathrm{pQCD}}. \qquad (94)
\end{aligned}$$

Note that, unlike $B^0 \to f_1(\rho^0, \omega)$ decays, $B_s^0 \to f_1(\rho^0, \omega)$ ones are all governed by the penguin-dominated amplitudes with very small,

color-suppressed tree contributions. Because of dominant factorizable emission contributions with a $B_s^0 \to f_{1s}$ transition and no $B_s^0 \to (\rho^0, \omega)$ transition, $\mathrm{Br}(B_s^0 \to f_1(1285)(\rho^0, \omega))$ is smaller than $\mathrm{Br}(B_s^0 \to f_1(1420)(\rho^0, \omega))$ as a naive expectation. Relative to CKM-favored $B \to f_1 K^*$ decays, the $B_s^0 \to f_1 \overline{K}^{*0}$ ones have significantly smaller branching ratios because they involve a suppressed factor 0.22 in the decay amplitudes. The penguin-dominated $B_s^0 \to f_1\phi$ decays with negligibly small color-suppressed tree amplitudes have the branching ratios as $14.7^{+8.7}_{-6.4} \times 10^{-6}$ and $16.2^{+9.9}_{-7.6} \times 10^{-6}$, respectively. When the tree contaminations are turned off, the decay rates become 14.9×10^{-6} and 16.1×10^{-6}, correspondingly, as far as the central values are concerned. As shown in Table XIV, one can easily observe that the overall constructive (destructive) interferences in three polarizations between $B_s^0 \to f_{1q}\phi$ and $B_s^0 \to f_{1s}\phi$ modes result in the approximately equivalent CP-averaged branching ratios as mentioned previously. Furthermore, the dominance of the $B_s^0 \to f_{1s}\phi$ channel leads to a decay rate of $B_s^0 \to f_1(1420)\phi$ similar to that of $B_s^0 \to \phi\phi$ [6], while the comparable $B_s^0 \to f_{1q}\phi$ and $B_s^0 \to f_{1s}\phi$ with constructive effects make $\mathrm{Br}(B_s^0 \to f_1(1285)\phi)$ highly different from $\mathrm{Br}(B_s^0 \to \omega\phi)$, with a factor around $\mathcal{O}(10^2)$, which will be tested by the near future LHCb and/or Belle-II measurements. Because of the possibilities of new discoveries, the search for NP in the B_s system will be the main focus of the forthcoming experiments at LHCb and Belle-II. Several charmless penguin-dominated B_s decays such as $B_s^0 \to \phi\phi$ can provide ideal places to search for NP. In light of the similar behavior between f_1 and ϕ and the comparable and large decay rates between $B_s^0 \to f_1\phi$ and $B_s^0 \to \phi\phi$, it is therefore expected that the $B_s^0 \to f_1\phi$ decays can provide effective constraints on the $B_s^0 - \overline{B}_s^0$ mixing phase, CKM unitary triangle, and even NP signals complementarily.

(8) Frankly speaking, as can easily be seen in Tables I–X, the theoretical predictions calculated in the pQCD approach suffer from large errors induced by the still less constrained uncertainties in the light-cone distribution amplitudes involved in both initial and final states. Here, we then define some interesting ratios of the branching ratios for the selected decay modes. As generally expected, if the selected decay modes in a ratio have similar dependence on a specific input parameter, the error induced by the uncertainty of this input parameter will be largely canceled in the ratio, even if one cannot make an explicit factorization for this parameter. From the experimental side, we know that the ratios of the branching ratios generally could be measured with a better accuracy than that for individual branching ratios. For the sake of the possibility of the experimental measurements, we here define the following nine ratios out of the branching ratios of ten decay modes, i.e., $B^+ \to f_1\rho^+$, $B^{+,0} \to f_1 K^{*+,0}$, $B^0 \to f_1\omega$, and $B_s \to f_1\phi$, with relatively large branching ratios around 10^{-6}:

$$R^u_{f_1\rho} \equiv \frac{\mathrm{Br}(B^+ \to f_1(1285)\rho^+)}{\mathrm{Br}(B^+ \to f_1(1420)\rho^+)} = 4.81^{+0.21}_{-0.35},$$
$$R^u_{f_1K^*} \equiv \frac{\mathrm{Br}(B^+ \to f_1(1285)K^{*+})}{\mathrm{Br}(B^+ \to f_1(1420)K^{*+})} = 1.44^{+0.69}_{-0.56}, \tag{95}$$

$$R^d_{f_1K^*} \equiv \frac{\mathrm{Br}(B^0 \to f_1(1285)K^{*0})}{\mathrm{Br}(B^0 \to f_1(1420)K^{*0})} = 1.14^{+0.54}_{-0.47},$$
$$R^d_{f_1\omega} \equiv \frac{\mathrm{Br}(B^0 \to f_1(1285)\omega)}{\mathrm{Br}(B^0 \to f_1(1420)\omega)} = 5.29^{+0.58}_{-0.71}, \tag{96}$$

$$R^s_{f_1\phi} \equiv \frac{\mathrm{Br}(B_s^0 \to f_1(1285)\phi)}{\mathrm{Br}(B_s^0 \to f_1(1420)\phi)} = 0.91^{+0.40}_{-0.30}; \tag{97}$$

$$R^{uu}_{\rho/K^*}[f_1(1285)] \equiv \frac{\mathrm{Br}(B^+ \to f_1(1285)\rho^+)}{\mathrm{Br}(B^+ \to f_1(1285)K^{*+})} = 1.72^{+0.86}_{-0.88}, \tag{98}$$

$$R^{uu}_{\rho/K^*}[f_1(1420)] \equiv \frac{\mathrm{Br}(B^+ \to f_1(1420)\rho^+)}{\mathrm{Br}(B^+ \to f_1(1420)K^{*+})} = 0.52^{+0.36}_{-0.32}, \tag{99}$$

$$R^{sd}_{\phi/K^*}[f_1(1285)] \equiv \frac{\mathrm{Br}(B_s^0 \to f_1(1285)\phi)}{\mathrm{Br}(B^0 \to f_1(1285)K^{*0})} = 2.97^{+1.16}_{-0.94}, \tag{100}$$

$$R^{sd}_{\phi/K^*}[f_1(1420)] \equiv \frac{\mathrm{Br}(B_s^0 \to f_1(1420)\phi)}{\mathrm{Br}(B^0 \to f_1(1420)K^{*0})} = 3.71^{+0.86}_{-0.90}, \tag{101}$$

where the individual errors have been added in quadrature. One can see from the numerical results in the above equations that the total error has been reduced to ~10% for the ratio $R^u_{f_1\rho}$, but still remains large, around ~70%, for the ratio $R^{uu}_{\rho/K^*}[f_1(1420)]$. These ratios will be tested by future precise B meson experiments and could be used to explore the flavor symmetry in these modes and to further determine the mixing angle ϕ_{f_1} between f_{1q} and f_{1s} states in the quark-flavor basis. Note that the variations of hadronic parameters in ρ, K^*, and ϕ distribution

amplitudes are not considered in the last four ratios for convenience.

B. *CP*-averaged polarization fractions and relative phases

In this section we will analyze the *CP*-averaged polarization fractions and relative phases for 20 nonleptonic $B \to f_1 V$ decays in the pQCD approach. Based on the helicity amplitudes, we can define the transversity ones as follows:

$$\mathcal{A}_L = \xi m_B^2 A_L, \qquad \mathcal{A}_\parallel = \xi\sqrt{2} m_B^2 A_N,$$
$$\mathcal{A}_\perp = \xi m_V m_{f_1}\sqrt{2(r^2-1)} A_T, \tag{102}$$

for the longitudinal, parallel, and perpendicular polarizations, respectively, with the normalization factor $\xi = \sqrt{G_F^2 P_c/(16\pi m_B^2\Gamma)}$ and the ratio $r = P_2\cdot P_3/(m_V\cdot m_{f_1})$. These amplitudes satisfy the relation

$$|\mathcal{A}_L|^2 + |\mathcal{A}_\parallel|^2 + |\mathcal{A}_\perp|^2 = 1, \tag{103}$$

following the summation in Eq. (89). Since the transverse-helicity contributions can manifest themselves through polarization observables, we therefore define *CP*-averaged fractions in three polarizations f_L, $f_\parallel$, and $f_\perp$ as the following,

$$f_{L,\parallel,\perp} \equiv \frac{|\mathcal{A}_{L,\parallel,\perp}|^2}{|\mathcal{A}_L|^2 + |\mathcal{A}_\parallel|^2 + |\mathcal{A}_\perp|^2} = |\mathcal{A}_{L,\parallel,\perp}|^2. \tag{104}$$

With the above transversity amplitudes shown in Eq. (102), the relative phases $\phi_\parallel$ and $\phi_\perp$ can be defined as

$$\phi_\parallel = \arg\frac{\mathcal{A}_\parallel}{\mathcal{A}_L}, \qquad \phi_\perp = \arg\frac{\mathcal{A}_\perp}{\mathcal{A}_L}. \tag{105}$$

As aforementioned, by picking up higher power r_i^2 terms that were previously neglected, especially in the virtual gluon and/or quark propagators, the global agreement with data for $B \to VV$ decays has been greatly improved in the pQCD approach theoretically [6]. In particular, the polarization fractions for penguin-dominated $B \to VV$ decays contributed from large transverse amplitudes are well understood with this improvement. In the present work, we followed this treatment in charmless hadronic $B \to f_1 V$ decays. The theoretical predictions of polarization fractions and relative phases have been collected in Tables I–X within errors. Based on these numerical results, some remarks are given as follows:

(i) Overall, as can straightforwardly be seen in Tables I–X, the decays with large longitudinal polarization contributions include $B^+ \to f_1\rho^+$, $B^{+,0} \to f_1(1420)K^{*+,0}$, $B^0 \to f_1(1285)(\rho^0,\omega)$, $B^0 \to f_1\phi$, $B_s^0 \to f_1\rho^0$, $B_s^0 \to f_1(1285)\omega$, and $B_s^0 \to f_1(1420)\phi$, while the $B^{+,0} \to f_1(1285)K^{*+,0}$, $B^0 \to f_1(1420)\rho^0$, and $B_s^0 \to f_1(1285)\overline{K}^{*0}$ modes are governed by large transverse contributions. The other channels, such as $B_{(s)}^0 \to f_1(1420)\omega$, $B_s^0 \to f_1(1420)\overline{K}^{*0}$, and $B_s^0 \to f_1(1285)\phi$, have longitudinal polarization fractions around 50%, competing with transverse ones within theoretical uncertainties. These predicted *CP*-averaged polarization fractions will be tested at LHCb and/or Belle-II to further explore the decay mechanism with helicities associated with experimental confirmations on the decay rates.

(ii) Theoretically, the pQCD predictions of polarization fractions f_L and $f_T(=f_\parallel + f_\perp = 1 - f_L)$ for $B^+ \to f_1\rho^+$ modes are

$$f_L(B^+ \to f_1(1285)\rho^+) = 96.3^{+0.5}_{-0.4}\%,$$
$$f_T(B^+ \to f_1(1285)\rho^+) = 3.7^{+0.3}_{-0.3}\%; \tag{106}$$

$$f_L(B^+ \to f_1(1420)\rho^+) = 90.5^{+3.1}_{-5.1}\%,$$
$$f_T(B^+ \to f_1(1420)\rho^+) = 9.5^{+3.5}_{-2.4}\%. \tag{107}$$

In the QCDF approach, the longitudinal polarization fractions for $B^+ \to f_1\rho^+$ decays have also been available as follows [3]:

$$f_L(B^+ \to f_1(1285)\rho^+) = 90^{+4}_{-3}\%,$$
$$f_L(B^+ \to f_1(1420)\rho^+) = 93^{+4}_{-3}\%. \tag{108}$$

It is obvious to see that the fractions predicted in both pQCD and QCDF approaches are consistent with each other within errors, which will be further examined by combining with large *CP*-averaged branching ratios through the LHCb and/or Belle-II measurements in the near future. As a matter of fact, the studies on color-allowed tree-dominated *B* decays in the pQCD approach usually agree with those in the QCDF one within theoretical uncertainties, e.g., $B^0 \to \rho^+\rho^-$ [5,6]. But, it is not the case in penguin-dominated and weak-annihilation-dominated modes.

(iii) For penguin-dominated $B^{+,0} \to f_1 K^{*+,0}$ decays with a $\overline{b} \to \overline{s}$ transition, one can find the polarization fractions from Tables II and IV predicted in the pQCD approach as follows:

$$f_L(B^+ \to f_1(1285)K^{*+}) = 23.5^{+5.8}_{-4.0}\%,$$
$$f_T(B^+ \to f_1(1285)K^{*+}) = 76.5^{+2.9}_{-4.1}\%; \tag{109}$$

$$f_L(B^+ \to f_1(1420)K^{*+}) = 69.3^{+11.4}_{-12.5}\%,$$
$$f_T(B^+ \to f_1(1420)K^{*+}) = 30.7^{+8.5}_{-8.0}\%, \tag{110}$$

and

$$f_L(B^0 \to f_1(1285)K^{*0}) = 15.8^{+6.7}_{-3.4}\%,$$
$$f_T(B^0 \to f_1(1285)K^{*0}) = 84.2^{+2.5}_{-4.8}\%; \quad (111)$$

$$f_L(B^0 \to f_1(1420)K^{*0}) = 71.0^{+12.0}_{-13.1}\%,$$
$$f_T(B^0 \to f_1(1420)K^{*0}) = 29.0^{+9.4}_{-8.6}\%, \quad (112)$$

which show the pattern of polarization fractions in the pQCD approach,

$$f_L(B^{+,0} \to f_1(1285)K^{*+,0}) < f_T(B^{+,0} \to f_1(1285)K^{*+,0}),$$
$$f_L(B^{+,0} \to f_1(1420)K^{*+,0}) > f_T(B^{+,0} \to f_1(1420)K^{*+,0}), \quad (113)$$

and

$$f_L(B^{+,0} \to f_1(1285)K^{*+,0}) < f_L(B^{+,0} \to f_1(1420)K^{*+,0}),$$
$$f_T(B^{+,0} \to f_1(1285)K^{*+,0}) > f_T(B^{+,0} \to f_1(1420)K^{*+,0}). \quad (114)$$

The decay amplitudes with three polarizations presented in Table XII show that, for $B^{+,0} \to f_1(1285)[f_1(1420)]K^{*+,0}$ decays, the significantly constructive (destructive) interferences in transverse polarizations between $B^{+,0} \to f_{1q}K^{*+,0}$ and $B^{+,0} \to f_{1s}K^{*+,0}$ finally result in somewhat smaller (larger) longitudinal polarization fractions, correspondingly, although the cancellations of the real (imaginary) decay amplitudes occur at different levels in the longitudinal polarization.

In Ref. [3], the authors predicted longitudinal polarization fractions for the $B^{+,0} \to f_1K^{*+,0}$ modes in the QCDF approach as follows:

$$f_L(B^+ \to f_1(1285)K^{*+}) = 47^{+49}_{-45}\%,$$
$$f_L(B^+ \to f_1(1420)K^{*+}) = 64^{+37}_{-61}\%, \quad (115)$$

and

$$f_L(B^0 \to f_1(1285)K^{*0}) = 45^{+55}_{-50}\%,$$
$$f_L(B^0 \to f_1(1420)K^{*0}) = 64^{+38}_{-61}\%, \quad (116)$$

which show the longitudinal polarization fractions roughly competing with the transverse ones for $B^{+,0} \to f_1K^{*+,0}$ and the relation $f_L(B^{+,0} \to f_1(1285)K^{*+,0}) \sim f_L(B^{+,0} \to f_1(1420)K^{*+,0})$ within large theoretical errors, though, as far as central values are concerned, the same pattern as in Eqs. (113) and (114) can also be obtained in the QCDF framework.

However, with the same $\bar{b} \to \bar{s}$ transition, the almost pure penguin $B_s^0 \to f_1\phi$ decays are dominated by longitudinal contributions with the polarization fractions as

$$f_L(B_s^0 \to f_1(1285)\phi) = 56.7^{+4.4}_{-4.7}\%,$$
$$f_T(B_s^0 \to f_1(1285)\phi) = 43.3^{+3.3}_{-3.2}\%; \quad (117)$$

$$f_L(B_s^0 \to f_1(1420)\phi) = 82.1^{+4.9}_{-5.5}\%,$$
$$f_T(B_s^0 \to f_1(1420)\phi) = 17.9^{+4.0}_{-3.2}\%, \quad (118)$$

which are different from $B^{+,0} \to f_1K^{*+,0}$ decays, apart from the similar pattern $f_L(B_s^0 \to f_1(1285)\phi) < f_L(B_s^0 \to f_1(1420)\phi)$. To our best knowledge, $B_s^0 \to f_1V$ decays in this paper are indeed investigated theoretically for the first time in the literature. It is therefore expected that these polarization fractions combined with large CP-averaged branching ratios of the order of 10^{-5} will be tested soon at the LHCb and/or Belle-II experiments with a large amount of events of $B_s\overline{B}_s$ production.

(iv) For $B^0 \to f_1(\rho^0, \omega, \phi)$ decays with $\bar{b} \to \bar{d}$ transition, the polarization fractions have also been predicted in the QCDF and pQCD approaches. From Tables III, V, and VI, one can observe that the pQCD predictions of longitudinal polarization fractions agree roughly with those QCDF values within very large theoretical errors. However, in terms of central values, it is noted that the above-mentioned six modes are all governed by the longitudinal contributions in the QCDF approach, which is different from those given in the pQCD approach to some extent.

For $B^0 \to f_1\omega$ decays for example, the leading-order QCD dynamics and the interferences between $B^0 \to f_{1q}\omega$ and $B^0 \to f_{1s}\omega$ make $f_L(B^0 \to f_1(1285)\omega) = 60.1^{+8.9}_{-8.3}\%$, while $f_L(B^0 \to f_1(1420)\omega) = 45.3^{+12.1}_{-11.7}\%$, where, in terms of the central value, the latter polarization fraction presents a striking contrast to the value of $f_L(B^0 \to f_1(1420)\omega) = 86\%$ obtained in the QCDF approach. Due to the analogous behavior between f_1 and V and the dominance of f_{1q} in the $f_1(1285)$ state, it is then expected that the longitudinal polarization fraction $f_L(B^0 \to f_1(1285)\omega)$ is more like that of $f_L(B^0 \to \omega\omega)$. The theoretical prediction of $f_L(B^0 \to \omega\omega) \sim 66\%$ made in the pQCD approach [6] indeed confirms this similarity. Of course, the analogy between $f_L(B^0 \to f_1(1285)\omega) \sim 86\%$ and $f_L(B^0 \to \omega\omega) \sim 94\%$ can also be manifested in the QCDF framework. Therefore, this phenomenology should be tested by the near future measurements at LHCb and/or Belle-II experiments to distinguish these two

popular factorization approaches based on QCD dynamics.

As we know, the color-suppressed tree-dominated $B^0 \to \rho^0\rho^0$ decay is governed by large transverse amplitudes, but with a too small branching ratio to be comparable to the data at leading order in the pQCD approach [6,46]. After including partial next-to-leading order contributions such as vertex corrections, quark loop, and chromomagnetic penguin [46], even the Glauber-gluon factor [23], the predicted branching ratio and longitudinal polarization fraction of $B^0 \to \rho^0\rho^0$ decay are simultaneously in good agreement with the existing measurements [45]. Of course, it is noted that the small longitudinal polarization fraction $0.21^{+0.18}_{-0.22} \pm 0.13$ [47] provided by the Belle Collaboration cannot match with that given by the *BABAR* [48] and LHCb [49] collaborations, respectively. Therefore, it is important to make a refined measurement at the forthcoming Belle-II experiment to give a definitive conclusion. The stringent measurements on the $B^0 \to f_1\omega$ decays are also sensitive to the color-suppressed tree amplitude, which may tell us whether they have the same issue as the $B^0 \to \rho^0\rho^0$ mode.

Moreover, for pure penguin $B^0 \to f_1\phi$ decays, although the central values of longitudinal polarization fractions in the pQCD approach are somewhat smaller than those in the QCDF method, the predictions of polarization fractions within large theoretical errors are consistent with each other, and $B^0 \to f_1\phi$ decays are dominated by the longitudinal polarization contributions in both the pQCD and QCDF approaches. However, the predictions of polarization fractions for $B^0 \to f_1\rho^0$ decays in the pQCD approach show that the $B^0 \to f_1(1285)[f_1(1420)]\rho^0$ channel seems to be governed by the longitudinal (transverse) polarization amplitudes (see Table III for detail), which indicates a significantly different understanding in the QCDF framework. In QCDF, the $B^0 \to f_1\rho^0$ decays have similar and dominantly large longitudinal polarization fractions. These phenomenologies await precise measurements in the future to further explore the unknown dynamics in the axial-vector f_1 states, as well as in the decay channels.

(v) For $B_s^0 \to f_1(\rho^0, \omega, \overline{K}^{*0})$ decays, the pQCD predictions of polarization fractions have been presented in Tables VII, IX, and VIII, respectively. One can easily observe that (a) the $B_s^0 \to f_1\rho^0$ decays are dominated by the longitudinal contributions with polarization fractions $f_L(B_s^0 \to f_1(1285)\rho^0) = 79.8^{+2.1}_{-3.7}\% \sim f_L(B_s^0 \to f_1(1420)\rho^0) = 80.8^{+1.8}_{-2.8}\%$; (b) the longitudinal amplitudes dominate the $B_s^0 \to f_1(1285)\omega$ mode with $f_L(B_s^0 \to f_1(1285)\omega) = 81.8^{+11.1}_{-11.5}\%$ and contribute to the $B_s^0 \to f_1(1420)\omega$ channel, almost competing with the transverse ones with $f_L(B_s^0 \to f_1(1420)\omega) = 50.9^{+5.3}_{-5.1}\%$, respectively; and (c) the $B_s^0 \to f_1(1285)\overline{K}^{*0}$ decay is governed by the transverse amplitudes, contrary to $B_s^0 \to f_1(1285)(\rho^0, \omega)$, with longitudinal polarization fraction $39.2^{+9.2}_{-8.5}\%$. However, similar to the $B_s^0 \to f_1(1420)\omega$ mode, the $B_s^0 \to f_1(1420)\overline{K}^{*0}$ channel also has nearly equivalent contributions from both longitudinal and transverse polarizations. These predictions of $B_s^0 \to f_1 V$ decays in the pQCD approach could be tested by future measurements at LHCb and/or Belle-II, or even at Circular Electron Positron Collider (CEPC) factories.

(vi) In this work, the relative phases (in units of rad) $\phi_\parallel$ and $\phi_\perp$ of $B \to f_1 V$ decays are also studied for the first time in the literature and the relevant numerical results have been given in Tables I–X. Up to now, no data or theoretical predictions of these relative phases in the considered 20 nonleptonic decays of $B \to f_1 V$ have been available. It is therefore expected that our predictions in the pQCD approach could be confronted with future LHCb and/or Belle-II experiments, as well as the theoretical comparison within the framework of QCDF, SCET, and so forth.

Again, as stressed in the above section, no results are available yet for both theoretical and experimental aspects of $B \to f_1 V$ decays. Hence, we have to wait for the examinations to our pQCD analyses in the $B \to f_1 V$ decays from (near) future experiments.

C. Direct *CP*-violating asymmetries

Now we come to the evaluations of direct *CP*-violating asymmetries of $B \to f_1 V$ decays in the pQCD approach. The direct *CP* violation $\mathcal{A}_{CP}^{\rm dir}$ can be defined as

$$\mathcal{A}_{CP}^{\rm dir} \equiv \frac{\overline{\Gamma} - \Gamma}{\overline{\Gamma} + \Gamma} = \frac{|\overline{A}_{\rm final}|^2 - |A_{\rm final}|^2}{|\overline{A}_{\rm final}|^2 + |A_{\rm final}|^2}, \tag{119}$$

where Γ and $A_{\rm final}$ stand for the decay rate and decay amplitude of $B \to f_1 V$, while $\overline{\Gamma}$ and $\overline{A}_{\rm final}$ denote the charge conjugation ones, correspondingly. It should be mentioned that here we will not distinguish charged B^+ mesons from neutral B^0 and B_s^0 ones in Eq. (119) because we are only considering the direct *CP* violation. Meanwhile, according to Ref. [7], the direct-induced *CP* asymmetries can also be studied with the help of helicity amplitudes. Usually, we need to combine three polarization fractions, as shown in Eq. (104), with those corresponding conjugation ones of B decays and then to quote the resultant six observables to define direct *CP* violations of $B \to f_1 V$ decays in the transversity basis as follows:

$$\mathcal{A}_{CP}^{\mathrm{dir},\ell} = \frac{\overline{f}_\ell - f_\ell}{\overline{f}_\ell + f_\ell}, \tag{120}$$

where $\ell = L, \parallel, \perp$ and the definition of $\overline{f}$ is the same as that in Eq. (104), but for the corresponding $\overline{B}$ decays.

Using Eq. (119), we calculate the pQCD predictions of direct CP-violating asymmetries in the $B \to f_1 V$ decays and present the results as shown in Tables I–X. Based on these numerical values, some comments are in order:

(1) Generally speaking, the $\Delta S = 0$ decays including $B^0 \to f_1(\rho^0, \omega)$ and $B_s^0 \to f_1 \overline{K}^{*0}$ and the $\Delta S = 1$ decays such as $B^+ \to f_1 K^{*+}$ and $B_s^0 \to f_1(\rho^0, \omega)$ have large direct CP violations $\mathcal{A}_{CP}^{\mathrm{dir}}$ within still large theoretical errors, except for $B^+ \to f_1\rho^+$, $B^0 \to f_1(\phi, K^{*0})$, and $B_s^0 \to f_1\phi$ modes giving CP-violating asymmetries less than 10%, because of either extremely small penguin contaminations, e.g., $B^+ \to f_1\rho^+$, or negligible tree pollution, e.g., $B^0 \to f_1 K^{*0}$. In particular, the $B^0 \to f_1\phi$ modes have zero direct CP asymmetries in the SM because of pure penguin contributions. However, if the experimental measurements of the direct CP asymmetries of $B^0 \to f_1\phi$ decays exhibit large nonzero values, this will indicate the existence of new physics beyond the SM and will provide a very promising place to search for possible exotic effects.

(2) As can be seen in Tables I and III, the direct CP asymmetries of $B \to f_1\rho$ decays in the pQCD approach are

$$\begin{aligned}
&\mathcal{A}_{CP}^{\mathrm{dir}}(B^+ \to f_1(1285)\rho^+) = -6.7^{+2.2}_{-3.0}\%, \\
&\mathcal{A}_{CP}^{\mathrm{dir}}(B^+ \to f_1(1420)\rho^+) = -3.7^{+2.1}_{-2.4}\%,
\end{aligned} \tag{121}$$

$$\begin{aligned}
&\mathcal{A}_{CP}^{\mathrm{dir}}(B^0 \to f_1(1285)\rho^0) = 18.0^{+42.9}_{-30.5}\%, \\
&\mathcal{A}_{CP}^{\mathrm{dir}}(B^0 \to f_1(1420)\rho^0) = 24.1^{+20.0}_{-24.3}\%,
\end{aligned} \tag{122}$$

in which various errors as specified previously have been added in quadrature. One can find that the large branching ratio of the order of 10^{-5} combined with direct CP asymmetry around $-9.7 \sim -4.5\%$ in $B^+ \to f_1(1285)\rho^+$ is expected to be detected in the near future at the LHCb and/or Belle-II experiments. With a somewhat large decay rate $\mathcal{O}(10^{-6})$, the small direct CP violation in $B^+ \to f_1(1420)\rho^+$ may not be easily accessed. However, it is worth mentioning that large direct CP-violating asymmetries exist in both transverse polarizations, i.e., parallel and perpendicular, as follows:

$$\begin{aligned}
&\mathcal{A}_{CP}^{\mathrm{dir},\parallel}(B^+ \to f_1(1420)\rho^+) = 13.8^{+11.7}_{-11.8}\%, \\
&\mathcal{A}_{CP}^{\mathrm{dir},\perp}(B^+ \to f_1(1420)\rho^+) = 10.5^{+12.8}_{-13.2}\%,
\end{aligned} \tag{123}$$

which may be detectable and helpful to explore the physics involved in $B^+ \to f_1(1420)\rho^+$ decays. Note that the $B^0 \to f_1\rho^0$ modes cannot be measured in the near future due to their very small decay rates, although the seemingly large direct CP violations have been predicted in the pQCD approach.

(3) It is interesting to note from Tables II, IV, and X that the direct-induced CP asymmetries for the penguin-dominated $B^+ \to f_1 K^{*+}$, $B^0 \to f_1 K^{*0}$, and $B_s^0 \to f_1\phi$ decays with contaminations arising from tree amplitudes at different levels are predicted in SM as follows:

$$\begin{aligned}
&\mathcal{A}_{CP}^{\mathrm{dir}}(B^+ \to f_1(1285)K^{*+}) = -16.0^{+5.2}_{-4.9}\%, \\
&\mathcal{A}_{CP}^{\mathrm{dir}}(B^+ \to f_1(1420)K^{*+}) = 13.9^{+5.3}_{-5.3}\%;
\end{aligned} \tag{124}$$

$$\begin{aligned}
&\mathcal{A}_{CP}^{\mathrm{dir}}(B^0 \to f_1(1285)K^{*0}) = -7.8^{+2.5}_{-2.3}\%, \\
&\mathcal{A}_{CP}^{\mathrm{dir}}(B^0 \to f_1(1420)K^{*0}) = 4.7^{+1.4}_{-1.5}\%;
\end{aligned} \tag{125}$$

$$\begin{aligned}
&\mathcal{A}_{CP}^{\mathrm{dir}}(B_s^0 \to f_1(1285)\phi) = -5.3^{+1.4}_{-1.0}\%, \\
&\mathcal{A}_{CP}^{\mathrm{dir}}(B_s^0 \to f_1(1420)\phi) = 2.5^{+1.0}_{-0.9}\%,
\end{aligned} \tag{126}$$

which indicates that the former $B^+ \to f_1 K^{*+}$ decays suffer from somewhat stronger interferences induced by larger tree contributions than the latter two modes.

By combining three polarization fractions in the transversity basis with those of CP-conjugated $\overline{B}$ decays, we also computed the direct CP violations of the above-mentioned decays with a $\overline{b} \to \overline{s}$ transition in every polarization in the pQCD approach correspondingly.

$\underline{B^+ \to f_1(1285)K^{*+}}$:

$$\begin{aligned}
&\mathcal{A}_{CP}^{\mathrm{dir,L}} = -94.5^{+24.0}_{-7.7}\%, \qquad \mathcal{A}_{CP}^{\mathrm{dir},\parallel} = 8.2^{+2.4}_{-2.4}\%, \\
&\mathcal{A}_{CP}^{\mathrm{dir},\perp} = 7.9^{+2.4}_{-2.3}\%;
\end{aligned} \tag{127}$$

$\underline{B^+ \to f_1(1420)K^{*+}}$:

$$\begin{aligned}
&\mathcal{A}_{CP}^{\mathrm{dir,L}} = 25.4^{+6.7}_{-6.8}\%, \qquad \mathcal{A}_{CP}^{\mathrm{dir},\parallel} = -14.1^{+6.5}_{-7.1}\%, \\
&\mathcal{A}_{CP}^{\mathrm{dir},\perp} = -9.7^{+5.2}_{-5.0}\%;
\end{aligned} \tag{128}$$

$\underline{B^0 \to f_1(1285)K^{*0}}$:

$$\begin{aligned}
&\mathcal{A}_{CP}^{\mathrm{dir,L}} = 1.7^{+7.6}_{-11.3}\%, \qquad \mathcal{A}_{CP}^{\mathrm{dir},\parallel} = -9.3^{+1.7}_{-1.6}\%, \\
&\mathcal{A}_{CP}^{\mathrm{dir},\perp} = -9.9^{+1.6}_{-1.8}\%;
\end{aligned} \tag{129}$$

$\underline{B^0 \to f_1(1420)K^{*0}}$:

$$\begin{aligned}
&\mathcal{A}_{CP}^{\mathrm{dir,L}} = 3.4^{+1.5}_{-1.9}\%, \qquad \mathcal{A}_{CP}^{\mathrm{dir},\parallel} = 7.9^{+2.9}_{-2.7}\%, \\
&\mathcal{A}_{CP}^{\mathrm{dir},\perp} = 8.0^{+2.1}_{-2.4}\%;
\end{aligned} \tag{130}$$

$B_s^0 \to f_1(1285)\phi$:

$$\mathcal{A}_{CP}^{\mathrm{dir,L}} = -7.2^{+2.1}_{-1.0}\%, \qquad \mathcal{A}_{CP}^{\mathrm{dir},\parallel} = -2.7^{+0.7}_{-0.4}\%,$$
$$\mathcal{A}_{CP}^{\mathrm{dir},\perp} = -2.8^{+0.6}_{-0.6}\%; \tag{131}$$

$B_s^0 \to f_1(1420)\phi$:

$$\mathcal{A}_{CP}^{\mathrm{dir,L}} = 2.4^{+1.0}_{-0.7}\%, \qquad \mathcal{A}_{CP}^{\mathrm{dir},\parallel} = 2.6^{+1.4}_{-0.9}\%,$$
$$\mathcal{A}_{CP}^{\mathrm{dir},\perp} = 3.1^{+1.5}_{-1.2}\%, \tag{132}$$

where the various errors as specified previously have also been added in quadrature. These pQCD predictions and phenomenological analyses of the direct CP violations of $B^{+,0} \to f_1 K^{*+,0}$ and $B_s^0 \to f_1\phi$ decays could be tested in future measurements. Furthermore, the $B^+ \to f_1 K^{*+}$ modes with large branching ratios and large direct CP asymmetries are likely to be detected much easier in the near future.

(4) It is worth stressing that no theoretical predictions or experimental measurements of the direct CP-violating asymmetries of 20 nonleptonic $B \to f_1 V$ decays are available yet. Therefore, examinations of these leading order pQCD predictions have to be left to LHCb and/or Belle-II, or even CEPC experiments in the future.

D. Weak annihilation contributions in $B \to f_1 V$ decays

As proposed in [1], a strategy correlated with penguin annihilation contributions was suggested to explore the $B \to \phi K^*$ polarization anomaly in SM. The subsequently systematic studies on $B \to VV$ decays combined with rich data further confirm the important role of annihilation contributions played, in particular, in the penguin-dominated modes [3–7]. Here, it should be mentioned that, up to now, different treatments on annihilation contributions have been proposed in QCDF, SCET, and pQCD. For the former two approaches based on the collinear factorization theorem, both QCDF and SCET cannot directly evaluate the diagrams with annihilation topologies because of the existence of end-point singularities. However, different from parametrizing and then fitting the annihilation contributions through rich data in QCDF [31], the SCET method calculates the annihilation diagrams with the help of a zero-bin subtraction scheme and, consequently, obtains a real and small value for the annihilation decay amplitudes [50]. As mentioned in the Introduction, the pQCD approach based on the k_T factorization theorem, together with k_T resummation and threshold resummation techniques, makes the calculations of annihilation types of diagrams free of end-point singularities with a large imaginary part [51]. Recently, experimental measurements and theoretical studies on $B \to PP, PV, VV$ decays, especially on the pure annihilation-type decays such as $B^0 \to K^+K^-$, $B_s^0 \to \pi^+\pi^-$ [44,52], indicate that the pQCD approach may be a reliable method to deal with annihilation diagrams in heavy b flavor meson decays.

Because of similar behavior between vector and $^3P_1$-axial-vector mesons, it is reasonable to conjecture that the weak annihilation contributions can also play an important role, as in the $B \to VV$ ones [3,5–7], in the $B \to AV(VA)$ modes, in particular the penguin-dominated ones. Therefore, we will explore the important contributions from weak annihilation diagrams to $B \to f_1 V$ decays considered in this work. For the sake of simplicity, we will present the central values of pQCD predictions of the CP-averaged branching ratios, the polarization fractions, and the direct CP-violating asymmetries with mixing angle $\phi_{f_1} = 24°$ by taking the factorizable emission plus the nonfactorizable emission decay amplitudes into account. Some numerical results and phenomenological discussions are given as follows:

(i) Branching ratios

When the annihilation contributions are turned off, the CP-averaged branching ratios of $B \to f_1 V$ decays in the pQCD approach then become

$$\mathrm{Br}(B^+ \to f_1(1285)\rho^+) = 11.2 \times 10^{-6},$$
$$\mathrm{Br}(B^+ \to f_1(1420)\rho^+) = 2.3 \times 10^{-6}; \tag{133}$$

$$\mathrm{Br}(B^+ \to f_1(1285)K^{*+}) = 1.4 \times 10^{-6},$$
$$\mathrm{Br}(B^+ \to f_1(1420)K^{*+}) = 2.7 \times 10^{-6}; \tag{134}$$

$$\mathrm{Br}(B^0 \to f_1(1285)\rho^0) = 1.5 \times 10^{-7},$$
$$\mathrm{Br}(B^0 \to f_1(1420)\rho^0) = 7.5 \times 10^{-8}; \tag{135}$$

$$\mathrm{Br}(B^0 \to f_1(1285)K^{*0}) = 4.3 \times 10^{-7},$$
$$\mathrm{Br}(B^0 \to f_1(1420)K^{*0}) = 2.5 \times 10^{-6}; \tag{136}$$

$$\mathrm{Br}(B^0 \to f_1(1285)\omega) = 7.7 \times 10^{-7},$$
$$\mathrm{Br}(B^0 \to f_1(1420)\omega) = 1.4 \times 10^{-7}; \tag{137}$$

$$\mathrm{Br}(B^0 \to f_1(1285)\phi) = 5.2 \times 10^{-9},$$
$$\mathrm{Br}(B^0 \to f_1(1420)\phi) = 1.0 \times 10^{-9}; \tag{138}$$

$$\mathrm{Br}(B_s^0 \to f_1(1285)\rho^0) = 5.0 \times 10^{-8},$$
$$\mathrm{Br}(B_s^0 \to f_1(1420)\rho^0) = 2.5 \times 10^{-7}; \tag{139}$$

$$\mathrm{Br}(B_s^0 \to f_1(1285)\overline{K}^{*0}) = 3.5 \times 10^{-7},$$
$$\mathrm{Br}(B_s^0 \to f_1(1420)\overline{K}^{*0}) = 2.2 \times 10^{-7}; \tag{140}$$

$$\mathrm{Br}(B_s^0 \to f_1(1285)\omega) = 7.1 \times 10^{-8},$$
$$\mathrm{Br}(B_s^0 \to f_1(1420)\omega) = 3.5 \times 10^{-7}; \tag{141}$$

$$\mathrm{Br}(B_s^0 \to f_1(1285)\phi) = 14.7 \times 10^{-6},$$
$$\mathrm{Br}(B_s^0 \to f_1(1420)\phi) = 15.4 \times 10^{-6}. \tag{142}$$

(ii) Longitudinal polarization fractions

By neglecting the weak annihilation contributions, the CP-averaged longitudinal polarization fractions of $B \to f_1 V$ decays in the pQCD approach are written as

$$f_L(B^+ \to f_1(1285)\rho^+) = 96.1\%,$$
$$f_L(B^+ \to f_1(1420)\rho^+) = 90.6\%; \quad (143)$$

$$f_L(B^+ \to f_1(1285)K^{*+}) = 42.9\%,$$
$$f_L(B^+ \to f_1(1420)K^{*+}) = 70.4\%; \quad (144)$$

$$f_L(B^0 \to f_1(1285)\rho^0) = 91.7\%,$$
$$f_L(B^0 \to f_1(1420)\rho^0) = 17.5\%; \quad (145)$$

$$f_L(B^0 \to f_1(1285)K^{*0}) = 2.8\%,$$
$$f_L(B^0 \to f_1(1420)K^{*0}) = 75.9\%; \quad (146)$$

$$f_L(B^0 \to f_1(1285)\omega) = 46.4\%,$$
$$f_L(B^0 \to f_1(1420)\omega) = 27.2\%; \quad (147)$$

$$f_L(B^0 \to f_1(1285)\phi) = 46.8\%,$$
$$f_L(B^0 \to f_1(1420)\phi) = 47.1\%; \quad (148)$$

$$f_L(B_s^0 \to f_1(1285)\rho^0) = 80.2\%,$$
$$f_L(B_s^0 \to f_1(1420)\rho^0) = 80.4\%; \quad (149)$$

$$f_L(B_s^0 \to f_1(1285)\overline{K}^{*0}) = 42.3\%,$$
$$f_L(B_s^0 \to f_1(1420)\overline{K}^{*0}) = 75.6\%; \quad (150)$$

$$f_L(B_s^0 \to f_1(1285)\omega) = 51.0\%,$$
$$f_L(B_s^0 \to f_1(1420)\omega) = 51.4\%; \quad (151)$$

$$f_L(B_s^0 \to f_1(1285)\phi) = 54.6\%,$$
$$f_L(B_s^0 \to f_1(1420)\phi) = 78.9\%. \quad (152)$$

(iii) Direct CP-violating asymmetries

Without the contributions arising from annihilation types of diagrams, the direct CP-violating asymmetries of $B \to f_1 V$ decays in the pQCD approach are given as

$$\mathcal{A}_{CP}^{\rm dir}(B^+ \to f_1(1285)\rho^+) = -6.7\%,$$
$$\mathcal{A}_{CP}^{\rm dir}(B^+ \to f_1(1420)\rho^+) = -2.2\%; \quad (153)$$

$$\mathcal{A}_{CP}^{\rm dir}(B^+ \to f_1(1285)K^{*+}) = -15.0\%,$$
$$\mathcal{A}_{CP}^{\rm dir}(B^+ \to f_1(1420)K^{*+}) = 12.8\%; \quad (154)$$

$$\mathcal{A}_{CP}^{\rm dir}(B^0 \to f_1(1285)\rho^0) = -83.5\%,$$
$$\mathcal{A}_{CP}^{\rm dir}(B^0 \to f_1(1420)\rho^0) = 35.4\%; \quad (155)$$

$$\mathcal{A}_{CP}^{\rm dir}(B^0 \to f_1(1285)K^{*0}) = -2.1\%,$$
$$\mathcal{A}_{CP}^{\rm dir}(B^0 \to f_1(1420)K^{*0}) = 3.4\%; \quad (156)$$

$$\mathcal{A}_{CP}^{\rm dir}(B^0 \to f_1(1285)\omega) = -50.8\%,$$
$$\mathcal{A}_{CP}^{\rm dir}(B^0 \to f_1(1420)\omega) = -2.0\%; \quad (157)$$

$$\mathcal{A}_{CP}^{\rm dir}(B_s^0 \to f_1(1285)\rho^0) = 15.2\%,$$
$$\mathcal{A}_{CP}^{\rm dir}(B_s^0 \to f_1(1420)\rho^0) = 15.3\%; \quad (158)$$

$$\mathcal{A}_{CP}^{\rm dir}(B_s^0 \to f_1(1285)\overline{K}^{*0}) = 20.5\%,$$
$$\mathcal{A}_{CP}^{\rm dir}(B_s^0 \to f_1(1420)\overline{K}^{*0}) = -53.2\%; \quad (159)$$

$$\mathcal{A}_{CP}^{\rm dir}(B_s^0 \to f_1(1285)\omega) = 25.1\%,$$
$$\mathcal{A}_{CP}^{\rm dir}(B_s^0 \to f_1(1420)\omega) = 25.1\%; \quad (160)$$

$$\mathcal{A}_{CP}^{\rm dir}(B_s^0 \to f_1(1285)\phi) = -5.1\%,$$
$$\mathcal{A}_{CP}^{\rm dir}(B_s^0 \to f_1(1420)\phi) = 2.5\%. \quad (161)$$

Note that because of the inclusion of pure penguin amplitudes, the direct CP-violating asymmetries of $B^0 \to f_1\phi$ decays are still zero, which are not presented here, even if the penguin annihilation contributions are turned off in the SM. However, it should be mentioned again that once the future experimental measurements release evidently nonzero and large direct CP violations, there might be NP beyond the SM hidden in these two decay modes.

Generally speaking, compared with the numerical results by considering the weak annihilation contributions in the pQCD approach as shown in Tables I–X, the branching ratios and longitudinal polarization fractions of $B^+ \to f_1\rho^+$, $B^0 \to f_1(1420)\rho^0$, $B_s^0 \to f_1\rho^0$, $B_s^0 \to f_1(1420)\omega$, and $B_s^0 \to f_1(1285)\phi$ decays almost remain unchanged when the annihilation contributions are neglected, while the other channels are affected by the annihilation decay amplitudes at different levels. Particularly, the contributions induced by the weak annihilation diagrams can make the $B^0 \to f_1(1285)K^{*0}$ decay rate (longitudinal polarization fraction) amazingly change from $4.3 \times 10^{-7}(2.8\%)$ to $5.0 \times 10^{-6}(15.8\%)$. From the pQCD point of view, because the annihilation amplitudes can contribute to CP violation as a source of the large strong phase, the direct CP-violating asymmetries of $B \to f_1 V$ decays without annihilation contributions will deviate from the predictions presented in Tables I–X more or less, except for the $B^0 \to f_1\phi$ modes with still invariant zero direct CP violations. Of course, the above general expectations in the pQCD approach will be examined by the relevant experiments in the future, which could be helpful

TABLE XIII. Same as Table XI but for $B^0 \to f_1 K^{*0}$ decays.

Decay modes	$B^0 \to f_1(1285)K^{*0}$		$B^0 \to f_1(1420)K^{*0}$	
Channels	$B^0 \to K^{*0} f_{1q}$	$B^0 \to K^{*0} f_{1s}$	$B^0 \to K^{*0} f_{1q}$	$B^0 \to K^{*0} f_{1s}$
A_L	$0.563 - i0.380$	$-0.647 - i0.814$	$0.251 - i0.169$	$1.454 + i1.829$
	$(0.602 + i0.197)$	$(-0.665 - i0.219)$	$(0.268 + i0.088)$	$(1.495 + i0.491)$
A_N	$-0.934 + i0.649$	$-0.104 + i0.466$	$-0.416 + i0.289$	$0.235 - i1.047$
	$(-0.588 + i0.066)$	$(0.126 - i0.027)$	$(-0.262 + i0.029)$	$(-0.284 + i0.061)$
A_T	$-1.949 + i1.296$	$-0.159 + i0.920$	$-0.868 + i0.577$	$0.358 - i2.067$
	$(-1.253 + i0.113)$	$(0.289 - i0.044)$	$(-0.558 + i0.050)$	$(-0.648 + i0.099)$

TABLE XIV. Same as Table XI but for $B_s^0 \to f_1 \phi$ decays.

Decay modes	$B_s^0 \to f_1(1285)\phi$		$B_s^0 \to f_1(1420)\phi$	
Channels	$B_s^0 \to \phi f_{1q}$	$B_s^0 \to \phi f_{1s}$	$B_s^0 \to \phi f_{1q}$	$B_s^0 \to \phi f_{1s}$
A_L	$-1.624 + i0.044$	$-2.502 - i0.542$	$-0.723 + i0.020$	$5.621 + i1.218$
	$(-1.624 + i0.044)$	$(-2.463 - i0.139)$	$(-0.723 + i0.020)$	$(5.533 + i0.312)$
A_N	$-1.077 + i0.093$	$-0.763 + i0.164$	$-0.480 + i0.041$	$1.714 - i0.368$
	$(-1.077 + i0.093)$	$(-0.813 + i0.081)$	$(-0.480 + i0.041)$	$(1.827 - i0.181)$
A_T	$-2.245 + i0.163$	$-1.479 + i0.307$	$-1.000 + i0.073$	$3.322 - i0.690$
	$(-2.245 + i0.163)$	$(-1.576 + i0.169)$	$(-1.000 + i0.073)$	$(3.539 - i0.379)$

to understand the annihilation decay mechanism in vector-vector and vector-axial-vector B decays in depth.

In order to clearly examine the important contributions from annihilation diagrams, we present the explicit decay amplitudes decomposed as $B \to f_{1q} V$ and $B \to f_{1s} V$ for $B^+ \to f_1 \rho^+$, $B^{+,0} \to f_1 K^{*+,0}$, and $B_s^0 \to f_1 \phi$ modes with large branching ratios in Tables XI–XIV with and without annihilation contributions on three polarizations. One can easily find from Table XIII, for $B^0 \to f_1 K^{*0}$ for example, that the significant variations induced by weak annihilation contributions mainly arise in the imaginary part of decay amplitudes on every polarization. Furthermore, when the annihilation decay amplitudes are not considered, then one can straightforwardly see from the numerical results shown in the parentheses that, combined with the dominant $A_T(B^0 \to f_{1q} K^{*0})$ amplitude, almost exact cancellation of the longitudinal polarization and somewhat stronger destructive interferences on the other two transverse polarizations between $B^0 \to f_{1q} K^{*0}$ and $B^0 \to f_{1s} K^{*0}$ modes in the $B^0 \to f_1(1285) K^{*0}$ decay resulted in a significantly smaller branching fraction, about $\mathcal{O}(10^{-7})$, and a surprisingly large transverse polarization fraction, around 97%. Consequently, lack of a large strong phase coming from annihilation contributions in the pQCD approach lead to a much smaller direct CP-violating asymmetry in magnitude, around 2%. Contrary to $B^0 \to f_1(1285) K^{*0}$ decay, because of the dominance of $B^0 \to f_{1s} K^{*0}$ on the longitudinal polarization in the $B^0 \to f_1(1420) K^{*0}$ channel, the constructive interferences between $B^0 \to f_{1q} K^{*0}$ and $B^0 \to f_{1s} K^{*0}$ modes on every polarization make the decay rate somewhat smaller, with a factor of around 0.6, and the longitudinal polarization fraction slightly larger than those corresponding results shown in Table IV, although the similarly large annihilation contributions are also turned off, which can be easily seen from the decay amplitudes given in Table XIII. Again, these important annihilation contributions should be tested by future experiments to further deepen our knowledge of the annihilation decay mechanism in the heavy b flavor sector.

IV. CONCLUSIONS AND SUMMARY

In this work, we studied 20 nonleptonic decays of $B \to f_1 V$ by employing the pQCD approach based on the framework of the k_T factorization theorem. The singularities that appeared in collinear factorization were then naturally smeared by picking up the transverse momentum k_T of valence quarks when the quark momentum fraction x approaches the end-point region. Consequently, with the pQCD formalism, the Feynman diagrams of every topology can be calculated perturbatively without introducing any new parameters, which is a unique point, different from the QCDF and the SCET based on the collinear factorization theorem. In order to explore the perturbative and nonperturbative QCD dynamics to further understand the helicity structure of the decay mechanism in $B \to f_1 V$ decays, we calculated the CP-averaged branching ratios, the polarization fractions, the direct CP-violating asymmetries, and the relative phases of those considered decay modes, where the mixing angle $\phi_{f_1} \sim 24°$ between two axial-vector $f_1(1285)$ and $f_1(1420)$ states adopted from

the first measurements of $B_{d/s} \to J/\psi f_1(1285)$ decays in the heavy b flavor sector.

From our numerical pQCD predictions and phenomenological analysis, we found the following points:

(a) The large CP-averaged branching ratios for $B^+ \to f_1\rho^+$, $B^{+,0} \to f_1 K^{*+,0}$, and $B_s^0 \to f_1\phi$ decays are predicted in the pQCD approach as follows:

$$\mathrm{Br}(B^+ \to f_1(1285)\rho^+) = 11.1^{+8.7}_{-6.8} \times 10^{-6}, \quad \mathrm{Br}(B^+ \to f_1(1420)\rho^+) = 2.3^{+1.9}_{-1.4} \times 10^{-6}; \tag{162}$$

$$\mathrm{Br}(B^+ \to f_1(1285)K^{*+}) = 6.4^{+3.6}_{-2.5} \times 10^{-6}, \quad \mathrm{Br}(B^+ \to f_1(1420)K^{*+}) = 4.5^{+1.7}_{-1.5} \times 10^{-6}; \tag{163}$$

$$\mathrm{Br}(B^0 \to f_1(1285)K^{*0}) = 5.0^{+2.7}_{-2.1} \times 10^{-6}, \quad \mathrm{Br}(B^0 \to f_1(1420)K^{*0}) = 4.4^{+1.7}_{-1.5} \times 10^{-6}; \tag{164}$$

$$\mathrm{Br}(B_s^0 \to f_1(1285)\phi) = 14.7^{+8.7}_{-6.4} \times 10^{-6}, \quad \mathrm{Br}(B_s^0 \to f_1(1420)\phi) = 16.2^{+9.9}_{-7.6} \times 10^{-6}, \tag{165}$$

which are expected to be measured at the running LHCb and the forthcoming Belle-II experiments in the near future. It is noted that the decay rates and decay pattern of $B^+ \to f_1\rho^+$ predicted in the pQCD approach are very consistent with those given in the QCDF approach within theoretical errors. But, it is not the same case for the $B^{+,0} \to f_1 K^{*+,0}$ decay modes. The future experimental measurements with good precision for the branching ratios and the pattern of $B^{+,0} \to f_1 K^{*+,0}$ decays will be helpful for us to examine these two different factorization approaches.

(b) In order to decrease the effects of the large theoretical errors of the branching ratios induced by those input parameters, we also define the ratios of the decay rates among the ten $B^+ \to f_1\rho^+$, $B^{+,0} \to f_1 K^{*+,0}$, $B^0 \to f_1\omega$, and $B_s^0 \to f_1\phi$ decay modes as given in Eqs. (95)–(101), where the large uncertainties of the predicted branching ratios are canceled to a large extent in such ratios. The future experimental measurements of these newly defined ratios will be helpful to further determine the mixing angle ϕ_{f_1} between f_{1q} and f_{1s} states for an axial-vector $f_1(1285) - f_1(1420)$ mixing system in the quark-flavor basis.

(c) The predictions of polarization fractions for the 20 nonleptonic $B \to f_1 V$ decays are given explicitly in the pQCD approach. Furthermore, associated with large branching ratios, the large longitudinal (transverse) polarization fractions in $B^+ \to f_1\rho^+$, $B^{+,0} \to f_1(1420)K^{*+,0}$, $B^0 \to f_1(1285)\omega$, and $B_s^0 \to f_1\phi$ [$B^{+,0} \to f_1(1285)K^{*+,0}$ and $B^0 \to f_1(1420)\omega$] decays are expected to be detected at LHCb and Belle-II experiments and to provide useful information to understand the famous polarization puzzle in rare vector-vector B meson decays, which will be helpful to shed light on the helicity structure of the decay mechanism.

(d) Some large direct CP-violating asymmetries of $B \to f_1 V$ decays are provided with the pQCD approach, such as $\mathcal{A}_{CP}^{\mathrm{dir}}(B^+ \to f_1(1285)K^{*+}) = -16.0^{+5.2}_{-4.9}\%$, $\mathcal{A}_{CP}^{\mathrm{dir}}(B^+ \to f_1(1420)K^{*+}) = 13.9^{+5.3}_{-5.3}\%$, $\mathcal{A}_{CP}^{\mathrm{dir}}(B^0 \to f_1(1285)K^{*0}) = -7.8^{+2.5}_{-2.3}\%$, and even $\mathcal{A}_{CP}^{\mathrm{dir},\parallel}(B^+ \to f_1(1420)\rho^+) = 13.8^{+11.7}_{-11.8}\%$ and $\mathcal{A}_{CP}^{\mathrm{dir},\perp}(B^+ \to f_1(1420)\rho^+) = 10.5^{+12.8}_{-13.2}\%$, and so forth, which are believed to be detectable at the LHCb, Belle-II, or even the future CEPC experiments. At the same time, a stringent examination of the zero direct CP asymmetries in the SM of $B^0 \to f_1\phi$ decays is of great interest to provide useful information for the possible signal of the new physics beyond the SM. Moreover, the theoretical estimations on physical observables of $B_s \to f_1 V$ decays are given for the first time in the pQCD approach, which can also be tested in the future.

(e) The weak annihilation contributions play an important role in many $B \to f_1 V$ decays. The near future measurements with good precision on some decay modes affected significantly by the annihilation amplitudes, such as $B^{+,0} \to f_1 K^{*+,0}$ with large branching ratios, can provide evidence to verify the reliability of the pQCD approach on the calculations of annihilation-type diagrams, and help us to understand the annihilation mechanism in the heavy flavor sector.

ACKNOWLEDGMENTS

This work is supported by the National Natural Science Foundation of China under Grants No. 11205072, No. 11235005, and No. 11447032 and by a project funded by the Priority Academic Program Development of Jiangsu Higher Education Institutions (PAPD), by the Research Fund of Jiangsu Normal University under Grant No. 11XLR38, and by the Natural Science Foundation of Shandong Province under Grant No. ZR2014AQ013.

TABLE XV. Input values of the decay constants of the light vector mesons (in MeV) [42,55].

f_ρ	f_ρ^T	f_ω	f_ω^T	f_{K^*}	$f_{K^*}^T$	f_ϕ	f_ϕ^T
209 ± 2	165 ± 9	195 ± 3	145 ± 10	217 ± 5	185 ± 10	231 ± 4	200 ± 10

TABLE XVI. Gegenbauer moments in the distributions amplitudes of the lightest vector mesons taken at $\mu = 1$ GeV [38].

K^* meson				ρ and ω mesons		ϕ meson	
$a_1^\parallel$	$a_2^\parallel$	$a_1^\perp$	$a_2^\perp$	$a_2^\parallel$	$a_2^\perp$	$a_2^\parallel$	$a_2^\perp$
0.03 ± 0.02	0.11 ± 0.09	0.04 ± 0.03	0.10 ± 0.08	0.15 ± 0.07	0.14 ± 0.06	0.18 ± 0.08	0.14 ± 0.07

APPENDIX: MESONIC DISTRIBUTION AMPLITUDES

As we know, mesonic distribution amplitudes in hadron wave functions are the essential nonperturbative inputs in the pQCD approach. Now, we will give a brief introduction to these items involved in the present work.

For the B meson, the distribution amplitude in the impact b space has been proposed as

$$\phi_B(x,b) = N_B x^2(1-x)^2 \exp\left[-\frac{1}{2}\left(\frac{xm_B}{\omega_b}\right)^2 - \frac{\omega_b^2 b^2}{2}\right] \quad \text{(A1)}$$

in Ref. [20] and widely adopted, for example, in [6,16–18,20,22,23,53], where the normalization factor N_B is related to the decay constant f_B through Eq. (4). The shape parameter ω_b was fixed at 0.40 GeV by using the rich experimental data on the B^+ and B^0 mesons, with $f_B = 0.19$ GeV, based on many calculations of form factors [36] and other well-known modes of B^+ and B^0 mesons [20] in the pQCD approach. Here, the assumption of isospin symmetry has been made. For the B_s^0 meson, relative to the lightest u or d quark, the heavier s quark leads to a somewhat larger momentum fraction than that of the u or d quark in the B^+ or B^0 mesons. Therefore, by taking a small SU(3) symmetry-breaking effect into account, we adopt the shape parameter $\omega_b = 0.50$ GeV, with $f_B = 0.23$ GeV, for the B_s meson [53], and the corresponding normalization constant is $N_B = 63.67$. In order to estimate the theoretical uncertainties induced by the inputs, we consider varying the shape parameter ω_b by 10%, i.e., $\omega_b = 0.40 \pm 0.04$ GeV for B^+ and B^0 mesons and $\omega_b = 0.50 \pm 0.05$ GeV for the B_s^0 meson, respectively.

The twist-2 light-cone distribution amplitudes ϕ_V and ϕ_V^T can be parametrized as

$$\phi_V(x) = \frac{3f_V}{\sqrt{2N_c}} x(1-x)\left[1 + 3a_{1V}^\parallel(2x-1) + a_{2V}^\parallel \frac{3}{2}(5(2x-1)^2-1)\right], \quad \text{(A2)}$$

$$\phi_V^T(x) = \frac{3f_V^T}{\sqrt{2N_c}} x(1-x)\left[1 + 3a_{1V}^\perp(2x-1) + a_{2V}^\perp \frac{3}{2}(5(2x-1)^2-1)\right], \quad \text{(A3)}$$

in which f_V and f_V^T are the decay constants of the vector meson with longitudinal and transverse polarization, respectively, whose values are shown in Table XV. The decay constants can be extracted from $V^0 \to l^+l^-$ and $\tau \to V^-\overline{\nu}$ [38,54]. The Gegenbauer moments taken from the recent updates [38] are collected in Table XVI.

The asymptotic forms of the twist-3 distribution amplitudes $\phi_V^{t,s}$ and $\phi_V^{v,a}$ are [11,56]

$$\phi_V^t(x) = \frac{3f_V^T}{2\sqrt{2N_c}}(2x-1)^2, \qquad \phi_V^s(x) = -\frac{3f_V^T}{2\sqrt{2N_c}}(2x-1), \quad \text{(A4)}$$

$$\phi_V^v(x) = \frac{3f_V}{8\sqrt{2N_c}}(1+(2x-1)^2), \qquad \phi_V^a(x) = -\frac{3f_V}{4\sqrt{2N_c}}(2x-1). \quad \text{(A5)}$$

For the axial-vector state $f_{1q(s)}$, its twist-2 light-cone distribution amplitudes can generally be expanded as the Gegenbauer polynomials [27]:

$$\phi_{f_{1q(s)}}(x) = \frac{f_{f_{1q(s)}}}{2\sqrt{2N_c}} 6x(1-x)\left[1 + a_2^{\parallel}\frac{3}{2}(5(2x-1)^2-1)\right], \tag{A6}$$

$$\phi^T_{f_{1q(s)}}(x) = \frac{f_{f_{1q(s)}}}{2\sqrt{2N_c}} 6x(1-x)[3a_1^{\perp}(2x-1)]. \tag{A7}$$

For twist-3 ones, we use the following form as in Ref. [39]:

$$\phi^s_{f_{1q(s)}}(x) = \frac{f_{f_{1q(s)}}}{4\sqrt{2N_c}}\frac{d}{dx}[6x(1-x)(a_1^{\perp}(2x-1))], \tag{A8}$$

$$\phi^t_{f_{1q(s)}}(x) = \frac{f_{f_{1q(s)}}}{2\sqrt{2N_c}}\left[\frac{3}{2}a_1^{\perp}(2x-1)(3(2x-1)^2-1)\right], \tag{A9}$$

TABLE XVII. Same as Table XVI but for light axial-vector f_{1q} and f_{1s} states [27].

f_{1q} state		f_{1s} state	
$a_2^{\parallel}$	$a_1^{\perp}$	$a_2^{\parallel}$	$a_1^{\perp}$
-0.05 ± 0.03	-1.08 ± 0.48	$0.10^{+0.15}_{-0.19}$	$0.30^{+0.00}_{-0.33}$

$$\phi^v_{f_{1q(s)}}(x) = \frac{f_{f_{1q(s)}}}{2\sqrt{2N_c}}\left[\frac{3}{4}(1+(2x-1)^2)\right],$$
$$\phi^a_{f_{1q(s)}}(x) = \frac{f_{f_{1q(s)}}}{8\sqrt{2N_c}}\frac{d}{dx}[6x(1-x)], \tag{A10}$$

where $f_{f_{1q(s)}}$ is the "normalization" constant for both longitudinally and transversely polarized mesons and the Gegenbauer moments $a^{\parallel(\perp)}_{2(1)}$ can be found in Table XVII.

[1] A. L. Kagan, Phys. Lett. B **601**, 151 (2004).
[2] P. Colangelo, F. De Fazio, and T. N. Pham, Phys. Lett. B **597**, 291 (2004).
[3] H. Y. Cheng and K. C. Yang, Phys. Rev. D **78**, 094001 (2008); **79**, 039903(E) (2009).
[4] H. Y. Cheng and J. G. Smith, Annu. Rev. Nucl. Part. Sci. **59**, 215 (2009).
[5] H. Y. Cheng and C. K. Chua, Phys. Rev. D **80**, 114008 (2009).
[6] Z. T. Zou, A. Ali, C. D. Lü, X. Liu, and Y. Li, Phys. Rev. D **91**, 054033 (2015).
[7] M. Beneke, J. Rohrer, and D. Yang, Nucl. Phys. **B774**, 64 (2007).
[8] K. A. Olive *et al.* (Particle Data Group Collaboration), Chin. Phys. C **38**, 090001 (2014).
[9] B. Aubert *et al.* (*BABAR* Collaboration), Phys. Rev. Lett. **91**, 171802 (2003); **93**, 231804 (2004); **98**, 051801 (2007); **99**, 201802 (2007).
[10] K. F. Chen *et al.* (Belle Collaboration), Phys. Rev. Lett. **91**, 201801 (2003); **94**, 221804 (2005).
[11] H.-n. Li, Phys. Lett. B **622**, 63 (2005).
[12] H. Y. Cheng, C. K. Chua, and A. Soni, Phys. Rev. D **71**, 014030 (2005).
[13] Y. D. Yang, R. M. Wang, and G. R. Lu, Phys. Rev. D **72**, 015009 (2005); C. S. Kim and Y. D. Yang, arXiv:hep-ph/0412364; R. Wang, G. R. Lu, E. K. Wang, and Y. D. Yang, Eur. Phys. J. C **47**, 815 (2006); C. S. Huang, P. Ko, X. H. Wu, and Y. D. Yang, Phys. Rev. D **73**, 034026 (2006); Q. Chang, X. Q. Li, and Y. D. Yang, J. High Energy Phys. 06 (2007) 038; C. H. Chen and C. Q. Geng, Phys. Rev. D **71**, 115004 (2005); S. Baek, A. Datta, P. Hamel, O. F. Hernandez, and D. London, Phys. Rev. D **72**, 094008 (2005); W. S. Hou and M. Nagashima, arXiv:hep-ph/0408007; A. K. Giri and R. Mohanta, Eur. Phys. J. C **44**, 249 (2005); E. Alvarez, L. N. Epele, D. G. Dumm, and A. Szynkman, Phys. Rev. D **70**, 115014 (2004); P. K. Das and K. C. Yang, Phys. Rev. D **71**, 094002 (2005); W. J. Zou and Z. J. Xiao, Phys. Rev. D **72**, 094026 (2005).
[14] H. Y. Cheng and K. C. Yang, Phys. Rev. D **76**, 114020 (2007).
[15] T. Feldmann, arXiv:1408.0300; W. Wang, R. H. Li, and C. D. Lü, Phys. Rev. D **78**, 074009 (2008).
[16] X. Liu, Z. T. Zou, and Z. J. Xiao, Phys. Rev. D **90**, 094019 (2014).
[17] X. Liu and Z. J. Xiao, Phys. Rev. D **89**, 097503 (2014).
[18] X. Liu, Z. J. Xiao, J. W. Li, and Z. T. Zou, Phys. Rev. D **91**, 014008 (2015).
[19] R. Aaij *et al.* (LHCb Collaboration), Phys. Rev. Lett. **112**, 091802 (2014).
[20] Y. Y. Keum, H.-n. Li, and A. I. Sanda, Phys. Lett. B **504**, 6 (2001); Phys. Rev. D **63**, 054008 (2001); C. D. Lü, K. Ukai, and M. Z. Yang, Phys. Rev. D **63**, 074009 (2001); H.-n. Li, Prog. Part. Nucl. Phys. **51**, 85 (2003).
[21] X. Liu and Z. J. Xiao, J. Phys. G **38**, 035009 (2011); Z. J. Xiao and X. Liu, Chin. Sci. Bull. **59**, 3748 (2014).
[22] H.-n. Li, Y. L. Shen, Y. M. Wang, and H. Zou, Phys. Rev. D **83**, 054029 (2011); **85**, 074004 (2012); J. High Energy Phys. 02 (2013) 008; H. C. Hu and H.-n. Li, Phys. Lett. B **718**, 1351 (2013); Z. Rui, G. Xiangdong, and C. D. Lü, Eur. Phys. J. C **72**, 1923 (2012); S. Cheng, Y. Y. Fan, X. Yu,

C. D. Lü, and Z. J. Xiao, Phys. Rev. D **89**, 094004 (2014); Y. L. Zhang, X. Y. Liu, Y. Y. Fan, S. Cheng, and Z. J. Xiao, Phys. Rev. D **90**, 014029 (2014); S. Cheng, Z. J. Xiao, and Y. L. Zhang, Nucl. Phys. **B896**, 255 (2015); H.-n. Li and S. Mishima, Phys. Rev. D **83**, 034023 (2011); **90**, 074018 (2014).

[23] X. Liu, H.-n. Li, and Z. J. Xiao, Phys. Rev. D **91**, 114019 (2015); **93**, 014024 (2016).

[24] G. Buchalla, A. J. Buras, and M. E. Lautenbacher, Rev. Mod. Phys. **68**, 1125 (1996).

[25] H. Y. Cheng, Phys. Lett. B **707**, 116 (2012).

[26] G. Calderon, J. H. Munoz, and C. E. Vera, Phys. Rev. D **76**, 094019 (2007).

[27] K. C. Yang, Nucl. Phys. **B776**, 187 (2007).

[28] M. Beneke, G. Buchalla, M. Neubert, and C. T. Sachrajda, Phys. Rev. Lett. **83**, 1914 (1999); Nucl. Phys. **B591**, 313 (2000).

[29] C. W. Bauer, S. Fleming, D. Pirjol, and I. W. Stewart, Phys. Rev. D **63**, 114020 (2001); C. W. Bauer, D. Pirjol, and I. W. Stewart, Phys. Rev. D **65**, 054022 (2002).

[30] H.-n. Li and H. L. Yu, Phys. Rev. Lett. **74**, 4388 (1995); Phys. Lett. B **353**, 301 (1995); Phys. Rev. D **53**, 2480 (1996).

[31] M. Beneke, G. Buchalla, M. Neubert, and C. T. Sachrajda, Nucl. Phys. **B606**, 245 (2001); M. Beneke and M. Neubert, Nucl. Phys. **B675**, 333 (2003).

[32] H.-n. Li, Phys. Rev. D **66**, 094010 (2002).

[33] H.-n. Li and K. Ukai, Phys. Lett. B **555**, 197 (2003).

[34] J. Botts and G. F. Sterman, Nucl. Phys. **B325**, 62 (1989).

[35] H.-n. Li and G. F. Sterman, Nucl. Phys. **B381**, 129 (1992).

[36] C. D. Lü and M. Z. Yang, Eur. Phys. J. C **28**, 515 (2003).

[37] P. Ball, V. M. Braun, Y. Koike, and K. Tanaka, Nucl. Phys. **B529**, 323 (1998).

[38] P. Ball and G. W. Jones, J. High Energy Phys. 03 (2007) 069.

[39] R. H. Li, C. D. Lu, and W. Wang, Phys. Rev. D **79**, 034014 (2009).

[40] R. C. Verma, J. Phys. G **39**, 025005 (2012).

[41] J. J. Dudek, R. G. Edwards, P. Guo, and C. E. Thomas, Phys. Rev. D **88**, 094505 (2013).

[42] J. Beringer *et al.* (Particle Data Group Collaboration), Phys. Rev. D **86**, 010001 (2012).

[43] L. Wolfenstein, Phys. Rev. Lett. **51**, 1945 (1983).

[44] T. Aaltonen *et al.* (CDF Collaboration), Phys. Rev. Lett. **108**, 211803 (2012); F. Ruffini, Report No. FERMILAB-THESIS-2013-02;R. Aaij *et al.* (LHCb Collaboration), J. High Energy Phys. 10 (2012) 037.

[45] Y. Amhis *et al.* (Heavy Flavor Averaging Group Collaboration), arXiv:1412.7515; updated in http://www.slac.stanford.edu/xorg/hfag.

[46] H.-n. Li and S. Mishima, Phys. Rev. D **73**, 114014 (2006).

[47] I. Adachi *et al.* (Belle Collaboration), Phys. Rev. D **89**, 072008 (2014); **89**, 119903 (2014).

[48] B. Aubert *et al.* (*BABAR* Collaboration), Phys. Rev. D **78**, 071104 (2008).

[49] R. Aaij *et al.* (LHCb Collaboration), Phys. Lett. B **747**, 468 (2015).

[50] C. M. Arnesen, Z. Ligeti, I. Z. Rothstein, and I. W. Stewart, Phys. Rev. D **77**, 054006 (2008).

[51] J. Chay, H.-n. Li, and S. Mishima, Phys. Rev. D **78**, 034037 (2008).

[52] Z. J. Xiao, W. F. Wang, and Y. Y. Fan, Phys. Rev. D **85**, 094003 (2012).

[53] A. Ali, G. Kramer, Y. Li, C. D. Lu, Y. L. Shen, W. Wang, and Y. M. Wang, Phys. Rev. D **76**, 074018 (2007).

[54] H.-n. Li and S. Mishima, Phys. Rev. D **74**, 094020 (2006).

[55] P. Ball and R. Zwicky, Phys. Rev. D **71**, 014029 (2005).

[56] H.-n. Li and S. Mishima, Phys. Rev. D **71**, 054025 (2005).